ABSTRACT

Title of dissertation: ENERGY COOPERATION IN
ENERGY HARVESTING COMMUNICATIONS

Berk Gurakan, Doctor of Philosophy, 2016

Dissertation directed by: Professor Şennur Ulukuş
Department of Electrical and Computer Engineering

In energy harvesting communications, users transmit messages using energy harvested from nature. In such systems, transmission policies of the users need to be carefully designed according to the energy arrival profiles. When the energy management policies are optimized, the resulting performance of the system depends only on the energy arrival profiles. In this dissertation, we introduce and analyze the notion of *energy cooperation* in energy harvesting communications where users can share a portion of their harvested energy with the other users via wireless energy transfer. This energy cooperation enables us to control and optimize the energy arrivals at users to the extent possible. In the classical setting of cooperation, users help each other in the transmission of their data by exploiting the broadcast nature of wireless communications and the resulting overheard information. In contrast to the usual notion of cooperation, which is at the *signal level*, energy cooperation we introduce here is at the *battery energy level*. In a multi-user setting, energy may be abundant in one user in which case the loss incurred by transferring it to another user may be less than the gain it yields for the other user. It is this cooperation that

we explore in this dissertation for several multi-user scenarios, where energy can be transferred from one user to another through a separate wireless energy transfer unit.

We first consider the offline optimal energy management problem for several basic multi-user network structures with energy harvesting transmitters and one-way wireless energy transfer. In energy harvesting transmitters, energy arrivals in time impose energy causality constraints on the transmission policies of the users. In the presence of wireless energy transfer, energy causality constraints take a new form: energy can flow in time from the past to the future for each user, and from one user to the other at each time. This requires a careful joint management of energy flow in two separate dimensions, and different management policies are required depending on how users share the common wireless medium and interact over it. In this context, we analyze several basic multi-user energy harvesting network structures with wireless energy transfer. To capture the main trade-offs and insights that arise due to wireless energy transfer, we focus our attention on simple two- and three-user communication systems, such as the relay channel, multiple access channel and the two-way channel.

Next, we focus on the delay minimization problem for networks. We consider a general network topology of energy harvesting and energy cooperating nodes. Each node harvests energy from nature and all nodes may share a portion of their harvested energies with neighboring nodes through energy cooperation. We consider the joint data routing and capacity assignment problem for this setting under fixed data and energy routing topologies. We determine the joint routing of energy and

data in a general multi-user scenario with data and energy transfer.

Next, we consider the cooperative energy harvesting diamond channel, where the source and two relays harvest energy from nature and the physical layer is modeled as a concatenation of a broadcast and a multiple access channel. Since the broadcast channel is degraded, one of the relays has the message of the other relay. Therefore, the multiple access channel is an extended multiple access channel with common data. We determine the optimum power and rate allocation policies of the users in order to maximize the end-to-end throughput of this system.

Finally, we consider the two-user cooperative multiple access channel with energy harvesting users. The users cooperate at the physical layer (data cooperation) by establishing common messages through overheard signals and then cooperatively sending them. For this channel model, we investigate the effect of intermittent data arrivals to the users. We find the optimal offline transmit power and rate allocation policy that maximize the departure region. When the users can further cooperate at the battery level (energy cooperation), we find the jointly optimal offline transmit power and rate allocation policy together with the energy transfer policy that maximize the departure region.

ENERGY COOPERATION IN ENERGY HARVESTING COMMUNICATIONS

by

Berk Gurakan

Dissertation submitted to the Faculty of the Graduate School of the
University of Maryland, College Park in partial fulfillment
of the requirements for the degree of
Doctor of Philosophy
2016

Advisory Committee:
Professor Şennur Ulukuş, Chair/Advisor
Professor Prakash Narayan
Professor Richard La
Professor Gang Qu
Professor Radu Balan

To my family.

ACKNOWLEDGEMENT

I would like to start by thanking my advisor Professor Sennur Ulukus for all her help and support throughout my PhD studies. She is very committed to both the professional and academic development of her students, always emphasizing the value of hard work and dedication when tackling difficult problems. She was always open for discussion and exchange of ideas and this was very valuable for my research progress. Her passion for research and problem solving has always been inspiring. She has also helped me a lot in improving my presentation and writing skills, for which I will always be grateful. I deeply appreciate and thank her for the guidance and support she provided.

I would like to thank Professors Prakash Narayan, Richard La, Gang Qu and Radu Balan for being in my dissertation committee and for their valuable feedback. I am especially grateful to Professor Narayan for the various conversations and discussions about different interesting problems and topics.

I would like to thank all members of Prof. Ulukus' group and CSPL for the friendly environment that I enjoyed over the last five years. I acknowledge Dr. Ersen Ekrem, Prof. Jing Yang, Dr. Omur Ozel, Dr. Raef Bassily, Prof. Himanshu Tyagi, Dr. Jianwei Xie, Pritam Mukherjee, Praneeth Boda, Ahmed Arafa, Karim Banawan, Abdulrahman Baknina and Yi-Peng Wei. I also thank Prof. Onur Kaya, Dr. Omur Ozel and Prof. Jing Yang for our joint work.

Finally, I pay my sincerest thanks and regards to my parents and my brother for always supporting me. Special thanks to Maya Kabkab for always being there for me!

Table of Contents

List of Figures

CHAPTER 1

Introduction

1.1 Overview

In energy harvesting communications, users transmit messages using energy harvested from nature [1–3]. In such systems, transmission policies of the users need to be carefully designed according to the energy arrival profiles. Energy management problem for various energy harvesting commmunication setting has been adressed in different works [4–19]. When the energy management policies are optimized as in [4–19], the resulting performance of the system depends only on the energy arrival profiles. In this dissertation, we introduce and analyze the notion of *energy cooperation* in energy harvesting communications where users can share a portion of their harvested energy with the other users via wireless energy transfer [20–22]. This energy cooperation enables us to control and optimize the energy arrivals at users to the extent possible. In the classical setting of cooperation [23], users help each other in the transmission of their data by exploiting the broadcast nature of wireless communications and the resulting overheard information. In contrast to the usual notion of cooperation, which is at the *signal level*, energy cooperation we introduce

here is at the *battery energy level*. In a multi-user setting, energy may be abundant in one user in which case the loss incurred by transferring it to another user may be less than the gain it yields for the other user. It is this cooperation that we explore in this dissertation for several multi-user scenarios, where energy can be transferred from one user to another through a separate wireless energy transfer unit.

Wireless energy transfer has been recently proposed as a promising technique for a wide variety of wireless networking applications [24–29]. In future wireless networks, nodes are envisioned to be capable of harvesting energy from the environment and transferring energy to other nodes, rendering the network energy self-sufficient and self-sustaining with a significantly prolonged lifetime. Wireless energy transfer is a relatively new concept for wireless communications; however, it has been considered in other contexts earlier: Wireless powering of engineering systems by microwave power transfer technology has been used in many applications [30–32] for a long time, such as space missions [31] and optical communications [32]. While microwave power transfer is viewed as the key technology for large-scale cellular networks [24], recent advances in wireless energy transfer technology supports feasibility of wireless network design in smaller scales. In [33, 34], wireless energy transfer with strong inductive coupling has been demonstrated with relatively high efficiency over relatively long distances with small device sizes. Another related line of research in medical implanting applications has been presented in [27–29] where wireless nodes are powered by wireless energy transfer, which also use the wirelessly transferred energy for communications. RFID technology is another prominent example along this direction, where nodes harvest received energy and use the harvested energy

(via reflection) for communication [35]. Relying on the possibility of efficient wireless energy transfer, in this dissertation, we investigate the optimum communication schemes in multi-user systems with nodes that have energy harvesting and energy transfer capabilities.

In communication systems with wireless energy transfer, energy and information flow simultaneously. Motivated by this nature of such systems, the trade-off between energy and information transmission has been addressed in several recent works [36–42]. Among these works, the one that is most pertinent to our work is [41], where multi-user communication systems with simultaneous energy and information transmission are studied. Our problem formulations capture different trade-offs than those studied in [36–42] since in our model wireless energy transfer is maintained by a separate wireless energy transfer unit, and the harvested energy source is independent of the received signal energy.

We first consider the offline optimal energy management problem for several basic multi-user network structures with energy harvesting transmitters and one-way wireless energy transfer. As extensively emphasized in [4–19], in energy harvesting transmitters, energy arrivals in time impose energy causality constraints on the transmission policies of the users. In the optimal policy, due to the concavity of the throughput in powers, energy needs to be allocated as constant as possible over time subject to energy causality constraints. In the presence of wireless energy transfer, energy causality constraints take a new form: energy can flow in time from the past to the future for each user, and from one user to the other at each time. This requires a careful joint management of energy flow in two separate dimensions,

and different management policies are required depending on how users share the common wireless medium and interact over it. In this context, we analyze several basic multi-user energy harvesting network structures with wireless energy transfer. To capture the main trade-offs and insights that arise due to wireless energy transfer, we focus our attention on simple two- and three-user communication systems.

Next, we focus on the delay minimization problem for networks. We consider a general network topology of energy harvesting and energy cooperating nodes. Each node harvests energy from nature and all nodes may share a portion of their harvested energies with neighboring nodes through energy cooperation. The delay on each link depends on the information carrying capacity of the link, and in particular, it decreases monotonically with the capacity of the link for a fixed data flow through it; see e.g., [43, eqn. (5.30)]. The capacity, in turn, is a function of the power allocated to the link, and in particular, it is a monotonically increasing function of the power, for instance, through a logarithmic Shannon type capacity-power relationship; see e.g., [44, eqns. (9.60) and (9.62)]. In addition, the delay on a link is a monotonically increasing function of the data flow through it, for a fixed link capacity [43, eqn. (5.30)]. We consider the joint data routing and capacity assignment problem for this setting under fixed data and energy routing topologies [43, Section 5.4.2]. Our work is related to and builds upon classical and recent works on data routing and capacity assignment in communication networks [43, 45–53], and recent works on energy harvesting communications [4–6, 9, 54] and energy cooperation [24, 26, 36–38, 55–67] in wireless networks. Inspired by joint routing and resource allocation problems in the classical works such as [45–48, 51, 53], we study

joint routing of energy and data in a general multi-user scenario with data and energy transfer. We specialize in the objective of minimizing the total delay in the system, which has not been addressed in the context of energy harvesting wireless networks with energy cooperation.

Next, we consider the energy harvesting diamond channel [68], where the source and two relays harvest energy from nature and the physical layer is modeled as a concatenation of a broadcast and a multiple access channel. Since the broadcast channel is degraded, one of the relays has the message of the other relay. Therefore, the multiple access channel is an extended multiple access channel with common data [69]. We determine the optimum power and rate allocation policies of the users in order to maximize the end-to-end throughput of this system.

Finally, we consider the two-user cooperative multiple access channel where both of the users harvest energy from nature. The users cooperate at the physical layer (data cooperation) by establishing common messages through overheard signals and then cooperatively sending them. For this channel model, we investigate the effect of intermittent data arrivals to the users. We find the optimal offline transmit power and rate allocation policy that maximize the departure region. When the users can further cooperate at the battery level (energy cooperation), we find the jointly optimal offline transmit power and rate allocation policy together with the energy transfer policy that maximize the departure region.

1.2 Outline

In Chapter 2, we investigate three channel models with energy harvesting and energy cooperation. First, we examine additive Gaussian two-hop relay channel with one-way energy transfer from the source node to the relay node where the objective is to maximize the end-to-end throughput. Next, we consider the Gaussian two-way channel with one-way energy transfer, and the two-user Gaussian multiple access channel with one-way energy transfer. For these two channel models, we determine the two-dimensional simultaneously achievable throughput regions. For all three cases, we use a Lagrangian approach and determine the optimum transmit powers and energy transfer policies via the KKT optimality conditions. In particular, we develop a *two-dimensional directional water-filling algorithm* which optimally controls the energy flow in time and among users. As observed in [6], energy harvesting setting gives rise to a *directional* water-filling algorithm, where energy can flow only from the past to the future due to the energy causality constraints. In addition, with wireless energy transfer, at any give time, energy can flow from one user to the other depending on the direction of wireless energy transfer. Therefore, the directionality of energy flow in two separate dimensions requires careful management of energy over time and users. Solutions obtained in each setting yield new insights on energy cooperation at the battery energy level in the presence of wireless energy transfer.

In Chapter 3, we consider the delay minimization problem in an energy harvesting communication network with energy cooperation. For fixed data and energy routing topologies, we determine the optimum data rates, transmit powers and

energy transfers, subject to flow and energy conservation constraints, in order to minimize the network delay. We start with a simplified problem where data flows are fixed and optimize energy management at each node for the case of a single energy harvest per node. This is tantamount to distributing each node's available energy over its outgoing data links and energy transfers to neighboring nodes. For this case, with no energy cooperation, we show that each node should allocate more power to links with more noise and/or more data flow. In addition, when there is energy cooperation, our numerical results indicate that, energy is routed from nodes with lower data loads to nodes with higher data loads. We then extend this setting to the case of multiple energy harvests per node over time. In this case, we optimize each node's energy management over its outgoing data links and its energy transfers to neighboring nodes, over multiple time slots. For this case, with no energy cooperation, we show that, for any given node, the sum of powers on the outgoing links over time is equal to the single-link optimal power over time. Then, we consider the problem of joint flow control and energy management for the entire network. We determine the necessary conditions for joint optimality of a power control, energy transfer and routing policy. We provide an iterative algorithm that updates the data flows, energy flows and power distribution over outgoing data links sequentially. We show that this algorithm converges to a Pareto-optimal operating point.

In Chapter 4, we consider the energy harvesting diamond channel, where the source and two relays harvest energy from nature and the physical layer is modeled as a concatenation of a broadcast and a multiple access channel. Since the broadcast channel is degraded, one of the relays has the message of the other relay and the

multiple access channel can be modeled as an extended multiple access channel with common data. We find the optimal offline transmit power and rate allocations that maximize the end-to-end throughput. For the broadcast side, we show that there exists an optimal source power allocation which is equal to the single-user optimal power allocation for the source energy arrivals. We then show that the fraction of the power spent on each broadcast link depends on the energy arrivals for the relays. For the multiple access side with no cooperation, with fixed source rates, we show that the problem can be cast as a multiple access channel with both data and energy arrivals and can be formulated in terms of data transmission rates only. We use a dual decomposition method to solve the overall problem efficiently. Then, we focus on the diamond channel with cooperative multiple access capacity region and find the optimal rates and powers using a decomposition into inner and outer maximization problems.

In Chapter 5, we consider an energy harvesting two-user cooperative Gaussian multiple access channel. The users cooperate at the physical layer (data cooperation) by establishing common messages through overheard signals and then cooperatively sending them. We study two scenarios within this model. In the first scenario, the data packets arrive intermittently over time. We find the optimal offline transmit power and rate allocation policy that maximizes the departure region. We first show that there exists an optimal policy, in which the single-user rate constraints in each time slot are tight, yielding a one-to-one relation between the powers and rates. Then, we formulate the departure region maximization problem as a weighted sum rate maximization in terms of rates only. Next, we propose a sequential convex

approximation method to approximate the problem at each step and show that it converges to the optimal solution. Then, we solve the approximate problems using an inner outer decomposition method. In the second scenario, the users cooperate at the battery level (energy cooperation) by wirelessly transferring energy to each other in addition to the data cooperation. We find the jointly optimal offline transmit power and rate allocation policy together with the energy transfer policy that maximize the departure region. We provide necessary conditions for energy transfer, and prove some properties of the optimal transmit policy, thereby shedding some light on the interplay between energy and data cooperation.

In Chapter 6, we provide conclusions to this dissertation.

CHAPTER 2

Energy Cooperation in Energy Harvesting Communications

2.1 Introduction

In this chapter, we study the offline optimal energy management problem for several basic multi-user network structures with energy harvesting transmitters and one-way wireless energy transfer. First, we examine additive Gaussian two-hop relay channel with one-way energy transfer from the source node to the relay node where the objective is to maximize the end-to-end throughput. Next, we consider the Gaussian two-way channel with one-way energy transfer, and the two-user Gaussian multiple access channel with one-way energy transfer. For these two channel models, we determine the two-dimensional simultaneously achievable throughput regions. For all three cases, we use a Lagrangian approach and determine the optimum transmit powers and energy transfer policies via the KKT optimality conditions. In particular, we develop a *two-dimensional directional water-filling algorithm* which optimally controls the energy flow in time and among users. As observed in [6], energy harvesting setting gives rise to a *directional* water-filling algorithm, where energy can flow only from the past to the future due to the energy causality con-

straints. In addition, with wireless energy transfer, at any give time, energy can flow from one user to the other depending on the direction of wireless energy transfer. Therefore, the directionality of energy flow in two separate dimensions requires careful management of energy over time and users. Solutions obtained in each setting yield new insights on energy cooperation at the battery energy level in the presence of wireless energy transfer.

2.2 Two-Hop Relay Channel with One-Way Energy Transfer

In this section, we consider a two-hop relay channel consisting of a source node, a relay node and a destination node as shown in Fig. 2.1. The two queues at the source and the relay nodes are the data and energy queues. The energies that arrive at the source and the relay nodes are saved in the corresponding energy queues. The data queue of the source always carries some data packets to be delivered to the destination. The data packets sent from the source node cause a depletion of energy from the source energy queue and an increase in the relay data queue. These data packets are then served out of the relay data queue with a cost of energy depletion from the relay energy queue. The relay operates in a full-duplex mode, i.e., it can receive and send data within a single slot; in addition, the relay can receive energy as well in the same slot. Therefore, the data and energy queues of the relay are updated simultaneously in every slot. We assume that the data and energy buffer sizes are unlimited. In addition, energy expenditure is only due to data transmissions; any other energy costs, e.g., processing, circuitry, are not considered in this chapter.

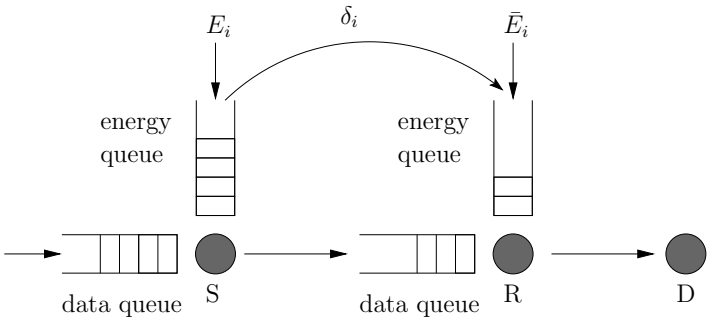

Figure 2.1: Two-hop relay channel with energy harvesting source and relay nodes, and one-way energy transfer from the source node to the relay node.

There is a separate wireless energy transfer unit at the source node. Information and energy transfer channels are orthogonal to each other. In this setting, the source node may wish to share a portion of its energy with the relay node so that the relay can forward more data.

The channels from the source to the relay and from the relay to the destination are additive white Gaussian noise (AWGN) channels. The received signals y_r and y_d at the relay and the destination, respectively, are given by $y_r = \sqrt{h_s}x_s + n_s$ and $y_d = \sqrt{h_r}x_r + n_r$, where h_s and h_r are the channel coefficients for the source-to-relay and relay-to-destination channels, respectively. n_s and n_r are Gaussian noises each with zero-mean and unit-variance. We assume that $h_s = h_r = 1$ without loss of generality as otherwise the energy arrivals can be properly scaled.

Time is slotted and there are a total of T equal length slots. Without loss of generality, we assume that the slots are of unit length. At times $t = 1, \ldots, T$, the source harvests energy with amounts $E_1, E_2, \ldots, E_T$ and the relay harvests energy with amounts $\bar{E}_1, \bar{E}_2, \ldots, \bar{E}_T$. Without loss of generality, we assume $E_1 > 0, \bar{E}_1 > 0$. The normalized energy transfer efficiency is α where $\alpha = \alpha' \frac{h_r}{h_s}$ and α' is the actual

energy transfer efficiency. We assume $0 \leq \alpha \leq 1$. This means that when the source transfers δ_i amount of energy to the relay through the wireless energy transfer unit in slot i, $\alpha\delta_i$ amount of energy enters the energy queue of the relay in the next slot. Similarly, when the source uses power P_i for data transmission, the data queue of the relay is increased by $\frac{1}{2}\log(1+P_i)$ bits in the next slot. The source and relay slots are indexed by one slot delay, so that, the slot subscripts are aligned at the source and the relay; see Fig. 2.2. Power policy of the source is the sequences P_i and δ_i, and the power policy of the relay is the sequence $\bar{P}_i$.

As the energy that has not arrived yet cannot be used for data transmission or energy transfer, the power policies of the source and the relay are constrained by the causality of energy in time. These constraints yield the following feasible set:

$$\mathcal{F} = \Big\{(\boldsymbol{\delta}, \mathbf{P}, \bar{\mathbf{P}}) : \ \sum_{i=1}^{k} P_i \leq \sum_{i=1}^{k}(E_i - \delta_i), \quad \sum_{i=1}^{k} \bar{P}_i \leq \sum_{i=1}^{k}(\bar{E}_i + \alpha\delta_i), \\ P_k, \bar{P}_k, \delta_k \geq 0, \quad \forall k \Big\} \tag{2.1}$$

where vectors $\mathbf{P}$, $\bar{\mathbf{P}}$ and $\boldsymbol{\delta}$ denote sequences $P_i, \bar{P}_i$ and δ_i, respectively. $\mathcal{F}$ is the feasible set due to energy causality in harvested and transferred energies and is valid for the two-way and multiple access system models as well. For the two-hop relay channel model, we have an additional constraint: The relay transmits data that arrives from the source. Therefore, the power policies of the source and the

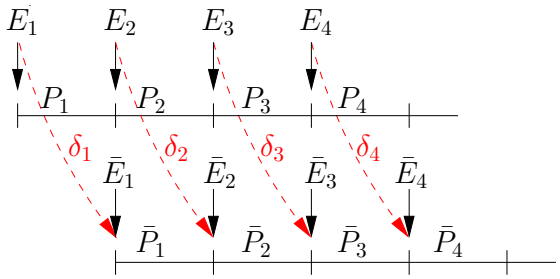

Figure 2.2: Slotted system model: The queues of the relay are updated with one slot delay with respect to the queues of the source so that the slot indices are aligned.

relay need to satisfy the following data causality constraints at the relay:

$$\sum_{i=1}^{k} \frac{1}{2} \log\left(1+\bar{P}_i\right) \leq \sum_{i=1}^{k} \frac{1}{2} \log\left(1+P_i\right), \quad k=1,\ldots,T \tag{2.2}$$

We formulate the end-to-end throughput maximization problem in the next section.

2.3 End-to-end Throughput Maximization for the Relay Channel

The optimal offline end-to-end throughput maximization problem with wireless energy transfer subject to energy causality at both nodes and data causality at the relay node is:

$$\begin{aligned} \max_{\bar{P}_i, P_i, \delta_i} \quad & \sum_{i=1}^{T} \frac{1}{2} \log\left(1+\bar{P}_i\right) \\ \text{s.t.} \quad & \sum_{i=1}^{k} \frac{1}{2} \log\left(1+\bar{P}_i\right) \leq \sum_{i=1}^{k} \frac{1}{2} \log\left(1+P_i\right), \quad \forall k \\ & (\boldsymbol{\delta}, \mathbf{P}, \bar{\mathbf{P}}) \in \mathcal{F} \end{aligned} \tag{2.3}$$

It can be shown that (2.3) is equivalent to a convex optimization problem (see [20]), by a change of variables from $\bar{P}_i, P_i, \delta_i$ to $\bar{r}_i = \frac{1}{2}\log\left(1+\bar{P}_i\right), r_i = \frac{1}{2}\log\left(1+P_i\right), \delta_i$. Thus, (2.3) can be solved using standard techniques [70]. The Lagrangian function for the problem in (2.3) is:

$$\begin{aligned}\mathcal{L} = &-\sum_{i=1}^{T}\log\left(1+\bar{P}_i\right)+\sum_{k=1}^{T}\mu_k\left(\sum_{i=1}^{k}P_i-(E_i-\delta_i)\right)+\sum_{k=1}^{T}\eta_k\left(\sum_{i=1}^{k}\bar{P}_i-(\bar{E}_i+\alpha\delta_i)\right)\\&+\sum_{k=1}^{T}\lambda_k\left(\sum_{i=1}^{k}\log\left(1+\bar{P}_i\right)-\sum_{i=1}^{k}\log\left(1+P_i\right)\right)-\sum_{k=1}^{T}\sigma_k P_k-\sum_{k=1}^{T}\psi_k\bar{P}_k-\sum_{k=1}^{T}\rho_k\delta_k\end{aligned} \tag{2.4}$$

We first argue that P_i and $\bar{P}_i$ are non-zero in an optimal policy since $E_1 > 0$ and $\bar{E}_1 > 0$. As (2.3) reduces to the problem in [12, 13] for fixed δ_i, the powers P_i and $\bar{P}_i$ are positive and non-decreasing for positive initial energy. Hence, it suffices to show that $\delta_1 < E_1$ in an optimal policy. Assume $\delta_1 = E_1$. Then, $P_1 = 0$ and from (2.2) $\bar{P}_1 = 0$. For now, assume that $P_2 > 0$. Then, we must also have $\bar{P}_2 > 0$. For some $0 < \epsilon \ll 1$, define a new energy transfer sequence $\delta_1^{'} = E_1 - \epsilon, \delta_2^{'} = \delta_2 + \epsilon$, and new source and relay power allocations $P_1^{'} = \epsilon, P_2^{'} = P_2 - \epsilon$ and $\bar{P}_1^{'} = \epsilon, \bar{P}_2^{'} = \bar{P}_2 - \epsilon$ while keeping the source and relay power levels and energy transfer values in the remaining slots unchanged. Note that this power allocation is feasible: For the source energy causality constraint over the first slot we have, $P_1^{'} = \epsilon = E_1 - (E_1 - \epsilon) = E_1 - \delta_1^{'}$. Together with the fact that $\sum_{i=1}^{k} P_i^{'} = \sum_{i=1}^{k} P_i$ and $\sum_{i=1}^{k}\delta_i^{'} = \sum_{i=1}^{k}\delta_i, \forall k \geq 2$, we have $\sum_{i=1}^{k} P_i^{'} \leq \sum_{i=1}^{k} E_i - \delta_i^{'}, \forall k$, since the original source power allocation and energy transfer profile are feasible. Similarly for the relay energy causality constraint over the first slot we have, $\bar{P}_1^{'} = \epsilon \leq$

$\bar{E}_1 + \alpha(E_1 - \epsilon)$ for small enough ϵ. Together with the fact that $\sum_{i=1}^{k} \bar{P}_i' = \sum_{i=1}^{k} \bar{P}_i$ and $\sum_{i=1}^{k} \delta_i' = \sum_{i=1}^{k} \delta_i, \forall k \geq 2$, we have $\sum_{i=1}^{k} \bar{P}_i' \leq \sum_{i=1}^{k} \bar{E}_i + \alpha\delta_i', \forall k$, since the original relay power allocation and energy transfer profile are feasible. The data causality constraint trivially holds for the first slot since, $\frac{1}{2}\log(1 + P_1') = \frac{1}{2}\log(1 + \bar{P}_1')$. Similarly, $\frac{1}{2}\log(1 + P_2') = \frac{1}{2}\log(1 + P_2 - \epsilon) \leq \frac{1}{2}\log(1 + \bar{P}_2 - \epsilon)$ since $\bar{P}_2 \leq P_2$ due to data causality of the original allocation in the second slot. Therefore, $\sum_{i=1}^{k} \frac{1}{2}\log(1 + \bar{P}_i') \leq \frac{1}{2}\sum_{i=1}^{k} \log(1 + P_i'), \forall k$, and data causality is satisfied in all slots. Hence, this new allocation satisfies the energy and data causality constraints in (2.3) and achieves higher end-to-end throughput due to the concavity of the objective function with respect to $\bar{P}_i$. Therefore this contradicts optimality. On the other hand, if $P_2 = 0$, then $\bar{P}_2 = 0$ also. We then go until the first slot k where $P_k > 0$. For that slot, we have $\bar{P}_k > 0$ and we use the above construction with P_2 and $\bar{P}_2$ replaced with P_k and $\bar{P}_k$, respectively. This discussion implies, P_i and $\bar{P}_i$ are non-zero for all i in an optimal policy, and we have $\sigma_i = \psi_i = 0, \ \forall i$.

The KKT conditions for this problem are:

$$\frac{-1 + \sum_{k=i}^{T} \lambda_k}{1 + \bar{P}_i} + \sum_{k=i}^{T} \eta_k = 0, \quad \forall i \tag{2.5}$$

$$\frac{-\sum_{k=i}^{T} \lambda_k}{1 + P_i} + \sum_{k=i}^{T} \mu_k = 0, \quad \forall i \tag{2.6}$$

$$\sum_{k=i}^{T} \mu_k - \alpha \sum_{k=i}^{T} \eta_k - \rho_i = 0, \quad \forall i \tag{2.7}$$

with the additional complementary slackness conditions as:

$$\lambda_k \left(\sum_{i=1}^{k} \log\left(1+\bar{P}_i\right) - \sum_{i=1}^{k} \log\left(1+P_i\right) \right) = 0, \quad \forall k \tag{2.8}$$

$$\mu_k \left(\sum_{i=1}^{k} P_i - \left(E_i - \delta_i\right) \right) = 0, \quad \forall k \tag{2.9}$$

$$\eta_k \left(\sum_{i=1}^{k} \bar{P}_i - \left(\bar{E}_i + \alpha\delta_i\right) \right) = 0, \quad \forall k \tag{2.10}$$

$$\rho_k \delta_k = 0, \quad \forall k \tag{2.11}$$

From (2.5), (2.6) and (2.7) we get:

$$\bar{P}_i = \frac{1 - \sum_{k=i}^{T} \lambda_k}{\sum_{k=i}^{T} \eta_k} - 1, \quad \forall i \tag{2.12}$$

$$P_i = \frac{\sum_{k=i}^{T} \lambda_k}{\sum_{k=i}^{T} \mu_k} - 1, \quad \forall i \tag{2.13}$$

$$\rho_i = \sum_{k=i}^{T} \mu_k - \alpha \sum_{k=i}^{T} \eta_k, \quad \forall i \tag{2.14}$$

Next, we obtain necessary optimality conditions for (2.3).

2.3.1 Necessary Optimality Conditions

The first necessary optimality condition for (2.3) is that the source has to send as many bits as the relay can send and the relay has to finish up all the data in its data buffer. In other words, in the optimal policy, no data should be left in the data queue of the relay at the end.

Lemma 2.1 *The optimal power sequences P_i^*, $\bar{P}_i^*$ must satisfy the constraint*

$\sum_{i=1}^{T} \frac{1}{2} \log(1 + \bar{P}_i^*) = \sum_{i=1}^{T} \frac{1}{2} \log(1 + P_i^*)$.

Proof: Suppose the stated constraint is satisfied with strict inequality. Then, we can increase δ_T, increase $\bar{P}_T$ and decrease P_T without violating the energy constraints and improve the overall throughput which contradicts the optimality of $\bar{P}_i^*$, P_i^*, δ_i^*.

■

We note that if the relay energy profile is sufficient to forward all the bits in the optimal source data stream with respect to the source energy profile, that is, if the separable policy in [12, 13] yields a policy that satisfies the necessary condition in Lemma 2.1, then it is the optimal solution for (2.3) and no energy transfer is needed.

The second observation about the optimal policy is that the source has to exhaust the energies that have been harvested throughout the communication session either for data transmission or in the form of wireless energy transfer.

Lemma 2.2 *The optimal power profiles P_i^*, $\bar{P}_i^*$ and energy transfers δ_i^* must satisfy* $\sum_{i=1}^{T} P_i^* = \sum_{i=1}^{T} (E_i - \delta_i^*)$.

Proof: Suppose this constraint is satisfied with strict inequality. Then, we can increase δ_T and $\bar{P}_T$ then decrease P_T to achieve a larger throughput and satisfy the constraints of (2.3). This contradicts the optimality of $P_i^*, \bar{P}_i^*, \delta_i^*$. ■

Next, we observe that if there is a non-zero energy transfer from the source to the relay, then the relay has to exhaust all of its energy in the optimal policy.

Lemma 2.3 *For the optimal power sequences P_i^*, $\bar{P}_i^*$ and energy transfer sequence δ_i^*, if $\delta_i^* \neq 0$ for some i, then $\sum_{i=1}^T \bar{P}_i^* = \sum_{i=1}^T (\bar{E}_i + \alpha\delta_i^*)$.*

Proof: Suppose this constraint is satisfied with strict inequality. Using a similar argument as in Lemma 2.2, we can decrease δ_T and increase $\bar{P}_T$ to achieve a larger throughput and satisfy the constraints of problem (2.3). This contradicts the optimality of $P_i^*, \bar{P}_i^*, \delta_i^*$. ■

Finally, we note that, in the optimal policy, the total energy expenditure at the relay must be higher than the total energy expenditure at the source.

Lemma 2.4 *The optimal power sequences P_i^* and $\bar{P}_i^*$ must satisfy $\sum_{i=1}^T P_i^* \leq \sum_{i=1}^T \bar{P}_i^*$, and with equality if and only if $P_i^* = \bar{P}_i^*$ for all i.*

Proof: We will give a proof based on majorization theory and Schur convexity [71]. We denote the optimal source and relay rate allocation vectors as $\mathbf{r}^* = [r_1^*, \ldots, r_T^*]$ and $\bar{\mathbf{r}}^* = [\bar{r}_1^*, \ldots, \bar{r}_T^*]$, where $r_i^* = \frac{1}{2}\log(1 + P_i^*)$ and $\bar{r}_i^* = \frac{1}{2}\log(1 + \bar{P}_i^*)$, for $i = 1, \ldots, T$. First, we note that the optimal rate allocations of both the source and the relay are monotone non-decreasing sequences by [4, Lemmas 1 and 4], i.e., $r_i^* \leq r_{i+1}^*$ and $\bar{r}_i^* \leq \bar{r}_{i+1}^*$, for $i = 1, \ldots, T$. Second, we note the data causality constraint at the relay $\sum_{i=1}^k \bar{r}_i^* \leq \sum_{i=1}^k r_i^*$, for all $k < T$, and the equality $\sum_{i=1}^T \bar{r}_i^* = \sum_{i=1}^T r_i^*$ by Lemma 2.1. These imply that $\mathbf{r}^*$ is majorized by $\bar{\mathbf{r}}^*$, which is denoted by $\mathbf{r}^* \preceq \bar{\mathbf{r}}^*$; see [71, Definition 1.A.1]. Since $P_i^* = 2^{2r_i^*} - 1$ and $g(x) = 2^{2x} - 1$ is strictly convex, $\sum_{i=1}^T P_i^* = \sum_{i=1}^T 2^{2r_i^*} - 1$ is a strictly Schur convex function of $\mathbf{r}^*$ [71, Proposition 3.C.1]. Then, since $\mathbf{r}^* \preceq \bar{\mathbf{r}}^*$, we have that $\sum_{i=1}^T P_i^* = \sum_{i=1}^T 2^{2r_i^*} - 1 \leq \sum_{i=1}^T 2^{2\bar{r}_i^*} - 1 =$

$\sum_{i=1}^{T} \bar{P}_i^*$ [71, Proposition 4.B.1]. Moreover, due to the strict convexity of $g(x)$, and the resulting strict Schur convexity, equality is possible only when $r_i^* = \bar{r}_i^*$ for all i.

■

An immediate application of Lemma 2.4 is that if $\sum_{i=1}^{T} \bar{E}_i < \sum_{i=1}^{T} E_i$, i.e., if the total energy of the relay is less than the total energy of the source, then the relay cannot forward the source data stream only with its own energy. In this case, we must have $\delta_i^* \neq 0$ for some i, i.e., some energy transfer is strictly needed. We state this in the following lemma.

Lemma 2.5 *If the data buffer of the relay is empty at some slot k, $k \leq T$, then $\sum_{i=1}^{k} P_i^* \leq \sum_{i=1}^{k} \bar{P}_i^*$, and with equality only when $P_i^* = \bar{P}_i^*$ for all $i = 1, \ldots, k$.*

Proof: If the data buffer of the relay is empty at some slot k, $k \leq T$, then we must have $\sum_{i=1}^{k} r_i^* = \sum_{i=1}^{k} \bar{r}_i^*$. Together with the data causality constraints at the relay $\sum_{i=1}^{\tilde{k}} \bar{r}_i^* \leq \sum_{i=1}^{\tilde{k}} r_i^*$, for $\tilde{k} = 1, \ldots, k-1$, we conclude that the subvector $\mathbf{r}_k^* = [r_1^*, \ldots, r_k^*]$ is majorized by the subvector $\bar{\mathbf{r}}_k^* = [r_1^*, \ldots, r_k^*]$, i.e., $\mathbf{r}_k^* \preceq \bar{\mathbf{r}}_k^*$. Then, $\sum_{i=1}^{k} P_i^* = \sum_{i=1}^{k} 2^{2r_i^*} - 1 \leq \sum_{i=1}^{k} 2^{2\bar{r}_i^*} - 1 = \sum_{i=1}^{k} \bar{P}_i^*$, and with equality iff $\mathbf{r}_k^* = \bar{\mathbf{r}}_k^*$ due to the strict Schur convexity. ■

Necessary conditions in Lemmas 2.1 through 2.5 do not provide detailed structural properties for the optimal policy for an algorithmic solution. In the next sections, we consider specific scenarios to gain insight on the optimal policy. In particular, we examine cases that correspond to practically interesting settings, such as the case of only one of the nodes harvesting energy.

2.3.2 Specific Scenario: Relay Energy Higher at the Beginning Lower at the End

We consider the scenario where the relay energy arrival profile is higher at the beginning, intersects the energy arrival profile of the source once, and remains lower until the end of the communication, as shown in Fig. 2.3. In particular, we assume that there exists $\tilde{i} \in [0, T]$ such that $\sum_{k=1}^{i} \bar{E}_k \geq \sum_{k=1}^{i} E_k$, for all $i = 1, \ldots, \tilde{i}$, and $\sum_{k=1}^{i} \bar{E}_k \leq \sum_{k=1}^{i} E_k$, for all $i = \tilde{i}+1, \ldots, T$. In Fig. 2.3, $\tilde{i} = 3$. We note that this case also covers the setting where the relay is not energy harvesting, and only the source harvests energy during the communication session.

For this case, we propose the following solution. Form a new energy arrival profile as: $\min\{\sum_{k=1}^{i} \frac{\bar{E}_k + \alpha E_k}{\alpha+1}, \sum_{k=1}^{i} E_k\}$ as shown in Fig. 2.3, and maximize the throughput with respect to this profile. In particular, use $\sum_{k=1}^{i} E_k$ for $i = 1, \ldots, \tilde{i}$, and $\sum_{k=1}^{i} \frac{\bar{E}_k + \alpha E_k}{\alpha+1}$ for $i = \tilde{i}+1, \ldots, T$; and perform energy transfer only at slots $\tilde{i}+1, \ldots, T$. The resulting power sequences are matched for the source and the relay. More specifically, we propose

$$P_i^* = \bar{P}_i^* = \frac{\min\left\{\frac{\sum_{j=n_{i-1}}^{n_i} \bar{E}_j + \alpha E_j}{\alpha+1}, \sum_{j=n_{i-1}}^{n_i} E_j\right\}}{n_i - n_{i-1}} \tag{2.15}$$

where

$$n_i = \arg \min_{n_{i-1} \leq k \leq T} \left\{ \frac{\min\{\sum_{j=n_{i-1}}^{k} \frac{\bar{E}_j + \alpha E_j}{\alpha+1}, \sum_{j=n_{i-1}}^{k} E_j\}}{k - n_{i-1}} \right\} \tag{2.16}$$

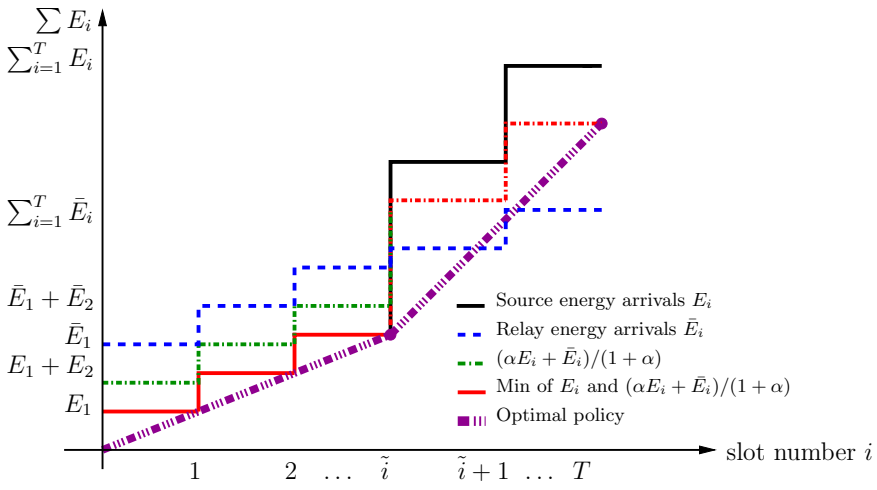

Figure 2.3: Optimal power sequence and energy transfer when the relay energy profile is higher at the beginning and lower at the end with crossing only once.

We next show that there exist $\lambda_i, \mu_i, \eta_i, \rho_i \geq 0$ that satisfy (2.5)-(2.11) and yield the solution in (2.15)-(2.16) via (2.12)-(2.14). In particular, $\rho_i = 0$ and $\eta_i = \frac{\mu_i}{\alpha}$ for $i = \tilde{i}+1, \ldots, T$. Since $\alpha \sum_{k=i}^{T} \eta_k = \sum_{k=i}^{T} \mu_k$ for all $i = \tilde{i}+1 \ldots, T$, we have from (2.12) and (2.13)

$$\bar{P}_i^* + \alpha P_i^* = \frac{1}{\sum_{k=i}^{T} \eta_k} - (1+\alpha), \quad i = \tilde{i}+1, \ldots, T \tag{2.17}$$

Hence, $\bar{P}_i^* = \frac{1}{(1+\alpha)\sum_{k=i}^{T} \eta_k} - 1$, which implies that $\lambda_T = \frac{1}{1+\alpha}$ and $\lambda_i = 0$ for $i = \tilde{i}+1, \ldots, T-1$. Moreover, $\eta_i = \frac{\mu_i}{\alpha} > 0$ whenever $\sum_{k=1}^{i} \frac{\bar{E}_k + \alpha E_k}{\alpha+1}$ is active for some $i = \tilde{i}+1, \ldots, T$. As in [6, 7], we can show that such $\eta_i = \frac{\mu_i}{\alpha}$ that yield the power sequence in (2.15)-(2.16) are uniquely found for $i = \tilde{i}+1, \ldots, T$.

It remains to find the Lagrange multipliers for $i = 1, \ldots, \tilde{i}$. We observe that $\eta_i = 0$ and $\rho_i = \sum_{k=i}^{\tilde{i}} \mu_k$ for $i = 1, \ldots, \tilde{i}$. That is, the relay power constraint is not active in the first $\tilde{i}$ slots, i.e., $\sum_{k=1}^{i} \bar{P}_k^* < \sum_{k=1}^{i} \bar{E}_k$, $i = 1, \ldots, \tilde{i}$. To justify this

claim, we note that since $P_i^* = \bar{P}_i^*$ for $i = \tilde{i}+1, \ldots, T$, we have $\sum_{i=1}^{\tilde{i}} \frac{1}{2}\log(1+P_i^*) = \sum_{i=1}^{\tilde{i}} \frac{1}{2}\log(1+\bar{P}_i^*)$. By Lemma 2.5, selecting $P_i = \bar{P}_i$ for $i = 1, \ldots, \tilde{i}$ is the minimum energy consuming policy at the relay. Since by assumption $\sum_{k=1}^{i} P_k \leq \sum_{k=1}^{i} \bar{P}_k$ for $i = 1, \ldots, \tilde{i}$, $P_i = \bar{P}_i$ is feasible and hence optimal, which in turn implies that $\sum_{k=1}^{i} \bar{P}_k^* < \sum_{k=1}^{i} \bar{E}_k$ for $i = 1, \ldots, \tilde{i}$. As a consequence, $\sum_{k=i}^{T} \eta_k = \sum_{k=\tilde{i}+1}^{T} \eta_k$, i.e., constant for all $i = 1, \ldots, \tilde{i}$. As $\bar{P}_i^* \leq \bar{P}_{\tilde{i}+1}^*$, we can specify $0 \leq \lambda_i \leq \frac{1}{1+\alpha}$ recursively, with $\lambda_i > 0$ only when $\sum_{k=1}^{i} E_k$ constraint is active, as follows

$$\lambda_i = 1 - \bar{P}_i^* \sum_{k=\tilde{i}+1}^{T} \eta_k - \sum_{k=i+1}^{T} \lambda_k \tag{2.18}$$

Moreover, $\mu_i > 0$ for slots where $\sum_{k=1}^{i} E_k$ constraint is active and $\mu_i = \frac{\sum_{k=i}^{T} \lambda_k}{P_i^*} - \sum_{k=i+1}^{T} \mu_k$. Note that if $\delta_i^* \neq 0$ for some i, the optimal source and relay power sequences are unique while there may exist infinitely many δ_i^* that yield the same optimal power levels.

A particular case covered is when only the source has energy replenishments and the relay has all its energy available initially, i.e., $\bar{E}_1 > 0$ and $\bar{E}_i = 0$ for $i > 1$. If $\bar{E}_1 > \sum_{i=1}^{T} E_i$, the relay can forward all the bits sent from the source and the optimal policy is trivial. If $\bar{E}_1 < \sum_{i=1}^{T} E_i$, the optimal policy is obtained by forming a common energy profile via energy transfer and matching the power and rate sequences. Another special case is when $\tilde{i} = 0$, i.e., when $\bar{E}_i < E_i$ for all i. In this case, $\min\{\sum_{k=1}^{i} \frac{\bar{E}_k + \alpha E_k}{\alpha+1}, \sum_{k=1}^{i} E_k\} = \sum_{k=1}^{i} \frac{\alpha \bar{E}_k + E_k}{\alpha+1}$ for all i and matching the relay and source power sequences is optimal with $\delta_i^* = E_i - \frac{\bar{E}_i + \alpha E_i}{\alpha+1}$. When $\tilde{i} = T$, we have $\bar{E}_i > E_i$, $\forall i$. The source optimizes the throughput according to $\{E_i\}_{i=1}^{T}$

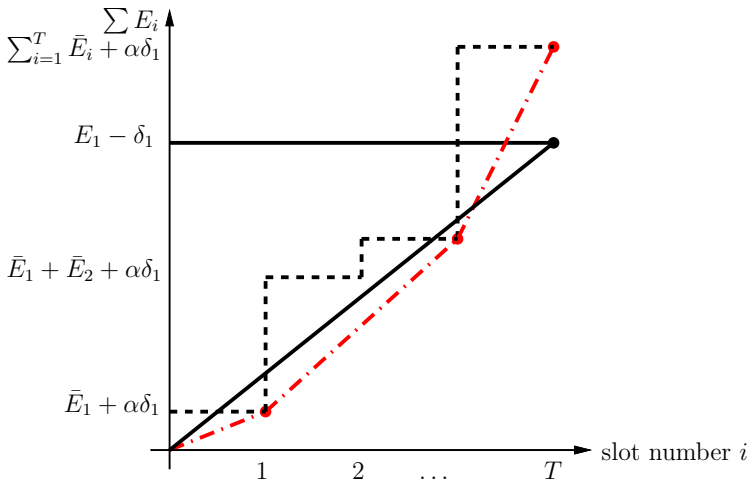

Figure 2.4: Optimal power sequences and energy transfer when the source energy is available at the beginning.

and the relay power is matched with the source.

2.3.3 Specific Scenario: Source Energy Available at the Beginning

We consider the scenario where the source has all of its energy available at the beginning (i.e., $E_1 > 0$ only), and the relay harvests energy throughout the communication. Let the relay energy profile not be satisfactory to forward the optimal source data stream which has constant rate $\frac{1}{2}\log\left(1+\frac{E_1}{T}\right)$. Assume $\delta_i \neq 0$ for some i. Since the source is not energy harvesting, the total energy of the source will then be $E_1 - \delta_i$ yielding an optimal transmission power of $\frac{E_1-\delta_i}{T}$. Hence, the throughput of the source is independent of the slot index i the energy is transferred. However, transferring the energy at slot $j < i$ can only increase the relay transmit powers after that slot; therefore, energy transfer has to be performed as early as possible, i.e., at the first slot. Hence, the jointly optimal policy is $\delta_1^* \neq 0$ and $\delta_i^* = 0$ for the remaining slots as shown in Fig. 2.4. Note that the power sequences of the source

and the relay are not matched. δ_1^* is found by solving a fixed point equation as:

$$f(\bar{E}_1 + \delta_1^*, \bar{E}_2, \ldots, \bar{E}_T) = \frac{T}{2} \log\left(1 + \frac{E_1 - \delta_1^*}{T}\right) \tag{2.19}$$

where $f(\bar{E}_1, \bar{E}_2, \ldots, \bar{E}_T)$ is the maximum number of bits corresponding to the energy arrival sequence $\bar{E}_1, \bar{E}_2, \ldots, \bar{E}_T$.

2.4 Gaussian Two-Way Channel with One-Way Energy Transfer

In this section, we consider a two-way channel as shown in Fig. 2.5. The two queues at the nodes are the data and energy queues. The energies that arrive at the nodes are saved in the corresponding energy queues. The data queues of both users always carry some data packets. The physical layer is a memoryless Gaussian two-way channel [72] where the channel inputs and outputs are x_1, x_2 and y_1, y_2, respectively. The input-output relations are $y_1 = x_1 + x_2 + n_1$ and $y_2 = x_1 + x_2 + n_2$ where n_1 and n_2 are independent Gaussian noises with zero-mean and unit-variance. In slot t, the first and second users harvest energy in amounts E_t and $\bar{E}_t$, respectively. There is a separate wireless energy transfer unit at the first user, that transfers energy from the first user to the second user with efficiency $0 \leq \alpha \leq 1$. The power policy of user 1 is composed of the sequences P_i and δ_i, and the power policy of user 2 is the sequence $\bar{P}_i$.

For the Gaussian two-way channel with individual power constraints P_1 and P_2, rate pairs (R_1, R_2) with $R_1 \leq \frac{1}{2}\log(1 + P_1), R_2 \leq \frac{1}{2}\log(1 + P_2)$ are achievable [72]. For a fixed energy transfer vector $\boldsymbol{\delta}$, and feasible power control policies $\mathbf{P}$ and

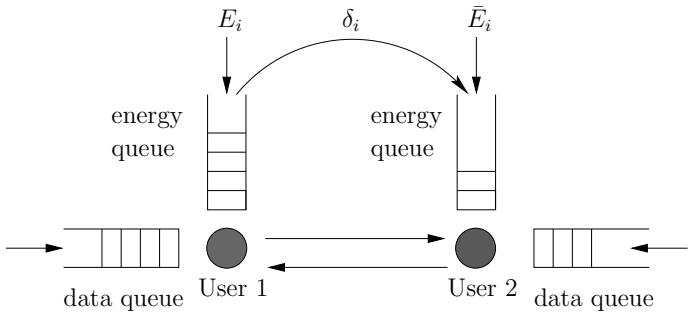

Figure 2.5: Two-way channel with one-way energy transfer.

$\bar{\mathbf{P}}$, the set of achievable rates is:

$$\mathcal{C}_{\boldsymbol{\delta}}(\mathbf{P}, \bar{\mathbf{P}}) = \left\{(R_1, R_2) : R_1 \leq \sum_{i=1}^{T} \frac{1}{2} \log\left(1 + P_i\right), \quad R_2 \leq \sum_{i=1}^{T} \frac{1}{2} \log\left(1 + \bar{P}_i\right)\right\} \quad (2.20)$$

The notation shows the dependence of the region on the energy transfer vector $\boldsymbol{\delta}$. This region is shown in Fig. 2.6 for different values of $\boldsymbol{\delta}$. Each of these regions are rectangles of the form $R_i \leq C_i$ where C_i is the maximum throughput achieved for user i found by maximizing (2.20) constrained to the feasibility constraints $\mathcal{F}$. As $\boldsymbol{\delta}$ is increased, energy is transferred from user 1 to user 2 therefore C_1 decreases while C_2 increases. By taking the union of the regions over all possible energy transfer vectors and power policies for the users, we obtain the capacity region of the Gaussian two-way channel as:

$$\mathcal{C}(\mathbf{E}, \bar{\mathbf{E}}) = \bigcup_{(\boldsymbol{\delta}, \mathbf{P}, \bar{\mathbf{P}}) \in \mathcal{F}} \mathcal{C}_{\boldsymbol{\delta}}(\mathbf{P}, \bar{\mathbf{P}}) \quad (2.21)$$

We determine the capacity region of the Gaussian two-way channel in the next section, by solving weighted rate maximization problems which trace the boundary

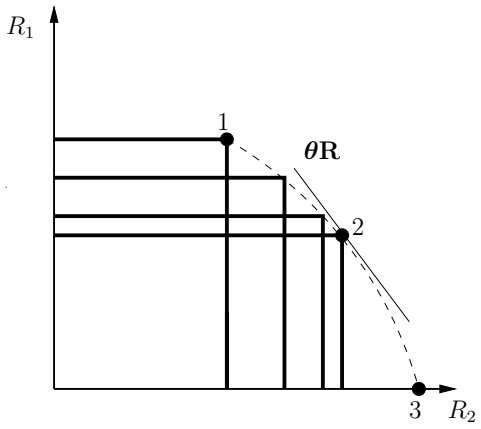

Figure 2.6: Capacity region of the Gaussian two-way channel.

of the capacity region.

2.5 Capacity Region of the Gaussian Two-Way Channel

In this section, we characterize the capacity region as well as the optimal power allocation and energy transfer policies. We start by noting that the capacity region is convex in the following lemma. The proof of this lemma is provided in Appendix 2.10.1.

Lemma 2.6 *$\mathcal{C}(\boldsymbol{E}, \bar{\boldsymbol{E}})$ is a convex region.*

Since $\mathcal{C}(\mathbf{E}, \bar{\mathbf{E}})$ is convex, each boundary point can be found by solving the following weighted rate maximization problem:

$$\begin{aligned} \max_{\bar{P}_i, P_i, \delta_i} \quad & \sum_{i=1}^{T} \theta_1 \frac{1}{2} \log\left(1 + P_i\right) + \theta_2 \frac{1}{2} \log\left(1 + \bar{P}_i\right) \\ \text{s.t.} \quad & (\boldsymbol{\delta}, \mathbf{P}, \bar{\mathbf{P}}) \in \mathcal{F} \end{aligned} \tag{2.22}$$

The problem in (2.22) is a convex optimization problem as the objective function is concave and the feasible set is a convex set [70]. We write the Lagrangian function for (2.22) as:

$$\mathcal{L} = -\sum_{i=1}^{T}\left[\theta_1 \log\left(1+P_i\right) + \theta_2 \log\left(1+\bar{P}_i\right)\right] + \sum_{k=1}^{T}\mu_k\left(\sum_{i=1}^{k} P_i - (E_i - \delta_i)\right) + \sum_{k=1}^{T}\eta_k\left(\sum_{i=1}^{k}\bar{P}_i - (\bar{E}_i + \alpha\delta_i)\right) - \sum_{k=1}^{T}\sigma_k P_k - \sum_{k=1}^{T}\psi_k\bar{P}_k - \sum_{k=1}^{T}\rho_k\delta_k \tag{2.23}$$

We note that $\bar{P}_i$ are always non-zero in the optimal policy as $\bar{E}_1 > 0$. Therefore, we have $\psi_k = 0, \forall k$. However, $P_k = 0$ may be optimal at some slots k and for some values of θ_1, θ_2 in which case $\sum_{i=1}^{k}\delta_i = \sum_{i=1}^{k} E_i$ as energy should not be wasted in an optimal policy. In the particular case of $\theta_1 = \theta_2$, $\sum_{i=1}^{k}\delta_i < \sum_{i=1}^{k} E_i, \forall k$ and $P_i > 0, \forall i$ [22]. The KKT conditions for this problem are:

$$-\frac{\theta_1}{1+P_i} + \sum_{k=i}^{T}\mu_k - \sigma_i = 0, \quad \forall i \tag{2.24}$$

$$-\frac{\theta_2}{1+\bar{P}_i} + \sum_{k=i}^{T}\eta_k = 0, \quad \forall i \tag{2.25}$$

$$\sum_{k=i}^{T}\mu_k - \alpha\sum_{k=i}^{T}\eta_k - \rho_i = 0, \quad \forall i \tag{2.26}$$

with the additional complementary slackness conditions as:

$$\mu_k\left(\sum_{i=1}^{k} P_i - (E_i - \delta_i)\right) = 0, \quad \forall k \tag{2.27}$$

$$\eta_k\left(\sum_{i=1}^{k}\bar{P}_i - (\bar{E}_i + \alpha\delta_i)\right) = 0, \quad \forall k \tag{2.28}$$

$$\rho_k \delta_k = 0, \quad \forall k \tag{2.29}$$

$$\sigma_k P_k = 0, \quad \forall k \tag{2.30}$$

From (2.24), (2.25) and (2.26) we get:

$$P_i = \left(\frac{\theta_1}{\sum_{k=i}^{T} \mu_k} - 1 \right)^+, \quad \forall i \tag{2.31}$$

$$\bar{P}_i = \frac{\theta_2}{\sum_{k=i}^{T} \eta_k} - 1, \quad \forall i \tag{2.32}$$

$$\rho_i = \sum_{k=i}^{T} \mu_k - \alpha \sum_{k=i}^{T} \eta_k, \quad \forall i \tag{2.33}$$

We will give the solution for general $\theta_1, \theta_2 > 0$ in the sequel. Before that, we note that in the extreme case when $\theta_2 = 0$, the problem reduces to maximizing the first user's throughput only and hence any energy transfer is strictly sub-optimal, i.e., $\boldsymbol{\delta} = \mathbf{0}$ is optimal. This corresponds to point 1 in Fig. 2.6. Similarly, when $\theta_1 = 0$, the problem reduces to maximizing the second user's throughput only and the first user must transfer all of its energy to the second user, i.e., $\boldsymbol{\delta} = \mathbf{E}$ is optimal. This corresponds to point 3 in Fig. 2.6. When $\theta_1, \theta_2 > 0$, we obtain the points between points 1 and 3 in Fig. 2.6. In this case, for a given energy transfer profile $\delta_1, \ldots, \delta_T$, the optimization problem can be separated into two optimization problems, each only in terms of the power control policy of the corresponding user. For fixed $\boldsymbol{\delta}$, the optimal power policies of the two users can be found by [4].

Next, we provide the necessary optimality condition for a non-zero energy transfer.

Lemma 2.7 *For the optimal power sequences $P_i^*, \bar{P}_i^*$ and energy transfer sequence δ_i^*, if $\delta_i^* \neq 0$ and $P_i^* \neq 0$ for a slot i, then*

$$\frac{1+P_i^*}{1+\bar{P}_i^*} = \frac{\theta_1}{\theta_2 \alpha} \tag{2.34}$$

Proof: From (2.31), (2.32) and (2.33), we have

$$\frac{1+P_i^*}{1+\bar{P}_i^*} = \frac{\theta_1 \sum_{k=i}^{T} \eta_k}{\theta_2(\alpha \sum_{k=i}^{T} \eta_k + \rho_i - \sigma_i)} \tag{2.35}$$

If there is a non-zero energy transfer, $\delta_i^* \neq 0$, we have from (2.29), $\rho_i = 0$ and if $P_i^* \neq 0$ we have from (2.30), $\sigma_i = 0$. Therefore, (2.34) must be satisfied if $\delta_i^* \neq 0$ and $P_i^* \neq 0$. ■

In order to devise an algorithmic solution, we apply a change of variable $\tilde{P}_i = \frac{\bar{P}_i}{\alpha}$ and re-write the optimization problem in terms of $P_i, \tilde{P}_i, \delta_i$ as follows:

$$\begin{aligned}
\max_{\tilde{P}_i, P_i, \delta_i} \quad & \sum_{i=1}^{T} \theta_1 \frac{1}{2} \log(1+P_i) + \theta_2 \frac{1}{2} \log(1+\alpha \tilde{P}_i) \\
\text{s.t.} \quad & \sum_{i=1}^{k} P_i \leq \sum_{i=1}^{k} (E_i - \delta_i), \quad \forall k \\
& \sum_{i=1}^{k} \tilde{P}_i \leq \sum_{i=1}^{k} \left(\frac{\bar{E}_i}{\alpha} + \delta_i \right), \quad \forall k \\
& P_k, \tilde{P}_k, \delta_k \geq 0, \quad \forall k
\end{aligned} \tag{2.36}$$

The optimal power allocation for this transformed problem is:

$$P_i^* = (\theta_1 \nu_i - 1)^+, \quad \forall i \tag{2.37}$$

$$\tilde{P}_i^* = \theta_2 \tilde{\nu}_i - \frac{1}{\alpha}, \quad \forall i \tag{2.38}$$

where ν_i and $\tilde{\nu}_i$ in slot i are defined by

$$\nu_i = \frac{1}{\sum_{k=i}^{T} \mu_k} \quad \text{and} \quad \tilde{\nu}_i = \frac{1}{\sum_{k=i}^{T} \eta_k} \tag{2.39}$$

The power level expressions in (2.37)-(2.38) lead to a directional water-filling interpretation [6]. In particular, we note that energy has to be jointly allocated in time and user dimensions together. This calls for a *two-dimensional directional water-filling* algorithm where energy is allowed to flow in two dimensions, from left to right (in time) and from up to down (among users). We, next, explain this algorithm.

2.5.1 Two-Dimensional Directional Water-filling Algorithm

We utilize *right permeable taps* for users to account for the energy which is saved in their individual batteries to be used in the future and *down permeable taps* to account for energy that is transferred from user 1 to user 2; see Figs. 2.7 and 2.8. The base levels for users 1 and 2 are 1 and $\frac{1}{\alpha}$, respectively, as shown in Fig. 2.7. Moreover, to facilitate the water flow interpretation, we scale the energy arrivals of user 2 by $\frac{1}{\alpha}$ as in the transformed problem (2.36). Then, we fill the scaled

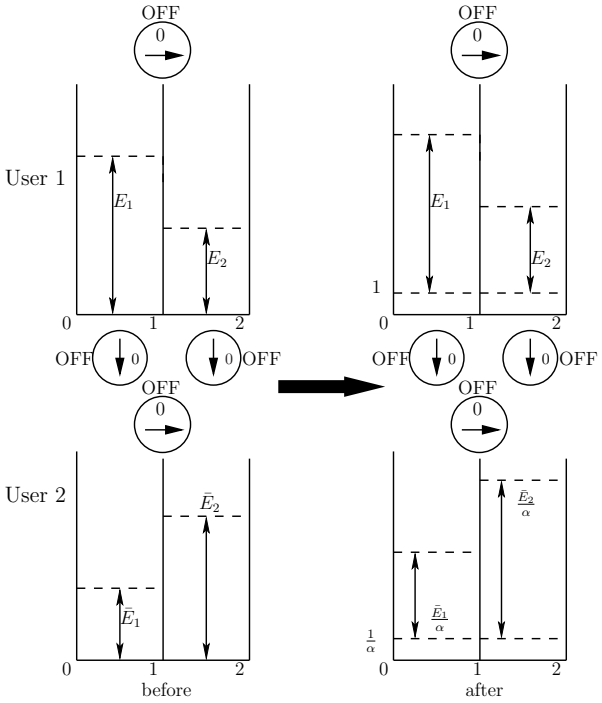

Figure 2.7: The proper scaling of the energy arrivals for a two slot system.

energies into slots to get the initial water levels. If the resulting water levels are not monotonically increasing in time for both users, then water has to flow through the horizontal taps until the levels are balanced. However, the water flow through the vertical taps follow a different rule: If water level of user 1, ν_i is higher than $\frac{\theta_1}{\theta_2}$ times the water level of user 2, $\tilde{\nu}_i$ at some slot, then water flows through the vertical taps till $\frac{\nu_i}{\tilde{\nu}_i} = \frac{\theta_1}{\theta_2}$ is satisfied. If user 1's energy is run out before this proportionality is satisfied, then the water flow stops. This follows from Lemma 2.7. Once the balanced water levels are found, P_i^* will be found from (2.37) and $\tilde{P}_i^*$ from (2.38). Then, $\bar{P}_i^* = \alpha \tilde{P}_i^*$ will give the optimal relay power allocation.

While finding the balanced water levels, the two dimensions of the water flow (i.e., in time and among users) are coupled and therefore it is not easy to determine

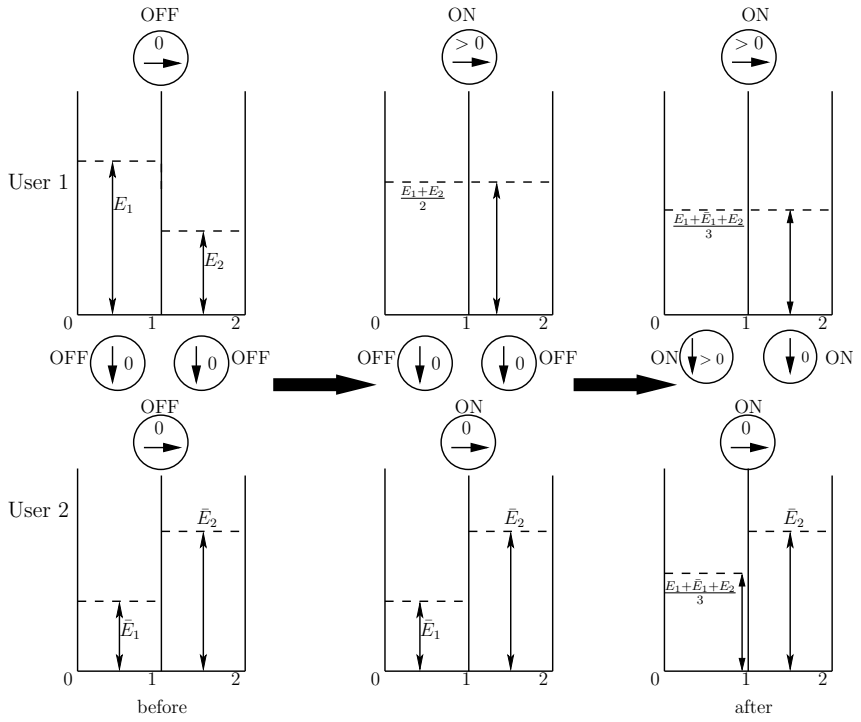

Figure 2.8: Two-dimensional directional water-filling with right/down permeable meter taps for $\theta_1 = \theta_2$ and $\alpha = 1$.

beforehand which taps will be open or closed in the optimal solution. In particular, the water flow of user 2 from time slot i to time slot $i + j$, $j > 0$, may become redundant if some energy is transferred from user 1 in time slot $i+j$. To circumvent this difficulty, we let each tap (right/down permeable) have a *meter* measuring the water that has already passed through it and we allow that tap to let the water flow back if an update in the allocation necessitates it. This way, we keep track of the source of the energy and whether it is transferred to future time slots or to the other user.

One can possibly propose many different procedures to obtain a solution for the balanced water levels and hence an optimal policy. For instance, the following particular procedure could be followed to obtain a solution: First, we fill energy

into the slots with all taps closed. Then, we open only the right permeable taps and perform directional water-filling (over time) for both users individually [6]. Then, we open the down taps one by one in a backward fashion. Water is allowed to flow from user 1 to user 2 only and only if the ratio of the water levels of user 1 and user 2 is higher than $\frac{\theta_1}{\theta_2}$. If water flows down through a tap, the amount is measured by the meter. Water levels in the slots connected by the bi-directional horizontal taps need to be equal. Whenever water flows down through a down permeable tap, the water levels must equalize in the transformed setting, or equivalently, they must satisfy the proportionality relationship in (2.34) in the original setting. When the water levels are properly balanced, the optimal solution is obtained. This procedure is depicted in Fig. 2.8 for the case of $\theta_1 = \theta_2$ and $\alpha = 1$. The advantage of this particular algorithm is that the initial temporal directional water-filling is simple and follows from [6].

The balanced water levels in the two-dimensional directional water-filling algorithm can alternatively be obtained by iteratively allowing the water to flow from a single tap at a time provided that all taps are visited infinitely often. In particular, we open only one of the horizontal and vertical taps at a time and we keep track of transferred energy in each tap by means of meters. Whenever a horizontal tap is opened, the two water levels are equalized if the directionality of the tap allows water to flow; otherwise, they are equalized to the extent possible according to the meter readings. Similarly, if a vertical tap is opened, water flows till the ratio of user 1's water level to user 2's water level equals $\frac{\theta_1}{\theta_2}$ if this ratio is higher than $\frac{\theta_1}{\theta_2}$; otherwise, this ratio is made closer to $\frac{\theta_1}{\theta_2}$ to the extent possible according to the

meter readings. This iterative algorithm is given in Algorithm 1. We note that if we go through all the possible taps sufficiently many times, our algorithm will converge to the balanced water levels and hence to an optimal solution. This is due to the fact that each iteration strictly increases the objective function in view of the strict concavity of log(.) function and that bounded real monotone sequences always converge.

An example run of the first algorithm proposed above (non-iterative) is given in Fig. 2.8 for $\theta_1 = \theta_2$ and $\alpha = 1$. Initially, we open the right permeable taps and the water levels are equalized for the first user. Then, we open the down permeable taps. In the second slot there is no need for energy transfer because $\frac{E_1+E_2}{2} < \bar{E}_2$. In the first slot there will be some non-zero energy transfer since $\frac{E_1+E_2}{2} > \bar{E}_1$, and some water flows through the first down permeable tap. Since user 1's right permeable tap has a positive meter at that point, some water is allowed to flow from right to left thereby equalizing the water levels of user 1's first and second slots and user 2's first slot.

2.5.2 A Specific Run of the Algorithm

In order to show more specifically how the algorithm runs, further explain the particular sequence of steps followed in the first two-dimensional water-filling algorithm proposed above (non-iterative), and justify the need to use metered taps to keep track of the water flow, we next provide a numerical example where $\mathbf{E} = [0, 12, 0]$ mJ, $\bar{\mathbf{E}} = [6, 6, 0]$ mJ and $\alpha = 1$. Let T_{1i}, T_{2i} denote the horizontal taps of the

Algorithm 1 Two dimensional directional water-filling (iterative algorithm)

Initialize

for $i = 1 : N$ **do**

  $U^1[i] = 1 + E_i$, $U^2[i] = \frac{1+\bar{E}_i}{\alpha}$ ▷ Fill energy into slots

end for

Define procedure

procedure WF(i, j, K, L) ▷ Water-filling from slot i to slot j, from user K to user L

  if $K = L$ **then** Tap $= T^K[i]$, $c = 1$

▷ If among the same user, the horizontal tap

  else Tap $= Q[i]$, $c = \frac{\theta_1}{\theta_2}$ ▷ Otherwise the vertical tap

  end if

  if $U^K[i] \geq cU^L[j]$ **then** ▷ If higher water level

    $t = \min\left(\frac{U^K[i]-cU^L[j]}{1+c}, U^K[i] - 1\right)$, Tap $=$ Tap $+ t$ ▷ Find water flow, update tap

    $U^K[i] = U^K[i] - t$, $U^L[j] = U^L[j] + t$

▷ Equalize water levels

  else if Tap > 0 **then** ▷ If meter is positive

    $t = \min\left(U^L[j] - \frac{1}{\alpha}, \text{Tap}, \frac{cU^L[j]-U^K[i]}{1+c}\right)$

▷ Find amount of water that can flow

    $U^K[i] = U^K[i] + t$, $U^L[j] = U^L[j] - t$

▷ Equalize as meter allows

    Tap $=$ Tap $- t$

  end if

end procedure

Main Algorithm

while diff $< \epsilon$ **do**

  for $i = 1 : N - 1$ **do**

    WF$(i, i + 1, 1, 1)$ ▷ User 1 horizontal tap

  end for

  for $i = N : 2$ **do**

    WF$(i, i, 1, 2)$ ▷ Vertical tap

    WF$(i - 1, i, 2, 2)$ ▷ User 2 horizontal tap

  end for

  $P_i = (U^1[i] - 1)^+$ and $\bar{P}_i = \alpha U^2[i] - 1$

  $\text{thr}_k = \sum_{i=1}^{T} \theta_1 \frac{1}{2} \log(1 + P_i) + \theta_2 \frac{1}{2} \log(1 + \bar{P}_i)$

  diff $= \text{thr}_k - \text{thr}_{k-1}$

  $k = k + 1$

end while

Return

$P_i^* = P_i$ and $\bar{P}_i^* = \bar{P}_i$

first and second users connecting the ith and $i+1$st slots, and let Q_i denote the ith vertical tap. The optimal solution is $\mathbf{P} = [0, 4.8, 4.8]$ and $\bar{\mathbf{P}} = [4.8, 4.8, 4.8]$, which is obtained by spreading the energy as equally as possible in two dimensions among the users and time slots, subject to energy causality. We next consider two sub-optimal orderings of tap openings.

Assume that we open the horizontal taps first and keep the vertical taps closed. This yields the transient water levels $\mathbf{P} = [0, 6, 6]$ and $\bar{\mathbf{P}} = [4, 4, 4]$. Now, if we open the vertical taps, water is transferred in the second and third slots and the balanced final levels are $\mathbf{P} = [0, 5, 5]$ and $\bar{\mathbf{P}} = [4, 5, 5]$. This profile is not optimal since the second user changes its power level when the battery is non-empty, violating [4, Lemma 2].

Now, assume that we open the vertical taps first and keep the horizontal taps closed. Energy is transferred in the second slot and the new transient water levels will be $\mathbf{P} = [0, 9, 0]$ and $\bar{\mathbf{P}} = [6, 9, 0]$. Then, when we open the horizontal taps, we will have $\mathbf{P} = [0, 4.5, 4.5]$ and $\bar{\mathbf{P}} = [5, 5, 5]$. This profile is not optimal either, as after energy transfer, the source power level is less than the relay power level, violating Lemma 2.7.

We now show how the first proposed (non-iterative) two-dimensional directional water-filling algorithm works. First, we open the horizontal taps to get $\mathbf{P} = [0, 6, 6]$ and $\bar{\mathbf{P}} = [4, 4, 4]$ with the water meters reading $[0, 6]$ and $[2, 2]$. Recall that the taps with positive meter readings allow bi-directional energy transfer. Next, we open the vertical taps in a backward fashion. Once Q_3 is opened, water flows to the second user and since T_{21}, T_{22} are bi-directional it starts to fill all the slots of the

second user. A balance is established when $\mathbf{P} = [0, 4.8, 4.8]$ and $\bar{\mathbf{P}} = [4.8, 4.8, 4.8]$, which is the optimal solution.

2.6 Multiple Access Channel with One-Way Energy Transfer

In this section, we consider the multiple access channel scenario shown in Fig. 2.9. In the multiple access channel, the received signal is $y = x_1 + x_2 + n$ where x_1 and x_2 are signals of user 1 and user 2, respectively, and n is a Gaussian noise with zero-mean and unit-variance. For the Gaussian two-user multiple access channel with individual power constraints P_1 and P_2, rate pairs (R_1, R_2) with $R_1 \leq \frac{1}{2}\log(1 + P_1), R_2 \leq \frac{1}{2}\log(1 + P_2)$, $R_1 + R_2 \leq \frac{1}{2}\log(1 + P_1 + P_2)$ are achievable [44]. For a fixed energy transfer vector $\boldsymbol{\delta}$, and feasible power control policies $\mathbf{P}$ and $\bar{\mathbf{P}}$, the set of achievable rates is a pentagon defined as [10]:

$$\begin{aligned}\mathcal{C}_{\boldsymbol{\delta}}(\mathbf{P}, \bar{\mathbf{P}}) = \Big\{(R_1, R_2) : R_1 &\leq \sum_{i=1}^{T} \frac{1}{2}\log(1 + P_i), \\ R_2 &\leq \sum_{i=1}^{T} \frac{1}{2}\log(1 + \bar{P}_i), \\ R_1 + R_2 &\leq \sum_{i=1}^{T} \frac{1}{2}\log(1 + \bar{P}_i + P_i)\Big\}\end{aligned} \tag{2.40}$$

For each feasible $(\mathbf{P}, \bar{\mathbf{P}}, \boldsymbol{\delta})$, the region is a pentagon. We obtain the capacity region by taking the union of these regions over all feasible power allocations and energy transfer profiles:

$$\mathcal{C}(\mathbf{E}, \bar{\mathbf{E}}) = \bigcup_{(\boldsymbol{\delta}, \mathbf{P}, \bar{\mathbf{P}}) \in \mathcal{F}} \mathcal{C}_{\boldsymbol{\delta}}(\mathbf{P}, \bar{\mathbf{P}}) \tag{2.41}$$

We determine the capacity region of the Gaussian multiple access channel in the next section.

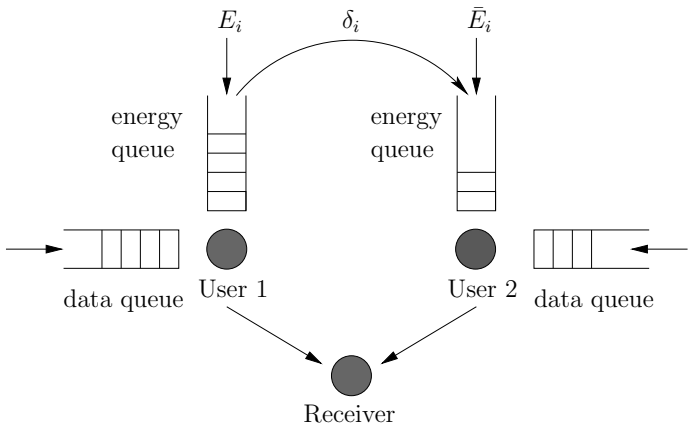

Figure 2.9: Multiple access channel with one-way energy transfer.

2.7 Capacity Region of the Gaussian Multiple Access Channel

In this section, we characterize the capacity region as well as the optimal power allocation and energy transfer policies. First, we note in the following lemma that the capacity region is convex. We prove this lemma in Appendix 2.10.2.

Lemma 2.8 *$\mathcal{C}(\boldsymbol{E}, \overline{\boldsymbol{E}})$ is a convex region.*

Since the region is convex, each boundary point is a solution to $\max_{\mathbf{R}\in\mathcal{C}^M} \boldsymbol{\theta}\mathbf{R}$ [73] for some $\boldsymbol{\theta} = [\theta_1, \theta_2]$. We examine two cases separately, $\theta_1 \geq \theta_2$ and $\theta_1 < \theta_2$.

2.7.1 $\theta_1 \geq \theta_2$

In this case, the boundary points between 1, 2 and 3 in Fig. 2.10 are found by solving the following problem:

$$\max_{\bar{P}_i,\, P_i,\, \delta_i} \sum_{i=1}^{T} (\theta_1 - \theta_2)\frac{1}{2}\log\left(1 + P_i\right) + \theta_2 \frac{1}{2}\log\left(1 + \bar{P}_i + P_i\right)$$
$$\text{s.t. } (\boldsymbol{\delta}, \mathbf{P}, \bar{\mathbf{P}}) \in \mathcal{F} \tag{2.42}$$

The problem in (2.42) is a convex optimization problem as the objective function is concave and the feasible set is a convex set [70]. We write the Lagrangian function for (2.42) as:

$$\mathcal{L} = -\sum_{i=1}^{T} \left[(\theta_1 - \theta_2)\log\left(1 + P_i\right) + \theta_2 \log\left(1 + \bar{P}_i + P_i\right)\right] + \sum_{k=1}^{T} \mu_k \left(\sum_{i=1}^{k} P_i - (E_i - \delta_i)\right)$$
$$+ \sum_{k=1}^{T} \eta_k \left(\sum_{i=1}^{k} \bar{P}_i - (\bar{E}_i + \alpha\delta_i)\right) - \sum_{k=1}^{T} \sigma_k P_k - \sum_{k=1}^{T} \psi_k \bar{P}_k - \sum_{k=1}^{T} \rho_k \delta_k \tag{2.43}$$

The KKT conditions are:

$$-\frac{\theta_1 - \theta_2}{1 + P_i} - \frac{\theta_2}{1 + P_i + \bar{P}_i} + \sum_{k=i}^{T} \mu_k - \sigma_i = 0, \quad \forall i \tag{2.44}$$

$$-\frac{\theta_2}{1 + P_i + \bar{P}_i} + \sum_{k=i}^{T} \eta_k - \psi_i = 0, \quad \forall i \tag{2.45}$$

$$\sum_{k=i}^{T} \mu_k - \alpha \sum_{k=i}^{T} \eta_k - \rho_i = 0, \quad \forall i \tag{2.46}$$

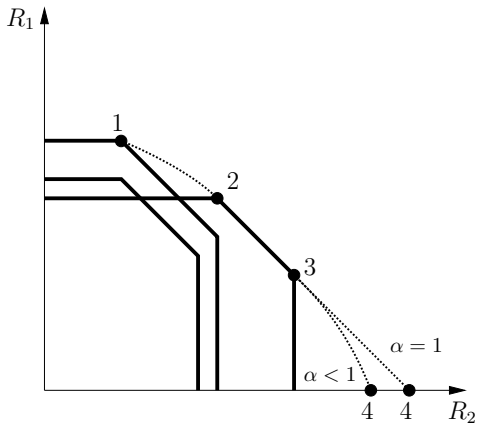

Figure 2.10: Capacity region of the Gaussian multiple access channel for $\alpha = 1$ and $\alpha < 1$.

We claim that in this case, $\delta_i = 0$, $\forall i$ is optimal. Therefore, the first user should not transfer any energy. To prove this claim, we first note that the first term in the objective function in (2.42) is a monotone concave function of P_i and the second term is a monotone concave function of $P_i + \bar{P}_i$. Assume $\delta_k > 0$ for some slot k and let $P_i, \bar{P}_i, \delta_i$ satisfy the constraints in (2.1). We first consider the case $\alpha = 1$. Now for some $0 < \epsilon \ll 1$, define a new energy transfer value in slot k as $\delta_k^{'} = \delta_k - \epsilon$, while keeping the energy transfer levels in the remaining slots unchanged. Also define new source and relay power allocations in slot k as $P_k^{'} = P_k + \epsilon, \bar{P}_k^{'} = \bar{P}_k - \epsilon$, while keeping the source and relay power levels in the remaining slots unchanged. It can be verified that this new allocation satisfies the constraints in (2.1) and $P_k^{'} + \bar{P}_k^{'} = P_k + \bar{P}_k$ together with $P_k^{'} > P_k$. This implies that by giving any transferred energy back to user 1, we can increase the objective function in (2.42). Therefore, in an optimal policy, energy transfer is not needed

for $\alpha = 1$. We note that if $\bar{P}_k^{'} = 0$, we can set $\delta_k^{'} = 0$ and $\delta_m^{'} = \delta_m + \delta_k^{'}$ where $m > k$ is the first slot after k such that $\bar{P}_m > 0$. As the transferred energy at slot k is not used at slots $k, \ldots, m-1$, the change in the energy transfer does not violate energy constraints. We can now use our construction on this modified energy transfer sequence and conclude that $\delta_k = 0$. Finally, if $k = T$ this allocation cannot be optimal since transferred energy is wasted. We conclude that if energy transfer is not needed for $\alpha = 1$, then it is also not needed for the general case of $\alpha < 1$ due to the inefficiency of wireless energy transfer. We also remark that for $\theta_2 = \theta_1$ and $\alpha = 1$, transferring no energy is sufficient but not necessary; there may exist multiple different optimal energy transfer profiles, including the one with no energy transfer.

Since energy transfer is not needed, optimal power control policies for the two users are the same as those in the energy harvesting multiple access channel with no energy transfer and can be found by the *generalized backward directional water-filling algorithm* described in [10]. That is, the capacity region boundary from point 1 to point 3 in Fig. 2.10 is found by the algorithm in [10]. Specifically, for $\theta_1 = \theta_2$, we have $\eta_k = \mu_k$ for all k and the sum-rate optimal power policies are obtained by applying single-user directional water-filling algorithm to the sum of the energy profiles of the two users [10].

2.7.2 $\theta_1 < \theta_2$

Here, we consider the remaining parts of the boundary, namely the points from point 3 to point 4 in Fig. 2.10. In this case, we need to solve the following optimization problem:

$$\begin{aligned} \max_{\bar{P}_i, P_i, \delta_i} \quad & \sum_{i=1}^{T} (\theta_2 - \theta_1) \log\left(1 + \bar{P}_i\right) + \theta_1 \log\left(1 + \bar{P}_i + P_i\right) \\ \text{s.t.} \quad & (\boldsymbol{\delta}, \bar{\mathbf{P}}, \mathbf{P}) \in \mathcal{F} \end{aligned} \tag{2.47}$$

which is a convex optimization problem and the corresponding KKT conditions are:

$$-\frac{\theta_1}{1 + P_i + \bar{P}_i} + \sum_{k=i}^{T} \mu_k - \sigma_i = 0, \quad \forall i \tag{2.48}$$

$$-\frac{\theta_2 - \theta_1}{1 + \bar{P}_i} - \frac{\theta_1}{1 + P_i + \bar{P}_i} + \sum_{k=i}^{T} \eta_k - \psi_i = 0, \quad \forall i \tag{2.49}$$

$$\sum_{k=i}^{T} \mu_k - \alpha \sum_{k=i}^{T} \eta_k - \rho_i = 0, \quad \forall i \tag{2.50}$$

We do not have an analytical closed form solution for (2.48)-(2.50). Since (2.47) is a convex optimization problem, standard numerical methods for convex optimization may be employed. We find that the solution of (2.47) has a simple form in some special cases, which we investigate next.

When $\alpha = 1$, we find that the optimal solution of (2.47) requires all the energy of user 1 transferred to user 2. To verify this fact, we use contradiction. Assume that $P_k > 0$ for some slot k. Then $\sigma_k = 0$ due to the slackness condition. Note from (2.48)-(2.49) that $\sum_{i=k}^{T} \eta_i - \psi_k > \sum_{i=k}^{T} \mu_i$, as $\theta_2 > \theta_1$. Combining this with (2.50),

we get $\psi_k + \rho_k < 0$, which is a contradiction. Thus, in the optimal solution, we must have $P_k = 0, \forall k$. Therefore, user 1 should not transmit any data, and instead should transfer all of its energy to user 2 by the end of T slots. This policy corresponds to point 4 in Fig. 2.10. On the other hand, sum-rate optimal point, point 3, achieves the same throughput as point 4. This implies that when $\alpha = 1$, points 2, 3 and 4 in Fig. 2.10 lie on the 45^o line. In particular, the optimal throughput of user 2, which is obtained by single-user throughput maximization subject to harvested energies of user 2 plus the harvested energies of user 1, coincides with the optimal sum-throughput.

When $\alpha < 1$, points 3 and 4 in Fig. 2.10 are not on the same line. We observe that when $\frac{\theta_2}{\theta_1}$ is sufficiently large, user 1 transfers all of its energy to user 2. In order to verify this claim, we note that, if user 1 transfers some but not all of its energy at the end of T slots, then $P_T > 0$ and $\sigma_T = 0$. In this case, from (2.48)-(2.50) and as $\rho_T \geq 0$, we have

$$\frac{1 + \bar{P}_T}{1 + \bar{P}_T + P_T} \geq \frac{\alpha(\theta_2 - \theta_1)}{(1-\alpha)\theta_1} \tag{2.51}$$

Since $\frac{1+\bar{P}_T}{1+\bar{P}_T+P_T} < 1$, we conclude that if $\frac{\alpha(\theta_2-\theta_1)}{(1-\alpha)\theta_1} \geq 1$, then (2.51) cannot be satisfied which forces all of the energy of user 1 to be transferred to user 2 so that $\sigma_T > 0$. Note that $\frac{\alpha(\theta_2-\theta_1)}{(1-\alpha)\theta_1} \geq 1$ is equivalent to $\frac{\theta_2}{\theta_1} \geq \frac{1}{\alpha}$. Hence, if $\frac{\theta_2}{\theta_1} \geq \frac{1}{\alpha}$, in the optimal solution, user 1 transfers all of its energy to user 2. This implies that the capacity region boundary intersects the horizontal line in Fig. 2.10 with slope less than or equal to $\frac{1}{\alpha}$.

2.8 Numerical Results

In this section, we provide numerical examples for studied multi-user settings and illustrate the resulting optimal policies. In all examples, we assume that the slot length is 1 second, noise spectral density is $N_0 = 10^{-19}$ W/Hz and the available bandwidth is 1 MHz.

2.8.1 Numerical Example for the Gaussian Two-Hop Relay Channel

We first consider the two-hop relay channel with energy harvesting and energy transfer in Section 2.2. In our first numerical study, the source and the relay have the energy arrival profiles $\mathbf{E} = [2; 3; 5; 4]$ mJ and $\bar{\mathbf{E}} = [5; 1; 2; 1]$ mJ, respectively, and the wireless energy transfer efficiency is $\alpha = 0.5$. We note that for these energy harvesting profiles the relay energy profile is higher at the beginning and lower at the end with crossing only once in the third slot. Therefore, the resulting optimal rate profiles are matched in the optimal policy. An optimal energy transfer vector is $\boldsymbol{\delta} = [0; 0; 1.33; 3.33]$ mJ and the resulting optimal power allocation vectors after the energy transfer are $\bar{\mathbf{P}} = \mathbf{P} = [2; 3; 4; 6.33]$ mW. We note that while the optimal energy transfer profile is not unique, resulting optimal powers are unique.

Next, we change the energy arrival profiles for the source and the relay as $\mathbf{E} = [12; 0; 0; 0]$ mJ and $\bar{\mathbf{E}} = [5; 1; 0; 2]$ mJ, respectively, with energy transfer efficiency $\alpha = 0.5$. Note that the source node is not energy harvesting. In this case, we find the optimal energy transfer vector as $\boldsymbol{\delta} = [2.67; 0; 0; 0]$ mJ and the resulting optimal power vectors are $\bar{\mathbf{P}} = \mathbf{P} = [2.33; 2.33; 2.33; 2.33]$ mW. Note that the optimal power

sequences for the source and the relay match in this specific example, which does not hold in general.

2.8.2 Numerical Example for the Gaussian Two-Way Channel

In this section, we consider the Gaussian two-way channel model in Section 2.4. The energy arrival profiles of user 1 and user 2 are $\mathbf{E} = [5; 10; 5]$ mJ and $\bar{\mathbf{E}} = [2; 1; 1]$ mJ, respectively, and the wireless energy transfer efficiency is set to $\alpha = 0.7$. Path loss of each link is set to 10 dB. We found the capacity region by running the two-dimensional directional water-filling algorithm for all $\theta_1, \theta_2 \geq 0$. We plot the resulting capacity region in Fig. 2.11, where we also plot the capacity region when energy transfer is not allowed. Note that when energy transfer is not allowed, the capacity region is the rectangle with single-user optimal rates subject to the individual energy arrivals. We observe that the availability of wireless energy transfer significantly improves the capacity region.

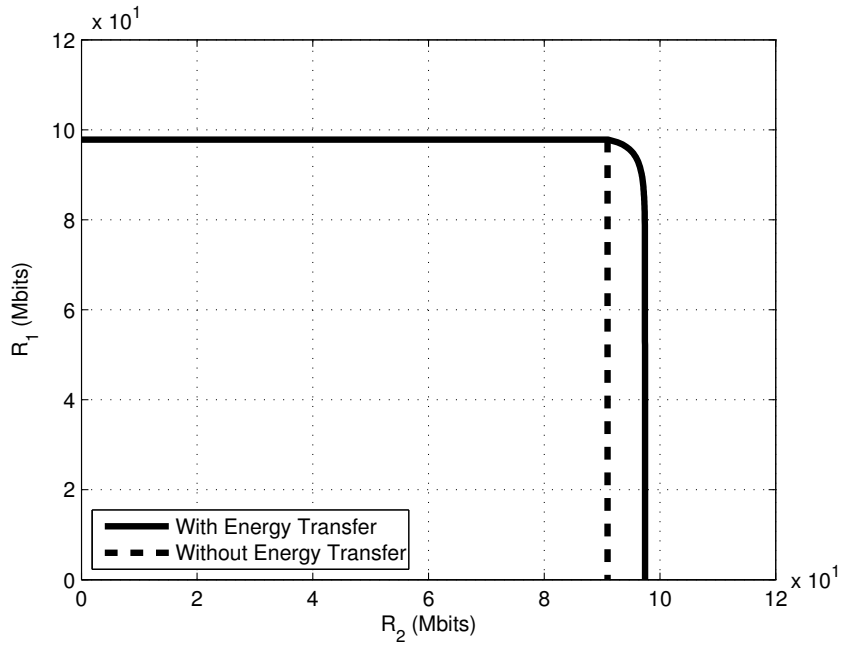

Figure 2.11: Capacity region of the two-way channel with energy transfer.

2.8.3 Numerical Example for the Gaussian Multiple Access Channel

In this section, we consider the Gaussian multiple access channel model in Section 2.6. The energy arrival profiles of user 1 and user 2 are $\mathbf{E} = [5; 2; 5]$ mJ and $\bar{\mathbf{E}} = [1; 3; 1]$ mJ, respectively, and wireless energy transfer efficiency is $\alpha = 0.5$. The path loss in user 1 to user 2 channel is set to 10dB, while user 1 to receiver and user 2 to receiver links have 100dB path losses. We plot the resulting capacity region in Fig. 2.12 and we compare it with the region when no energy transfer is allowed. Note that when no energy transfer is allowed, the region is found by the backward directional water-filling algorithm in [10]. We observe in Fig. 2.12 that the boundary of the capacity regions when energy transfer is allowed and not allowed match when

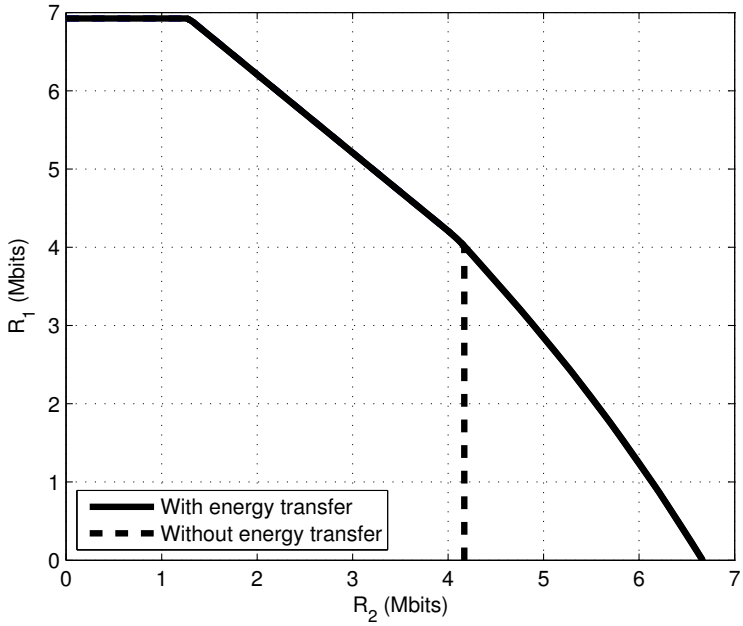

Figure 2.12: Capacity region of the multiple access channel with energy transfer.

the priority of user 1 is higher than the priority of user 2. However, the availability of wireless energy transfer significantly improves the capacity region when priority of user 2 is higher than the priority of user 1.

2.9 Concluding Remarks

Energy cooperation made possible by wireless energy transfer is a fundamental shift in terms of the energy dynamics of a wireless network, yielding new performance limits. In this chapter, we studied the communication performance of simple two- and three-node wireless networks in a deterministic setting where nodes harvest energy from the environment and wireless energy transfer is possible from one user to another in one-way and with efficiency α. We first considered the Gaussian two-

hop relay channel and studied the end-to-end throughput maximization problem. We showed that if the relay energy profile is higher first and then lower, the rates of the source and the relay nodes need to be matched in the optimal policy. We also showed that if the source is not energy harvesting, then transferring energy in the first slot is optimal. Next, we studied the capacity region of the Gaussian two-way channel. We showed that the boundary of the capacity region is achieved by policies that are given by a generalized version of two-dimensional directional water-filling algorithm. Finally, we studied the Gaussian multiple access channel. We showed that no energy transfer is needed if the priority of the first user is higher, and all of the energy needs to be transferred to the second user if the priority of the second user is sufficiently high. These results reveal new insights on how energy is optimally allocated in multi-user scenarios when wireless energy transfer is available as a new degree of freedom in network design. We remark that the analysis for finding the optimal policies in each multi-user setting can be extended for the cases when bi-directional energy transfer is allowed. In the two-hop relay setting, if bi-directional energy transfer is allowed, perfectly matching the energy profiles of the source and the relay nodes would be feasible and hence optimal: In this case, we collect energy arrivals of the source and the relay in a single energy queue and perform a single-user optimization. We then divide resulting power allocation equally for the source and the relay. Similarly, [56] recently presented the extension of the analysis for two-way and multiple access channels when bi-directional energy transfer is allowed.

2.10 Appendices

2.10.1 Proof of Lemma 2.6

Consider two feasible power policies and energy transfer profiles $(\mathbf{P}_1, \bar{\mathbf{P}}_1, \boldsymbol{\delta}_1)$ and $(\mathbf{P}_2, \bar{\mathbf{P}}_2, \boldsymbol{\delta}_2)$. Let us consider a new policy as a convex combination of these two policies, i.e., $(\mathbf{P_3}, \bar{\mathbf{P}}_\mathbf{3}, \boldsymbol{\delta}_3) = \lambda(\mathbf{P}_1, \bar{\mathbf{P}}_1, \boldsymbol{\delta}_1) + (1-\lambda)(\mathbf{P}_2, \bar{\mathbf{P}}_2, \boldsymbol{\delta}_2)$ for $0 < \lambda < 1$. First we show that this new policy is feasible:

$$\sum_{i=1}^{k} P_{3i} = \sum_{i=1}^{k} \lambda P_{1i} + (1-\lambda) P_{2i} \tag{2.52}$$

$$\leq \lambda \sum_{i=1}^{k} (E_i - \delta_{1i}) + (1-\lambda) \sum_{i=1}^{k} (E_i - \delta_{2i}) \tag{2.53}$$

$$= \sum_{i=1}^{k} (E_i - \delta_{3i}), \quad k = 1, \ldots, T \tag{2.54}$$

We use similar arguments for $\bar{P}_{3i}, \delta_{3i}$ and show that the policy $(\mathbf{P_3}, \bar{\mathbf{P}}_\mathbf{3}, \boldsymbol{\delta}_3)$ is feasible.

Now, consider the upper corner points of the achievable rate regions for $(\mathbf{P}_1, \bar{\mathbf{P}}_1, \boldsymbol{\delta}_1)$ and $(\mathbf{P}_2, \bar{\mathbf{P}}_2, \boldsymbol{\delta}_2)$. Since $\log(1+p)$ is concave in p, we have

$$\sum_{i=1}^{T} \log(1 + P_{3i}) > \sum_{i=1}^{T} \lambda \log(1 + P_{1i}) + (1-\lambda) \sum_{i=1}^{T} \log(1 + P_{2i}) \tag{2.55}$$

$$\sum_{i=1}^{T} \log(1 + \bar{P}_{3i}) > \sum_{i=1}^{T} \lambda \log(1 + \bar{P}_{1i}) + (1-\lambda) \sum_{i=1}^{T} \log(1 + \bar{P}_{2i}) \tag{2.56}$$

This means that the new policy $(\mathbf{P_3}, \bar{\mathbf{P}}_\mathbf{3}, \boldsymbol{\delta}_3)$ achieves a higher throughput for both users than the line connecting the two upper corner points under policies $(\mathbf{P}_1, \bar{\mathbf{P}}_1, \boldsymbol{\delta}_1)$ and $(\mathbf{P}_2, \bar{\mathbf{P}}_2, \boldsymbol{\delta}_2)$. Therefore, the region $\mathcal{C}(\mathbf{E}, \bar{\mathbf{E}})$ is a convex region.

2.10.2 Proof of Lemma 2.8

Consider two feasible power policies and energy transfer profiles $(\mathbf{P}_1, \bar{\mathbf{P}}_1, \boldsymbol{\delta}_1)$ and $(\mathbf{P}_2, \bar{\mathbf{P}}_2, \boldsymbol{\delta}_2)$. Let us consider a new policy as a convex combination of these two policies, i.e., $(\mathbf{P_3}, \bar{\mathbf{P}}_\mathbf{3}, \boldsymbol{\delta}_3) = \lambda(\mathbf{P}_1, \bar{\mathbf{P}}_1, \boldsymbol{\delta}_1) + (1-\lambda)(\mathbf{P}_2, \bar{\mathbf{P}}_2, \boldsymbol{\delta}_2)$ for $0 < \lambda < 1$. Since the constraints in set $\mathcal{F}$ are linear in the power vectors, it can be shown as in the proof of Lemma 2.6 in Appendix 2.10.1 that this new policy is feasible.

Now, let S_i be the pentagon created by the policy $(\mathbf{P}_i, \bar{\mathbf{P}}_i, \boldsymbol{\delta}_i)$, for $i = 1, 2, 3$. Choose $\boldsymbol{t}_1 \in S_1$ and $\boldsymbol{t}_2 \in S_2$ to form $\boldsymbol{t}_3 = \lambda \boldsymbol{t}_1 + (1-\lambda)\boldsymbol{t}_2$ for $0 \leq \lambda \leq 1$. We need to show that $\boldsymbol{t}_3 \in S_3$. We proceed as follows:

$$t_{31} = \lambda t_{11} + (1-\lambda) t_{21} \tag{2.57}$$

$$\leq \lambda \sum_{i=1}^{T} \log(1 + P_{1i}) + (1-\lambda) \sum_{i=1}^{T} \log(1 + P_{2i}) \tag{2.58}$$

$$\leq \sum_{i=1}^{T} \log(1 + \lambda P_{1i} + (1-\lambda) P_{2i}) \tag{2.59}$$

$$= \sum_{i=1}^{T} \log(1 + P_{3i}) \tag{2.60}$$

Similarly, we show $t_{32} \leq \sum_{i=1}^{T} \log(1 + \bar{P}_{3i})$. Finally

$$t_{31} + t_{32} = \lambda(t_{11} + t_{21}) + (1-\lambda)(t_{21} + t_{22}) \tag{2.61}$$

$$\leq \lambda \sum_{i=1}^{T} \log(1 + P_{1i} + \bar{P}_{1i}) + (1-\lambda) \sum_{i=1}^{T} \log(1 + P_{2i} + \bar{P}_{2i}) \tag{2.62}$$

$$\leq \sum_{i=1}^{T} \log\left(1 + \lambda(P_{1i} + \bar{P}_{1i}) + (1-\lambda)(P_{2i} + \bar{P}_{2i})\right) \tag{2.63}$$

$$= \sum_{i=1}^{T} \log(1 + P_{3i} + \bar{P}_{3i}) \tag{2.64}$$

These inequalities show that $\boldsymbol{t}_3 \in S_3$ since it satisfies the boundary conditions of S_3. Therefore, the region $\mathcal{C}(\mathbf{E}, \bar{\mathbf{E}})$ is a convex region.

CHAPTER 3

Optimal Energy and Data Routing in Networks with Energy Cooperation

3.1 Introduction

In this chapter, we consider an energy harvesting communication network with energy cooperation as shown in Fig. 3.1. We focus on the delay minimization problem for this network. We consider the joint data routing and capacity assignment problem for this setting under fixed data and energy routing topologies [43, Section 5.4.2]. We divide our development in this chapter into three parts. In the first part, we assume that the data flows through the links are fixed, and each node harvests energy only once. In this setting, we determine the optimum energies allocated to outgoing data links of the nodes and the optimum amounts of energies transferred between the nodes. In the second part, we extend this setting to the case of multiple energy harvests for each node. In the last part, we optimize both data flows on the links and energy management at the nodes. We determine the jointly optimal routing of data and energy in the network as well as distribution of power over the outgoing data links at each node.

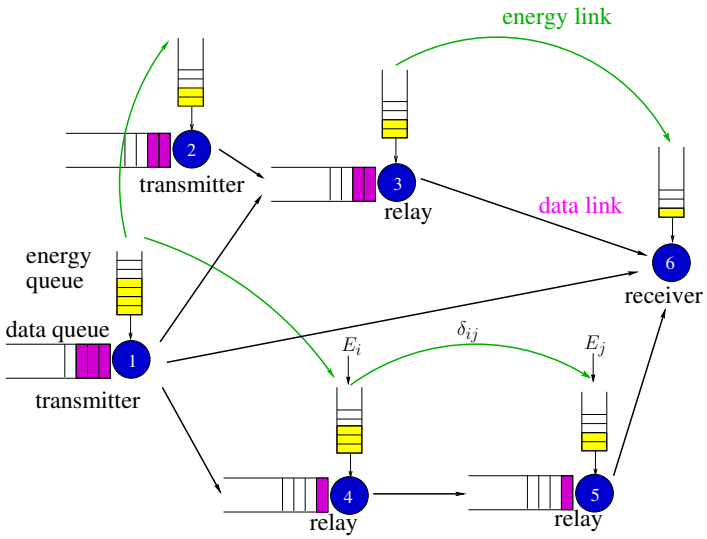

Figure 3.1: System model.

In the first part of the chapter, in Section 3.3, we focus on the optimal energy management problem at the nodes with a single energy harvest at each node. First, we consider the case without energy cooperation. We show that this problem can be decomposed into individual problems, each one to be solved for a single node. We show that more power should be allocated to links with more noise and/or more data flow, resembling channel inversion type of power control [74]. Next, we consider the case with energy cooperation, where nodes transfer a portion of their own energies to neighboring nodes. In this case, we have the joint problem of energy routing among the network nodes and energy allocation among the outgoing data links at each node. For this problem, we develop an iterative algorithm that visits all energy links sufficiently many times and decreases the network delay monotonically. We numerically observe that energy flows from nodes with lightly loaded data links to nodes with heavily loaded data links.

In the second part of the chapter, in Section 3.4, we extend our setting to the case of multiple energy harvests at each node, by allowing time-varying energy harvesting rates over large time frames. We incorporate the time variation in the energy harvests and solve for the optimal energy management at each node and energy routing among the nodes. First, we focus on the case without energy cooperation. We show that the sum powers on the outgoing data links of a node over time slots is equal to the single-link optimal transmit power of that node over time and can be found using [4–6]. When the optimal sum powers are known, we show that the problem reduces to a problem with a single energy arrival and can be solved using our method. Next, we focus on the case with energy cooperation. We show that this problem can be mapped to the original problem with no energy cooperation by constructing an equivalent directed graph.

In the last part of the chapter, in Section 3.5, we consider the problem of determining the jointly optimal data and energy flows in the network and the power distribution over the outgoing data links at all nodes. We determine a set of necessary conditions for the joint optimality of a power control, energy transfer and data routing policy. We then develop an iterative algorithm that updates the data flows, energy flows and distribution of power over the outgoing data links at each node in a sequential manner. We show that this algorithm converges to a Pareto-optimal operating point.

3.2 Network Flow and Energy Model

We use directed graphs to represent the network topology, and data and energy flows through the network. All nodes are energy harvesting, and are equipped with separate wireless energy transfer units. Information and energy transfer channels are orthogonal to each other.

3.2.1 Network Data Topology

We represent the data topology of the network by a directed graph. In this model, a collection of nodes, labeled $n = 1, \ldots, N$, can send and receive data across communication links.In particular, a node can be either a source node, a destination node or a relay node. A data communication link is represented as an ordered pair (i, j) of distinct nodes. The presence of a link (i, j) means that the network is able to send data from the start node i to the end node j. We label the data links as $l = 1, \ldots, L$. The network data topology can be represented by an $N \times L$ matrix, $\mathbf{A}$, in which every entry A_{nl} is associated with node n and link l via

$$A_{nl} = \begin{cases} 1, & \text{if } n \text{ is the start node of data link } l \\ -1, & \text{if } n \text{ is the end node of data link } l \\ 0, & \text{otherwise} \end{cases} \tag{3.1}$$

We define $\mathcal{O}_d(n)$ as the set of outgoing data links from node n, and $\mathcal{I}_d(n)$ as the set of incoming data links to node n. We define N-dimensional vector $\mathbf{s}$ whose

nth entry s_n denotes the non-negative amount of exogenous data flow injected into the network at node n. On each data link l, we let t_l denote the amount of flow and we call the L-dimensional vector $\mathbf{t}$ the flow vector. At each node n, the flow conservation implies:

$$\sum_{l \in \mathcal{O}_d(n)} t_l - \sum_{l \in \mathcal{I}_d(n)} t_l = s_n, \quad \forall n \tag{3.2}$$

The flow conservation law over all the network can be compactly written as:

$$\mathbf{At} = \mathbf{s} \tag{3.3}$$

We define c_l as the information carrying capacity of link l. Then, we require $t_l \leq c_l$, $\forall l$.

3.2.2 Network Energy Topology

All nodes are equipped with energy harvesting units. In this section, we describe the energy model for the case of a single energy harvest per node. We present the extension to the case of multiple energy harvests in Section 3.4. Here, each node n harvests energy in the amount of E_n. We use N-dimensional vector $\mathbf{E}$ to denote the energy arrival vector for the system. In the energy cooperation setting, there are energy links similar to data links. An energy link is represented as an ordered pair (i, j) of distinct nodes where the presence of an energy link means that it is possible to send energy from the start node to the end node. Energy links are

labeled as $q = 1, \ldots, Q$. Energy transfer efficiency on each energy link is denoted with $0 < \alpha_q \leq 1$ which means that when δ amount of energy is transferred on link q from node i to node j, node j receives $\alpha_q \delta$ amount of energy. We assume that the directionality and the position of energy transfer links are fixed whereas the amount of energy transferred on these links are unknown. The network energy topology can be represented by an $N \times Q$ matrix, $\mathbf{B}$, in which every entry B_{nq} is associated with node n and energy link q via

$$B_{nq} = \begin{cases} 1, & \text{if } n \text{ is the start node of energy link } q \\ -\alpha_q, & \text{if } n \text{ is the end node of energy link } q \\ 0, & \text{otherwise} \end{cases} \tag{3.4}$$

On each energy link q, we let y_q be the amount of energy transferred. We call the L-dimensional vector $\mathbf{y}$ the energy flow vector. We denote by $\mathcal{O}_e(n)$ and $\mathcal{I}_e(n)$, respectively, the sets of outgoing and incoming energy links at node n.

3.2.3 Communication Model and Delay Assumptions

Following the M/M/1 queueing model in [43], we represent the delay on data link l as:

$$D_l = \frac{t_l}{c_l - t_l} \tag{3.5}$$

where t_l is the flow and c_l is the information carrying capacity of link l, with $t_l \leq c_l, \forall l$. This delay expression is a good approximation for systems with Poisson arrivals at the entry points, exponential packet lengths and moderate-to-heavy traffic loads [43]. In view of energy scarcity in the network, moderate-to-heavy traffic load assumption generally holds. The packet arrival and packet length assumptions are made for convenience of analysis. Moreover, we assume that the slot length is sufficiently large to enable convergence to stationary distributions. In particular, we assume that the slot length is sufficiently longer than the average delay yielded by the M/M/1 approximation. Each node n, on the transmitting edge of data link l, with channel noise σ_l, enables a capacity c_l by expanding power p_l. These quantities are related by the Shannon formula [44, eqn. (9.60)] as:

$$c_l = \frac{1}{2} \log \left(1 + \frac{p_l}{\sigma_l} \right) \tag{3.6}$$

where all logs in this chapter are with respect to base e. At each node n, the total power expanded on data and energy links are constrained by the available energy, i.e.,

$$\sum_{l \in \mathcal{O}_d(n)} p_l + \sum_{q \in \mathcal{O}_e(n)} y_q \leq E_n + \sum_{q \in \mathcal{I}_e(n)} \alpha_q y_q, \quad \forall n \tag{3.7}$$

Using L-dimensional vector $\mathbf{p} = (p_1, \ldots, p_L)$ and $\mathbf{F} = \mathbf{A}^+$ where $(A^+)_{nl} = \max\{A_{nl}, 0\}$, the energy availability constraints can be compactly written as:

$$\mathbf{Fp} + \mathbf{By} \leq \mathbf{E} \tag{3.8}$$

We note that we use power and energy interchangeably in (3.8) and in the rest of the chapter by assuming slot lengths of 1 unit.

3.3 Capacity Assignment Problem for Single Time Slot

In this section, we consider the capacity assignment problem for the case of a single energy harvest per node. We assume that the flow assignments, t_l, on all links are fixed and are serviceable by the harvested energies and energy transfers. The total delay in the network is:

$$D = \sum_l \frac{t_l}{c_l - t_l} \tag{3.9}$$

The capacity assignment problem, with the goal of minimizing the total delay in the network is:

$$\begin{aligned} \min_{c_l, p_l, y_q} \quad & \sum_l \frac{t_l}{c_l - t_l} \\ \text{s.t.} \quad & \mathbf{Fp} + \mathbf{By} \leq \mathbf{E} \\ & t_l \leq c_l, \quad \forall l \end{aligned} \tag{3.10}$$

By using the capacities c_l in (3.6), we write the problem in terms of the link powers p_l and energy transfers y_q only as:

$$\begin{aligned} \min_{p_l, y_q} \quad & \sum_l \frac{t_l}{\frac{1}{2}\log\left(1+\frac{p_l}{\sigma_l}\right) - t_l} \\ \text{s.t.} \quad & \mathbf{Fp} + \mathbf{By} \leq \mathbf{E} \\ & p_l \geq \sigma_l \left(e^{2t_l} - 1\right), \quad \forall l \end{aligned} \tag{3.11}$$

We solve the problem in (3.11) in the rest of this section. We first identify some structural properties of the optimal solution in the next sub-section. The following analysis relies on the standing assumption that this problem has at least one feasible solution. To see if this problem is feasible, one can replace the objective function of (3.11) with a constant and solve a feasibility problem, which turns out to be a linear program.

3.3.1 Properties of the Optimal Solution

First, we note that the objective function can be written in the form $\sum_i f_i(g(x_i))$ where $f_i(x_i) = \frac{t_i}{x_i - t_i}$ and $g(x_i) = \frac{1}{2}\log(1+x_i)$. Since f is convex and non-increasing and g is concave, the resulting composition function is convex [70]. The constraint set is affine. Therefore, (3.11) is a convex optimization problem. The Lagrangian function is:

$$\mathcal{L} = \sum_l \frac{t_l}{\frac{1}{2}\log\left(1+\frac{p_l}{\sigma_l}\right) - t_l} + \sum_n \lambda_n \left[\sum_{l \in \mathcal{O}_d(n)} p_l + \sum_{q \in \mathcal{O}_e(n)} y_q - E_n - \sum_{q \in \mathcal{I}_e(n)} \alpha_q y_q \right]$$

$$- \sum_{l} \beta_l \left[p_l - \sigma_l \left(e^{2t_l} - 1 \right) \right] - \sum_{q} \theta_q y_q \tag{3.12}$$

where λ_n and β_l are Lagrange multipliers corresponding to the energy constraints of the nodes in (3.8) and the feasibility constraints $t_l \leq c_l$, respectively. The KKT optimality conditions are:

$$h_l'(p_l) + \lambda_{n(l)} - \beta_l = 0, \quad \forall l \tag{3.13}$$

$$\lambda_{m(q)} - \alpha_q \lambda_{k(q)} - \theta_q = 0, \quad \forall q \tag{3.14}$$

where $h_l(p_l) \triangleq t_l \left(\frac{1}{2} \log \left(1 + \frac{p_l}{\sigma_l} \right) - t_l \right)^{-1}$, $n(l)$ is the beginning node of data link l, $m(q)$ and $k(q)$ are the beginning and end nodes of energy link q, respectively. The additional complementary slackness conditions are:

$$\lambda_n \left(\sum_{l \in \mathcal{O}_d(n)} p_l + \sum_{q \in \mathcal{O}_e(n)} y_q - E_n - \sum_{q \in \mathcal{I}_e(n)} \alpha_q y_q \right) = 0, \, \forall n \tag{3.15}$$

$$\beta_l \left[p_l - \sigma_l \left(e^{2t_l} - 1 \right) \right] = 0, \quad \forall l \tag{3.16}$$

$$\theta_q y_q = 0, \quad \forall q \tag{3.17}$$

We now identify some properties of the optimal power allocation in the following three lemmas.

Lemma 3.1 *If the problem in (3.11) is feasible, then* $\beta_l = 0, \forall l$.

Proof: If the problem in (3.11) is feasible, its objective function must be bounded. Equality in the second set of constraints in (3.11) for any l implies that the objective

function is unbounded. Therefore, we must have strict inequality in those constraints for all l, and from (3.16), we conclude that $\beta_l = 0, \forall l$. ■

Lemma 3.2 *At every node n, the optimal power allocation amongst outgoing data links satisfies*

$$h_l'(p_l) = h_m'(p_m), \quad \forall l, m \in \mathcal{O}_d(n) \tag{3.18}$$

Proof: From (3.13) and Lemma 3.1 we have,

$$h_l'(p_l) = -\lambda_{n(l)}, \quad \forall l \tag{3.19}$$

For outgoing data links l and m that belong to the same node n,

$$h_l'(p_l) = -\lambda_n = h_m'(p_m) \tag{3.20}$$

which gives the desired result. ■

Lemma 3.3 *If some energy is transferred through energy link q across nodes (i, j), then,*

$$h_l'(p_l) = \alpha_q h_m'(p_m), \quad \forall l \in \mathcal{O}_d(i), \forall m \in \mathcal{O}_d(j) \tag{3.21}$$

Proof: If some energy is transferred through energy link q, then $y_q > 0$, and from

(3.17), $\theta_q = 0$. From (3.14), we have,

$$\lambda_i = \alpha_q \lambda_j \tag{3.22}$$

Writing (3.13) for nodes i and j, we have,

$$h_l'(p_l) = -\lambda_i, \quad \forall l \in \mathcal{O}_d(i) \tag{3.23}$$

$$h_m'(p_m) = -\lambda_j, \quad \forall m \in \mathcal{O}_d(j) \tag{3.24}$$

and the result follows from combining (3.22), (3.23) and (3.24). ■

In the following two sub-sections, we separately solve the problem for the cases of no energy transfer and with energy transfer.

3.3.2 Solution for the Case of No Energy Transfer

In the case of no energy transfer, we have $y_q = 0$, $\forall q$, and the problem becomes only in terms of p_l as stated below:

$$\begin{aligned} \min_{p_l} \quad & \sum_l \frac{t_l}{\frac{1}{2}\log\left(1+\frac{p_l}{\sigma_l}\right) - t_l} \\ \text{s.t.} \quad & \sum_{l \in \mathcal{O}_d(n)} p_l \leq E_n, \quad \forall n \\ & p_l \geq \sigma_l \left(e^{2t_l} - 1\right), \quad \forall l \end{aligned} \tag{3.25}$$

This problem can be decomposed into N sub-problems as:

$$\begin{aligned} \min_{p_l} \quad & \sum_{n} \sum_{l \in \mathcal{O}_d(n)} \frac{t_l}{\frac{1}{2}\log\left(1+\frac{p_l}{\sigma_l}\right) - t_l} \\ \text{s.t.} \quad & \sum_{l \in \mathcal{O}_d(n)} p_l \leq E_n, \quad \forall n \\ & p_l \geq \sigma_l(e^{2t_l}-1), \quad \forall l \end{aligned} \tag{3.26}$$

Since the constraint set depends only on the powers of node n, there is no interaction between the nodes. Every node will independently solve the following optimization problem:

$$\begin{aligned} \min_{p_l} \quad & \sum_{l \in \mathcal{O}_d(n)} \frac{t_l}{\frac{1}{2}\log\left(1+\frac{p_l}{\sigma_l}\right) - t_l} \\ \text{s.t.} \quad & \sum_{l \in \mathcal{O}_d(n)} p_l \leq E_n \\ & p_l \geq \sigma_l\left(e^{2t_l}-1\right), \quad \forall l \in \mathcal{O}_d(n) \end{aligned} \tag{3.27}$$

The feasibility of (3.27) requires $E_n \geq \sum_{l \in \mathcal{O}_d(n)} \sigma_l(e^{2t_l}-1)$ which we assume holds. Similar to (3.11), (3.27) is a convex optimization problem with the KKT optimality conditions:

$$h_l'(p_l) + \lambda = 0, \quad \forall l \in \mathcal{O}_d(n) \tag{3.28}$$

with the complementary slackness condition:

$$\lambda \left(\sum_{l \in \mathcal{O}_d(n)} p_l - E_n \right) = 0 \tag{3.29}$$

The Lagrange multipliers for the second set of constraints in (3.27) are not included, because similar to Lemma 3.1, they will always be satisfied with strict inequality. From (3.28), we have

$$-\lambda = h_l'(p_l) \tag{3.30}$$

$$= \frac{-t_l}{2\sigma_l} \left[\frac{1}{2} \log \left(1 + \frac{p_l}{\sigma_l} \right) - t_l \right]^{-2} \left(1 + \frac{p_l}{\sigma_l} \right)^{-1} \tag{3.31}$$

After some algebraic manipulations shown in Appendix 3.8.1, we have

$$p_l(\lambda) = \sigma_l \left(e^{2(W(z_l)+t_l)} - 1 \right) \tag{3.32}$$

where $z_l = \sqrt{\frac{t_l e^{-2t_l}}{2\lambda\sigma_l}}$ and $W(\cdot)$ is the Lambert W function defined as the inverse of the function $w \to we^w$ [75]. Next, we prove some monotonicity properties for the optimal solution, as a function of the qualities of the channels and the amounts of data flows through the channels.

Lemma 3.4 *For fixed t_l, p_l is monotone increasing in σ_l.*

Proof: By differentiating (3.32) and using the following property [75]

$$\frac{dW(x)}{dx} = \frac{W(x)}{x(1+W(x))} \tag{3.33}$$

it can be verified as shown in Appendix 3.8.2 that

$$\frac{\partial p_l}{\partial \sigma_l} = e^{2t_l} \frac{e^{2W(z_l)}}{1 + W(z_l)} - 1 > 0 \tag{3.34}$$

where the inequality follows from $e^{2t_l} > 1$, $\forall t_l > 0$, and $\frac{e^{2z}}{1+z} > 1$, $\forall z > 0$, proving the lemma. ■

This lemma shows that, for fixed data flows, more power should be allocated to channels with more noise power, similar to channel inversion power control [74].

Lemma 3.5 *For fixed σ_l, p_l is monotone increasing in t_l.*

Proof: By differentiating (3.32), it can be verified as shown in Appendix 3.8.3 that

$$\frac{\partial p_l}{\partial t_l} = \frac{\sigma_l (W(z_l) + 2t_l)\, e^{2(W(z_l)+t_l)}}{t_l (1 + W(z_l))} > 0 \tag{3.35}$$

proving the lemma. ■

This lemma shows that, for fixed channel qualities (i.e., fixed noise powers), more power should be allocated to links with more data flow.

Finally, we solve (3.27) as follows: From the total energy constraint, we have $\sum_l p_l(\lambda^*) = E_n$. We perform a one dimensional search on λ to find λ^* that satisfies $\sum_l p_l(\lambda^*) = E_n$, where $p_l(\lambda^*)$ is given in (3.32). Once λ^* is obtained, the optimal power allocations are found from (3.32).

3.3.3 Solution for the Case with Energy Transfer

Now, we consider the case with energy transfer, i.e., $y_q \geq 0$ for some q. Assume that some energy $y_q > 0$ is transferred from node i to node j on energy link q. Writing (3.32) for the outgoing data links of node i and node j, we have,

$$p_l(\lambda_i) = \sigma_l \left(e^{2(W(z_{il})+t_l)} - 1\right), \quad \forall l \in \mathcal{O}_d(i) \tag{3.36}$$

$$p_l(\lambda_j) = \sigma_l \left(e^{2(W(z_{jl})+t_l)} - 1\right), \quad \forall l \in \mathcal{O}_d(j) \tag{3.37}$$

where $z_{il} = \sqrt{\frac{t_l e^{-2t_l}}{2\lambda_i \sigma_l}}$ and $z_{jl} = \sqrt{\frac{t_l e^{-2t_l}}{2\lambda_j \sigma_l}}$. From (3.22), we have $\lambda_i = \alpha_q \lambda_j$. The energy causality constraints on node i and node j are:

$$\sum_{l \in \mathcal{O}_d(i)} p_l(\lambda_i^*) = E_i - y_q \tag{3.38}$$

$$\sum_{l \in \mathcal{O}_d(j)} p_l(\lambda_j^*) = E_j + \alpha_q y_q \tag{3.39}$$

Equations (3.22), (3.38) and (3.39) imply

$$\alpha_q \sum_{l \in \mathcal{O}_d(i)} p_l(\alpha_q \lambda_j^*) + \sum_{l \in \mathcal{O}_d(j)} p_l(\lambda_j^*) = \alpha_q E_i + E_j \tag{3.40}$$

which can be solved by a one-dimensional search on λ_j^*.

We solve (3.11) by iteratively allowing energy to flow through a single link at a time provided all links are visited infinitely often. Since we do not know which energy links will be active in the optimal solution, we may need to call back any

Algorithm 2 Algorithm to solve capacity assignment problem for single time slot

Initialize ▷ No energy transfer

1: **for** $i = 1 : N$ **do**
2: Find λ_i such that $\sum_{l \in \mathcal{O}_d(i)} p_l(\lambda_i) = E_i$, p_l is (3.32)
3: **end for**

Main Algorithm

4: **for** $q = 1 : Q$ **do** ▷ All energy links
5: Set $(i, j) \leftarrow$ (origin,destination) of energy link q
6: **if** $\lambda_i < \alpha_q \lambda_j$ **then** ▷ Perform energy transfer
Find λ_j^* such that
$\alpha_q \sum_{l \in \mathcal{O}_d(i)} p_l(\alpha_q \lambda_j^*) + \sum_{l \in \mathcal{O}_d(j)} p_l(\lambda_j^*) = \alpha_q E_i + E_j$
Set $\text{Tap}_q = E_i - \sum_{l \in \mathcal{O}_d(i)} p_l(\alpha_q \lambda_j^*)$ ▷ Update tap level
▷ Update battery levels
Set $E_i = \sum_{l \in \mathcal{O}_d(i)} p_l(\alpha_q \lambda_j^*), E_j = \sum_{l \in \mathcal{O}_d(j)} p_l(\lambda_j^*)$
7: **else if** $\lambda_i > \alpha_q \lambda_j$ **then** ▷ Recall some energy
8: **while** $\text{Tap}_q \geq 0, \lambda_i > \alpha_q \lambda_j, E_j \geq 0$ **do**
▷ Recall ϵ energy
Set $E_i = E_i + \epsilon, E_j = E_j - \alpha_q \epsilon, \text{Tap}_q = \text{Tap}_q - \epsilon$
Find λ_i, λ_j such that
$E_i = \sum_{l \in \mathcal{O}_d(i)} p_l(\lambda_i), E_j = \sum_{l \in \mathcal{O}_d(j)} p_l(\lambda_j)$
9: **end while**
10: **end if**
11: **end for**

transferred energy in the previous iterations. To perform this, we keep track of transferred energy over each energy link by means of meters as in [55]. Initially, we start from the no energy transfer solution and compute λ_n for every node n as described in the previous section. At every iteration, we open only one energy link q at a time, and whenever energy flows through link q, (3.40) must be satisfied with E_i and E_j in (3.40) replaced with the battery levels of nodes i and j at the current iteration. In particular, if $\lambda_i < \alpha_q \lambda_j$, we search for λ_j^* that satisfies (3.40). If no solution to (3.40) can be found, this means $\lambda_i > \alpha_q \lambda_j$, and then previously transferred energy must be called back to the extent possible according to the meter readings. The algorithmic description is given above as Algorithm 2. From the strict convexity of the objective function, we note that each iteration decreases the objective function as described similarly in [55, Section V.A]. Our algorithm converges since bounded real monotone sequences always converge, and the limit point is a local minimum because, the iterations can only stop when $\lambda_i = \alpha_q \lambda_j$ for the energy links where $y_q > 0$ which are the KKT optimality conditions from (3.22). This local minimum is also the unique global minimum due to the convexity of the problem.

3.4 Capacity Assignment Problem for Multiple Time Slots

In this section, we consider the capacity assignment problem for the scenario where the energy arrival rates to the nodes can change over time. We assume that the time is slotted and there are a total of T equal-length slots. In slots $i = 1, \ldots, T$, each

node n harvests energy with amounts $E_{n1}, E_{n2}, \ldots, E_{nT}$, and the arriving energies can be saved in a battery for use in future time slots. The subscript i denotes the time slot, and the quantities $t_{li}, c_{li}, p_{li}, \sigma_{li}$ and y_{qi} denote the flow, capacity, power, noise power, and energy transfer in slot i. We assume that the flow allocation and channel noises do not change over time, i.e., $t_{li} = t_l$ and $\sigma_{li} = \sigma_l, \forall i, \forall l$. We further assume that the slots are long enough so that the M/M/1 approximation is valid at every slot i. In particular, slot length is sufficiently larger than the average delay resulting from the M/M/1 approximation. Then, the average delay on link l at time slot i is given as,

$$D_{li} = \frac{t_l}{c_{li} - t_l} \tag{3.41}$$

where $c_{li} = \frac{1}{2}\log\left(1 + \frac{p_{li}}{\sigma_l}\right)$. As the energy that has not arrived yet cannot be used for data transmission or energy transfer, the power policies of the nodes are constrained by causality of energy in time. These constraints are written as:

$$\sum_{i=1}^{k}\left(\sum_{l\in\mathcal{O}_d(n)} p_{li} + \sum_{q\in\mathcal{O}_e(n)} y_{qi}\right) \leq \sum_{i=1}^{k}\left(E_{ni} + \sum_{q\in\mathcal{I}_e(n)} \alpha_q y_{qi}\right), \quad \forall n, \forall k \tag{3.42}$$

The capacity assignment problem with fixed link flows to minimize the total delay over all links and all time slots can be formulated as:

$$\min_{p_{li}, y_{qi}} \quad \sum_{i=1}^{T}\sum_{l} \frac{t_l}{\frac{1}{2}\log\left(1 + \frac{p_{li}}{\sigma_l}\right) - t_l}$$

$$\text{s.t.} \qquad \sum_{i=1}^{k}\left(\sum_{l\in\mathcal{O}_d(n)} p_{li} + \sum_{q\in\mathcal{O}_e(n)} y_{qi}\right) \leq \sum_{i=1}^{k}\left(E_{ni} + \sum_{q\in\mathcal{I}_e(n)} \alpha_q y_{qi}\right), \quad \forall n, \forall k$$

$$p_{li} \geq \sigma_l(e^{2t_l} - 1), \quad \forall l, \forall i \tag{3.43}$$

The problem in (3.43) is convex and the Lagrangian function can be written as:

$$\mathcal{L} = \sum_{i=1}^{T}\sum_{l} h_l(p_{li}) + \sum_{n}\sum_{k=1}^{T}\lambda_{nk}\left[\sum_{i=1}^{k}\left(\sum_{l\in\mathcal{O}_d(n)} p_{li} + \sum_{q\in\mathcal{O}_e(n)} y_{qi} - E_{ni} - \sum_{q\in\mathcal{I}_e(n)} \alpha_q y_{qi}\right)\right] - \sum_{q}\sum_{i=1}^{T}\theta_{qi}y_{qi} \tag{3.44}$$

where $h_l(p_{li}) \triangleq t_l\left[\frac{1}{2}\log\left(1+\frac{p_{li}}{\sigma_l}\right) - t_l\right]^{-1}$. The Lagrange multipliers for the second set of constraints for (3.43) are not included here because similar to before, they will always be satisfied with strict inequality. The KKT optimality conditions are:

$$h_l'(p_{li}) + \sum_{k=i}^{T}\lambda_{n(l)k} = 0, \quad \forall l, \forall i \tag{3.45}$$

$$\sum_{k=i}^{T}\lambda_{m(q)k} - \alpha_q\sum_{k=i}^{T}\lambda_{r(q)k} - \theta_{qi} = 0, \quad \forall q, \forall i \tag{3.46}$$

where $n(l)$ is the beginning node of data link l, $m(q)$ and $r(q)$ are the beginning and end nodes of energy link q. The additional complementary slackness conditions as:

$$\lambda_{nk}\left[\sum_{i=1}^{k}\left(\sum_{l\in\mathcal{O}_d(n)} p_{li} + \sum_{q\in\mathcal{O}_e(n)} y_{qi} - E_{ni} - \sum_{q\in\mathcal{I}_e(n)} \alpha_q y_{qi}\right)\right] = 0, \quad \forall n, \forall k \tag{3.47}$$

$$\theta_{qi}y_{qi} = 0, \quad \forall q, \forall i \tag{3.48}$$

Now, we extend Lemmas 3.2 and 3.3 to the case of multiple energy arrivals over time.

Lemma 3.6 *At every node n, the optimal power allocation amongst outgoing data links satisfies*

$$h_l'(p_{li}) = h_m'(p_{mi}), \quad \forall l, m \in \mathcal{O}_d(n), \forall i \tag{3.49}$$

Proof: From (3.45), we have,

$$h_l'(p_{li}) = -\sum_{k=i}^{T} \lambda_{n(l)k} \tag{3.50}$$

For outgoing data links l and m that belong to the same node n,

$$h_l'(p_{li}) = -\sum_{k=i}^{T} \lambda_{nk} = h_m'(p_{mi}), \quad \forall i \tag{3.51}$$

from which the result follows. ■

Lemma 3.7 *If some energy is transferred through energy link q across nodes (a, b) at time slot i,*

$$h_l'(p_{li}) = \alpha_q h_m'(p_{mi}), \quad \forall l \in \mathcal{O}_d(a), \forall m \in \mathcal{O}_d(b) \tag{3.52}$$

Proof: If some energy is transferred through energy link q at time slot i, then

$y_{qi} > 0$, and from (3.48), $\theta_{qi} = 0$. From (3.46), we have,

$$\sum_{k=i}^{T} \lambda_{ak} = \alpha_q \sum_{k=i}^{T} \lambda_{bk} \tag{3.53}$$

Then, we have,

$$h_l'(p_{li}) = -\sum_{k=i}^{T} \lambda_{ak} = -\alpha_q \sum_{k=i}^{T} \lambda_{bk} = \alpha_q h_m'(p_{mi}), \quad \forall l \in \mathcal{O}_d(a), \forall m \in \mathcal{O}_d(b) \tag{3.54}$$

where the first equality follows from writing (3.45) for node a, the second equality follows from (3.53), and the third equality follows from writing (3.45) for node b. ■

In the following two sub-sections, we separately solve the problem for the cases of no energy transfer and with energy transfer.

3.4.1 Solution for the Case of No Energy Transfer

In this case, we have $y_{qi} = 0, \forall i, \forall q$. The problem becomes only in terms of p_{li} as follows:

$$\begin{aligned} \min_{p_{li}} \quad & \sum_{i=1}^{T} \sum_{l} \frac{t_l}{\frac{1}{2}\log\left(1 + \frac{p_{li}}{\sigma_l}\right) - t_l} \\ \text{s.t.} \quad & \sum_{i=1}^{k} \sum_{l \in \mathcal{O}_d(n)} p_{li} \leq \sum_{i=1}^{k} E_{ni}, \quad \forall n, \forall k \\ & p_{li} \geq \sigma_l(e^{2t_l} - 1), \quad \forall l, \forall i \end{aligned} \tag{3.55}$$

The problem can be decomposed into N sub-problems as:

$$\begin{aligned} \min_{p_{li}} \quad & \sum_{i=1}^{T} \sum_{n} \sum_{l \in \mathcal{O}_d(n)} \frac{t_l}{\frac{1}{2}\log\left(1+\frac{p_{li}}{\sigma_l}\right) - t_l} \\ \text{s.t.} \quad & \sum_{i=1}^{k} \sum_{l \in \mathcal{O}_d(n)} p_{li} \leq \sum_{i=1}^{k} E_{ni}, \quad \forall n, \forall k \\ & p_{li} \geq \sigma_l(e^{2t_l}-1), \quad \forall l, \forall i \end{aligned} \tag{3.56}$$

Since the constraint set depends only on the powers of node n, there is no interaction between the nodes. Every node will independently solve the following optimization problem:

$$\begin{aligned} \min_{p_{li}} \quad & \sum_{i=1}^{T} \sum_{l \in \mathcal{O}_d(n)} \frac{t_l}{\frac{1}{2}\log\left(1+\frac{p_{li}}{\sigma_l}\right) - t_l} \\ \text{s.t.} \quad & \sum_{i=1}^{k} \sum_{l \in \mathcal{O}_d(n)} p_{li} \leq \sum_{i=1}^{k} E_{ni}, \quad \forall k \\ & p_{li} \geq \sigma_l(e^{2t_l}-1), \quad \forall l \in \mathcal{O}_d(n), \forall i \end{aligned} \tag{3.57}$$

Solving (3.57) entails finding the optimal energy management policy for each link l, over all time slots i. We define $b_{li} = p_{li} - \sigma_l(e^{2t_l}-1)$ and $G_{ni} = E_{ni} - |\mathcal{O}_d(n)|\sigma_l(e^{2t_l}-1)$. Then, (3.57) becomes:

$$\begin{aligned} \min_{b_{li}} \quad & \sum_{i=1}^{T} \sum_{l \in \mathcal{O}_d(n)} \frac{t_l}{\frac{1}{2}\log\left(e^{2t_l}+\frac{b_{li}}{\sigma_l}\right) - t_l} \\ \text{s.t.} \quad & \sum_{i=1}^{k} \sum_{l \in \mathcal{O}_d(n)} b_{li} \leq \sum_{i=1}^{k} G_{ni}, \quad \forall k \end{aligned}$$

$$b_{li} \geq 0, \quad \forall l \in \mathcal{O}_d(n), \forall i \tag{3.58}$$

For feasibility of (3.58) we need $G_{ni} \geq 0$ which we assume holds. Now, we state an important property of the optimal policy which is proved in Appendix 3.8.4.

Lemma 3.8 *The optimal total power allocated to outgoing data links at each slot* i, $\sum_{l\in\mathcal{O}_d(n)} b_{li}$, *is the same as the single-link optimal transmit power with energy arrivals* G_{ni}.

From Lemma 3.8 we have that the sum powers in outgoing data links are given by the single-link optimal transmit powers which can be found by the geometric method in [4] or by the directional water-filling method in [6]. Once the sum powers are obtained, individual link powers are found by solving $x(s_i)$ which is defined in (3.92) in Appendix 3.8.4. The problem in $x(s_i)$ includes a single energy harvest and is in the form of (3.27), therefore, we use the method proposed in Section 3.3.2 to find the individual link powers.

3.4.2 Solution for the Case with Energy Transfer

From (3.45) and some algebraic manipulations we have

$$p_{li} = \sigma_l \left(e^{2(W(z_{il})+t_l)} - 1\right) \tag{3.59}$$

where $z_{il} = \sqrt{\frac{t_l e^{-2t_l}}{2(\sum_{k=i}^{T} \lambda_{n(l)k})\sigma_l}}$ and $W(\cdot)$ is the Lambert W function. The Lagrangian structure of this problem is more complicated compared to the previous case since

the power allocation at time i depends on $\{\lambda_{n(l)k}\}_{k=i}^{T}$. Therefore, here, we offer an alternative solution.

In the scenario described above, the nodes have the capability to save their energies to use in future slots. We note that saving energy for use in future slots is equivalent to transferring energy to future slots with energy transfer efficiency of $\alpha = 1$. In light of this observation, an equivalent representation of (3.43) can be obtained by modifying the network graph where each time slot is treated as a new node with a single energy arrival and saving energy for future slots is represented by energy transfer links of efficiency 1. The modification to the network graph is performed in the following way. First, we make T replicas of the network graph including all the nodes and the existing data and energy transfer links. Each replica will denote the network at one time slot. We let each replica node receive one energy harvest which amounts to the energy harvested by that node in that time slot. We keep the existing energy and data links but we add new energy links between different replicas of the same node. For every node n, we add energy links of efficiency 1 between replicas k and $k+1$, where $k = 1, \ldots, T-1$. Relabeling the nodes, we obtain a new graph where all nodes have one energy harvest. Essentially, we have reduced this problem to the case in Section 3.3.3 and we use the solution provided in that section.

We finally remark that our framework can easily be extended to address variations in channel fading coefficients and energy transfer efficiencies by allowing the noise powers σ_l and energy transfer efficiencies α_l to vary from slot to slot, i.e.,

defining $c_{li} = \frac{1}{2}\log\left(1+\frac{p_{li}}{\sigma_{li}}\right)$ and replacing α_l with α_{li}.

3.5 Joint Capacity and Flow Optimization

In this section, we consider the joint optimization of capacity and flow assignments, in contrast to capacity assignment only with fixed flows, as considered in the previous sections. We focus on the case with a single energy harvest per node as in Section 3.3. The delay minimization problem with joint capacity and flow allocation can be formulated as:

$$\begin{aligned} \min_{p_l, y_q, t_l} \quad & \sum_l \frac{t_l}{\frac{1}{2}\log\left(1+\frac{p_l}{\sigma_l}\right) - t_l} \\ \text{s.t.} \quad & \mathbf{Fp} + \mathbf{By} \leq \mathbf{E} \\ & p_l \geq \sigma_l(e^{2t_l} - 1), \quad \forall l \\ & \mathbf{At} = \mathbf{s} \end{aligned} \tag{3.60}$$

where we optimize not only the powers p_l and energy transfers y_q, but also the data flows t_l. In (3.60), the first set of constraints are the energy constraints, the second set of constraints are the capacity constraints on individual links, and the last set of constraints are the flow conservation constraints at all nodes.

We assume that the exogenous arrivals $\mathbf{s}$ is serviceable by the energy harvests and energy transfers. This means that problem (3.60) has a bounded solution and furthermore no data link is operating at the capacity, i.e., the capacity constraints are never satisfied with equality unless $t_l = p_l = 0$. We solve the problem in (3.60)

in the remainder of this section. Here, the constraint set is convex, however, the objective function is not jointly convex in p_l and t_l [43], therefore, (3.60) is not a convex optimization problem. We study the necessary optimality conditions by writing the Lagrangian function as follows:

$$\begin{aligned}\mathcal{L} = &\sum_l \frac{t_l}{\frac{1}{2}\log\left(1+\frac{p_l}{\sigma_l}\right)-t_l} + \sum_n \lambda_n \left[\sum_{l\in\mathcal{O}_d(n)} p_l + \sum_{q\in\mathcal{O}_e(n)} y_q - E_n - \sum_{q\in\mathcal{I}_e(n)} \alpha_q y_q\right] \\ &- \sum_l \beta_l[p_l - \sigma_l(e^{2t_l}-1)] + \sum_n \nu_n \left[\sum_{l\in\mathcal{O}_d(n)} t_l - \sum_{l\in\mathcal{I}_d(n)} t_l - s_n\right] \\ &- \sum_q \theta_q y_q - \sum_l \gamma_l t_l \end{aligned} \tag{3.61}$$

The KKT optimality conditions are:[1]

$$\frac{-t_l}{2\sigma_l}\left[\frac{1}{2}\log\left(1+\frac{p_l}{\sigma_l}\right)-t_l\right]^{-2}\left(1+\frac{p_l}{\sigma_l}\right)^{-1} + \lambda_{n(l)} - \beta_l = 0, \quad \forall l \tag{3.62}$$

$$\frac{1}{2}\log\left(1+\frac{p_l}{\sigma_l}\right)\left[\frac{1}{2}\log\left(1+\frac{p_l}{\sigma_l}\right)-t_l\right]^{-2} + \nu_{n(l)} - \nu_{m(l)} - \gamma_l + 2\beta_l\sigma_l e^{2t_l} = 0, \quad \forall l \tag{3.63}$$

$$\lambda_{k(q)} - \alpha_q\lambda_{z(q)} - \theta_q = 0, \quad \forall q \tag{3.64}$$

where $n(l)$ and $m(l)$ are the source and destination nodes of data link l, $k(q)$ and $z(q)$ are the source and destination nodes of energy link q, respectively. The com-

[1]With the objective function of (3.60), there is an uncertainty when $t_l = p_l = 0$. Nonetheless, we argue as in [43, page 441] that the objective function of (3.60) is differentiable over the set of all p_l with $\frac{1}{2}\log\left(1+\frac{p_l}{\sigma_l}\right) > t_l$ and $\frac{\partial\mathcal{L}}{\partial p_l} = 0, \frac{\partial\mathcal{L}}{\partial t_l} = 0$ and $\frac{\partial\mathcal{L}}{\partial y_q} = 0$ are necessary conditions for optimality.

plementary slackness conditions are:

$$\lambda_n \left(\sum_{l \in \mathcal{O}_d(n)} p_l + \sum_{q \in \mathcal{O}_e(n)} y_q - E_n - \sum_{q \in \mathcal{I}_e(n)} \alpha_q y_q \right) = 0, \, \forall n \tag{3.65}$$

$$\nu_n \left(\sum_{l \in \mathcal{O}_d(n)} t_l - \sum_{l \in \mathcal{I}_d(n)} t_l - s_n \right) = 0, \quad \forall n \tag{3.66}$$

$$\theta_q y_q = \gamma_l t_l = 0, \quad \forall q, \, \forall l \tag{3.67}$$

$$\beta_l \left[p_l - \sigma_l (e^{2t_l} - 1) \right] = 0, \quad \forall l \tag{3.68}$$

$$\lambda_n, \beta_l, \theta_q, \gamma_l \geq 0, \quad \forall l, \, \forall q, \, \forall n \tag{3.69}$$

We note that $\nu_n < 0$ is allowed since the Lagrange multiplier ν corresponds to an equality constraint. Lemma 3.9, proved in Appendix 3.8.5, states the necessary optimality conditions.

Lemma 3.9 *For a feasible set of flow variables $\{t_l\}_{l=1}^L$, transmission power allocations $\{p_l\}_{l=1}^L$ and energy transfers $\{y_q\}_{q=1}^Q$ to be the solution to the problem in (3.60), the following conditions are necessary.*

1) For every node n, there exists a constant $\lambda_n > 0$ such that

$$\frac{t_l}{2\sigma_l} \left[\frac{1}{2} \log \left(1 + \frac{p_l}{\sigma_l} \right) - t_l \right]^{-2} \left(1 + \frac{p_l}{\sigma_l} \right)^{-1} \leq \lambda_n, \quad \forall l \in \mathcal{O}_d(n) \tag{3.70}$$

and with equality if $p_l > 0$.

2) For every node n, there exists a constant $\tilde{\nu}_n \geq 0$ such that

$$\sum_{l \in \mathcal{F}_{n,d}} \frac{1}{2} \log\left(1 + \frac{p_l}{\sigma_l}\right) \left[\frac{1}{2} \log\left(1 + \frac{p_l}{\sigma_l}\right) - t_l\right]^{-2} = \tilde{\nu}_n, \quad \forall d = 1, \ldots, D \tag{3.71}$$

where $\mathcal{F}_{n,d}$ is a data path that starts from node n and ends at destination node d and for which $p_l > 0, \forall l \in \mathcal{F}_{n,d}$. The condition in (3.71) is valid for all such data paths that start from node n and end at any destination node.

3) For all energy transfer links q, and $\forall l \in \mathcal{O}_d(n), \forall k \in \mathcal{O}_d(m)$ such that $p_l > 0$ and $p_k > 0$ where n and m are the origin and destination nodes of energy transfer link q

$$\begin{aligned} &\frac{t_l}{2\sigma_l} \left[\frac{1}{2} \log\left(1 + \frac{p_l}{\sigma_l}\right) - t_l\right]^{-2} \left(1 + \frac{p_l}{\sigma_l}\right)^{-1} \\ &\quad \geq \alpha_q \frac{t_k}{2\sigma_k} \left[\frac{1}{2} \log\left(1 + \frac{p_k}{\sigma_k}\right) - t_k\right]^{-2} \left(1 + \frac{p_k}{\sigma_k}\right)^{-1} \end{aligned} \tag{3.72}$$

where (3.72) is satisfied with equality if $y_q > 0$.

From Lemma 3.9, the structure of the optimal solution is as follows: We define $h_l(p_l, t_l)$ as the objective function of the problem in (3.60), $h_l(p_l, t_l) \triangleq t_l \left[\frac{1}{2} \log\left(1 + \frac{p_l}{\sigma_l}\right) - t_l\right]^{-1}$. We see from (3.70) that nodes should allocate more power on links where the quantity $\left|\frac{\partial h_l}{\partial p_l}\right|$ is large and less power on links where this quantity is small. Similarly, from (3.71), we see that less flow should be allocated on paths where the quantity $\sum_{l \in \mathcal{F}_{n,d}} \frac{\partial h_l}{\partial t_l}$ is large and more flow on paths where this quantity is small. Finally, (3.72) tells us the necessary conditions for energy transfer. We describe our solution to the problem in (3.60) in the next section.

3.5.1 Algorithmic Solution for the Joint Capacity and Flow Optimization Problem

In this section, we propose an iterative algorithm. There are three steps to each iteration as summarized below. We start from a feasible point $(\mathbf{t}_0, \mathbf{p}_0)$.

1. *Energy Management Step:* We fix a stepsize $\xi_p > 0$. Each node computes $\frac{\partial h_l}{\partial p_l}$ for their own outgoing data links where $p_l > 0$. Every node performs the following iteration:

$$p_l^{k+1} = \begin{cases} p_l^k + \xi_p, & \text{if } l = \arg\max_{l \in \mathcal{O}_d(n)} \left| \frac{\partial h_l}{\partial p_l} \right| \\ p_l^k - \xi_p, & \text{if } l = \arg\min_{l \in \mathcal{O}_d(n)} \left| \frac{\partial h_l}{\partial p_l} \right| \\ p_l^k, & \text{otherwise} \end{cases} \tag{3.73}$$

   where k denotes the iteration number, and the derivatives are computed at the current iteration, i.e., for $(\mathbf{t}^k, \mathbf{p}^k)$.

2. *Data Routing Step:* We fix a stepsize $\xi_t > 0$. Each node n computes $\sum_{l \in \mathcal{F}_{n,d}} \frac{\partial h_l}{\partial t_l}$ for the data paths originating from source node n and ending at any destination. Assume the path $\mathcal{F}_n^*$ maximizes $\sum_{l \in \mathcal{F}_{n,d}} \frac{\partial h_l}{\partial t_l}$ and the path $\mathcal{G}_n^*$ minimizes

$\sum_{l \in \mathcal{F}_{n,d}} \frac{\partial h_l}{\partial t_l}$ for each n. Every node performs the following iteration:

$$t_l^{k+1} = \begin{cases} t_l^k - \xi_t, & \text{if } l \in \mathcal{F}_n^* \\ t_l^k + \xi_t, & \text{if } l \in \mathcal{G}_n^* \\ t_l^k, & \text{otherwise} \end{cases} \tag{3.74}$$

3. *Energy Routing Step:* This step is the same as described in Section 3.3.3. Specifically, every node goes through its energy transfer links and makes the comparison $\left|\frac{\partial h_l}{\partial p_l}\right| \gtrless \alpha_q \left|\frac{\partial h_m}{\partial p_m}\right|$ where m is the receiving node of energy link q. If $\left|\frac{\partial h_l}{\partial p_l}\right| < \alpha_q \left|\frac{\partial h_m}{\partial p_m}\right|$, then some energy is transferred through link q. If $\left|\frac{\partial h_l}{\partial p_l}\right| > \alpha_q \left|\frac{\partial h_m}{\partial p_m}\right|$, then some energy must be called back, as explained in Section 3.3.3.

4. Go back to step 1, or terminate if sufficiently many iterations are performed.

We describe our Algorithm in tabular form as Algorithm 3 below. We note that our algorithm reduces to the one in [53] in the case of no energy harvesting or energy transfer. Next, we discuss the convergence and optimality properties of our algorithm.

3.5.2 Convergence and Optimality Properties of the Proposed Algorithm

Every iteration of the algorithm decreases the objective function and the iterations are bounded. Using the fact that real monotone bounded sequences converge, we

Algorithm 3 Algorithm to solve joint capacity and flow assignment problem for single time slot

Initialize

Generate initial point

Energy management step

for $n = 1 : N$ **do** ▷ All nodes

Find $\arg\max_{l \in \mathcal{O}_d(n)} \frac{\partial h_l}{\partial p_l}$, perform (3.73) as long as $p_l \geq \sigma_l(e^{2t_l} - 1)$ is still satisfied

end for

Data routing step

for $n = 1 : N$ **do** ▷ All Nodes

Find path $\mathcal{F}_n^*$ that maximizes and $\mathcal{G}_n^*$ that minimizes $\sum_{l \in \mathcal{F}_{n,d}} \frac{\partial h_l}{\partial t_l}$ where $d \in \mathcal{O}_d(n)$

  for $l \in \mathcal{F}_n^*$ **do** $t_l^{k+1} = t_l^k - \xi_t$

  end for

  for $l \in \mathcal{G}_n^*$ **do** $t_l^{k+1} = t_l^k + \xi_t$ as long as $p_l \geq \sigma_l(e^{2t_l} - 1)$ is still satisfied

  end for

end for

Energy routing step

for $q = 1 : Q$ **do** ▷ All energy links

  Set $(i, j) \leftarrow$ (origin,destination) of energy link q

  Set $\lambda_i = \left| \frac{\partial h_i}{\partial p_i} \right|$ and $\lambda_j = \frac{\partial h_j}{\partial p_j}$

  Use steps $6 : 10$ of Algorithm 2

end for

Repeat until convergence

conclude that the algorithm converges. Assume $(\mathbf{t}^*, \mathbf{p}^*, \mathbf{y}^*)$ is a convergence point of the algorithm. Next, we show that this point satisfies the KKT optimality conditions stated in Lemma 3.9.

Lemma 3.10 $(\mathbf{t}^*, \mathbf{p}^*, \mathbf{y}^*)$ *satisfies the conditions stated in Lemma 3.9.*

Proof: When the algorithm converges, we must have $p_l^{k+1} = p_l^k$. From (3.73), this is only possible when $\frac{\partial h_l}{\partial p_l}$ is constant for $l \in \mathcal{O}_d(n)$ which is equivalent to (3.70). Similarly, we must have $t_l^{k+1} = t_l^k$ and from (3.74), this is only possible when $\sum_{l \in \mathcal{F}_{n,d}} \frac{\partial h_l}{\partial t_l}$ is constant over all paths, which is equivalent to (3.71). Using a similar argument we conclude that energy transfers satisfy (3.72). This means that $(\mathbf{t}^*, \mathbf{p}^*, \mathbf{y}^*)$ satisfies Lemma 3.9. ■

Now, we remark that even though we cannot claim global optimality of the solution, we have the following *Pareto-optimality* condition.

Remark 3.1 *Assume that* $(\mathbf{t}^*, \mathbf{p}^*, \mathbf{y}^*)$ *satisfies the conditions stated in Lemma 3.9, then the vector of link delays is Pareto-optimal, i.e., there does not exist another pair of feasible allocations* $(\hat{\mathbf{t}}, \hat{\mathbf{p}}, \hat{\mathbf{y}})$ *such that*

$$h_l(\hat{p}_l, \hat{t}_l) \leq h_l(p_l^*, t_l^*), \quad \forall l \tag{3.75}$$

with at least one inequality being strict.

This remark means that at the Pareto-optimal point, the average delay cannot be strictly reduced on one link without it being increased on another. The proof of

this remark follows similar lines as the proof in [53, Thm. 4] and is omitted here for brevity. We note that, in particular, any local optimal point is Pareto-optimal due to the fact that local optimal points satisfy KKT conditions in Lemma 3.9.

3.6 Numerical Results

In this section, we give simple numerical results to illustrate the resulting optimal policies. We study three network topologies shown in Figs. 3.2, 3.3 and 3.4. For all examples, we assume $\sigma_l = 0.1$ units $\forall l$. The slot length is of 1 unit for convenience, so that we use power and energy; rate and data interchangeably.

3.6.1 Network Topology 1

We first consider the network topology in Fig. 3.2 with one source, one destination and three relays in between. The data and energy links are shown and labeled as in Fig. 3.2, where l_is represent data links and y_qs represent energy links. The fixed data flows are $\mathbf{t} = [t_1, \ldots, t_7] = [2, 1, 0.5, 0.125, 2.125, 0.375, 0.5]$ units. We consider two time slots. The energy arrival vector is $\mathbf{E} = [(E_{11}, E_{12}), \ldots, (E_{41}, E_{42})] = [(15, 10), (8, 6), (5, 9), (1, 6)]$ units and energy transfer efficiencies are $\boldsymbol{\alpha} = [\alpha_1, \alpha_2, \alpha_3] = [0.6, 0.5, 0.5]$.

The optimal energy transfer vector is found as $\mathbf{y} = [(y_{11}, y_{12}), (y_{21}, y_{22}), (y_{31}, y_{32})] = [(0, 3.75), (3.93, 9.52), (2.35, 9.81)]$ units and power allocation vector after energy transfer is $\mathbf{p} = [(p_{11}, p_{12}), \ldots, (p_{71}, p_{72})] = [(7.5, 7.5), (3.13, 3.13), (0.62, 1), (0.13, 0.22), (9.17, 11), (0.45, 0.74), (0.48, 0.73)]$ units. Lemmas 3.6 and 3.7 can be

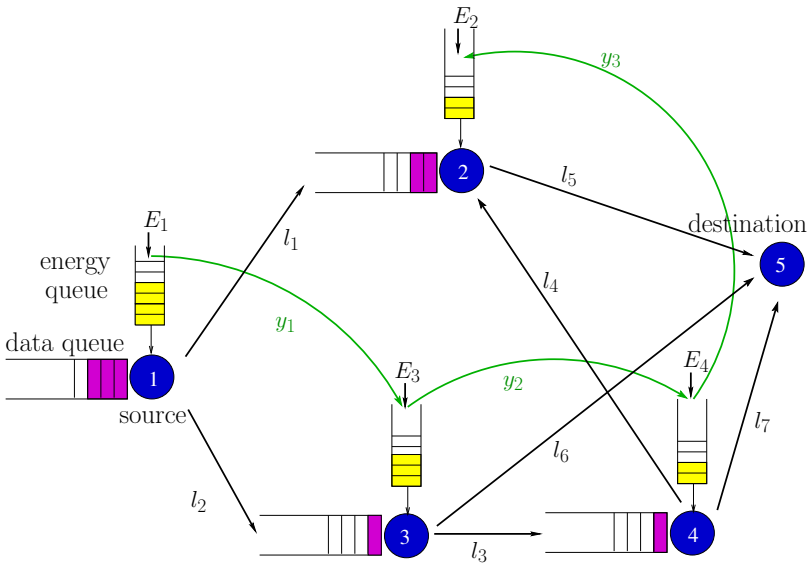

Figure 3.2: Network topology 1.

verified numerically: $h_l'(p_{li})$ equalizes for different outgoing links of the same node, for example, on links l_1 and l_2 (Lemma 3.6); and where some energy is transferred, $h_l'(p_{li})$ is proportional to the energy transfer efficiency of that energy transfer link, for example, $h_2'(p_{22})/h_3'(p_{32}) = \alpha_1$ (Lemma 3.7). Lemma 3.8 can also be verified numerically: after the energy transfers, the sum powers of the links are the optimal single-link powers. For example, node 1 has harvested $(15, 10)$ energies and transferred $(0, 3.75)$ of them. Equivalently node 1 has harvested $(15, 6.25)$ and the single-link optimal powers for these harvests are $(10.625, 10.625)$ which is $(p_{11} + p_{21}, p_{12} + p_{22})$. It is interesting to note that node 4 has transferred more energy than it initially had, which means that most of the transferred energy has been routed from other nodes. This is due to the high data flow on link l_5 which leads to a higher energy demand at node 2.

3.6.2 Network Topology 2

We next consider the star topology in Fig. 3.3 where five sources are communicating with one destination similar to a multiple access scenario. The data flows are $\mathbf{t} = [0.5, 2, 0.5, 0.5, 2]$ units. We consider a single time slot. The energy arrivals to all the nodes are the same, i.e., $E_n = 15$ units, $\forall n$. The wireless energy transfer efficiencies are $\alpha_q = 0.5, \forall q$.

The optimal energy transfer vector is found as $\mathbf{y} = [11.92, 0, 9.66, 16.29, 0]$ units and the power vector after energy transfer is $\mathbf{p} = [3.07, 20.96, 5.33, 3.53, 23.15]$ units. This system is symmetric in terms of energy arrivals, channel noises and energy transfer efficiencies, and furthermore $t_1 = t_3 = t_4$ and $t_2 = t_5$. In this scenario, one might expect $p_1 = p_3 = p_4$ and $p_2 = p_5$. However, in the optimal solution $p_5 > p_2$. The reason for this asymmetry is as follows. Due to the high data loads on links l_2 and l_5, there is no incentive for these nodes to share their energy. Then, in the optimal solution, $y_2 = y_5 = 0$ and nodes 2 and 5 act as energy sink nodes where energy is collected and not sent out. We see that node 5 has two nodes transferring energy to it while node 2 has only one node transferring energy. Then, $p_5 > p_2$.

3.6.3 Network Topology 3

In this last numerical example, we demonstrate the joint optimization of flow allocation and capacity assignment. We consider the diamond network topology shown in Fig. 3.4 where one source is communicating with one destination with two re-

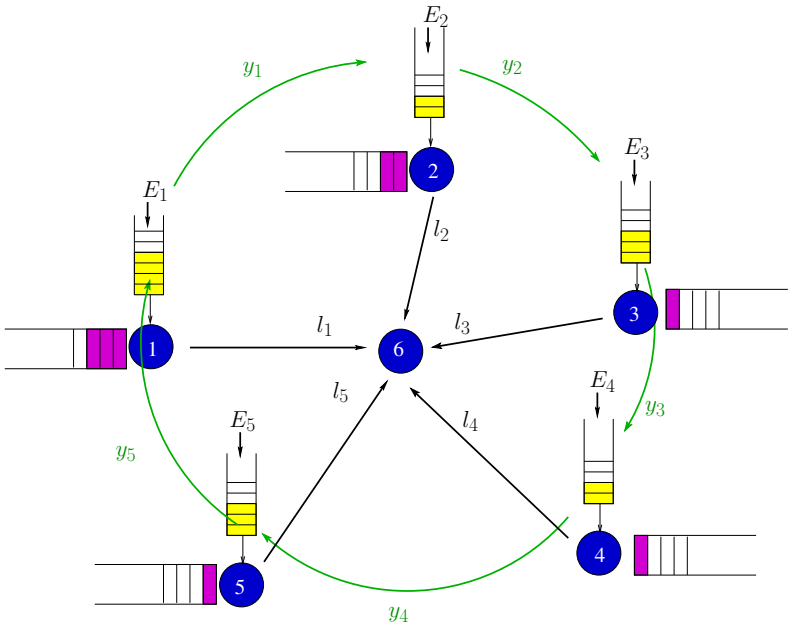

Figure 3.3: Network topology 2.

lays in between. The only exogenous data arrival to the network occurs at node 1 with the amount $t = 2$ units. The energy arrivals are $[E_1, E_2, E_3] = [2, 0.5, 1.5]$. Energy transfer efficiencies are given as $\alpha_1 = \alpha_2 = 0.8$. In this topology, there are six unknowns to be determined, i.e., $p_1, p_2, t_1, t_2, y_1, y_2$. By exhaustively searching over these parameters, we can obtain the minimum achievable delay region as shown in Fig. 3.5(top). In the diamond network, there are two paths of data flow. One is the top path which includes links l_1 and l_3 and the other is the bottom path which includes links l_2 and l_4. In Fig. 3.5(top), we plot the delay on bottom path versus the delay on top path. Any delay which is to the interior of this curve is achievable whereas other delays are not. All points on this boundary are Pareto-optimal points. We observe that energy cooperation enhances the achievable delay region. In Fig. 3.5(bottom), we demonstrate the convergence of our algorithm to a

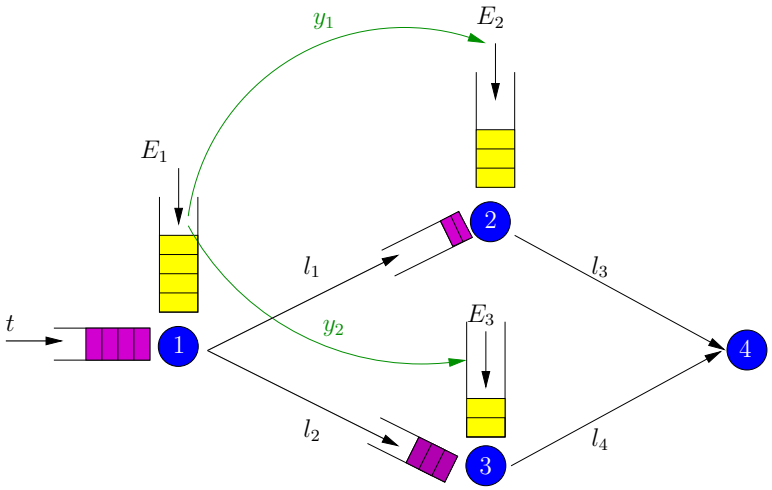

Figure 3.4: Network topology 3.

Pareto-optimal point. We start our algorithm from two different initial points and observe that they converge to a point which is on the boundary of the achievable delay region, demonstrating Remark 3.1.

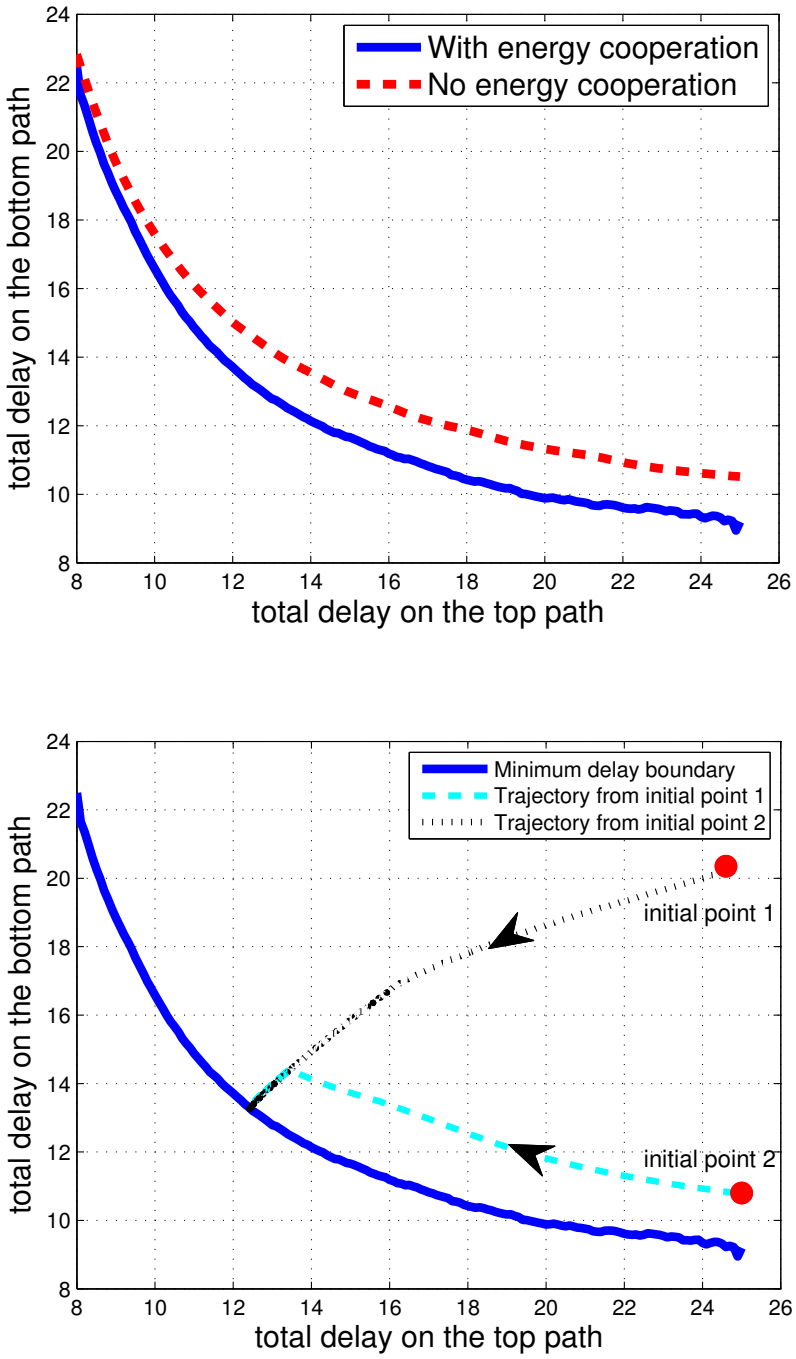

Figure 3.5: (top) Achievable delay regions with and without energy cooperation. (bottom) Convergence of our algorithm.

3.7 Concluding Remarks

In this chapter, we considered the energy management and energy routing problems for delay minimization in energy harvesting networks with energy cooperation. In this network, there are data links where data flows and energy links where energy flows. We determined the jointly optimal data and energy flows in the network and the energy distribution over outgoing data links at all nodes. We established necessary conditions for the solution, and proposed an iterative algorithm that updates powers, data routing and energy routing sequentially and converges to a Pareto-optimal operating point. In the special case of fixed data flows and no energy cooperation, we showed that each link should allocate more power to links with more noise and/or more data flow. In the case with multiple energy harvests, and no energy cooperation, we showed that the optimal sum powers on the outgoing data links of each node at every slot must be equal to the optimal single-link transmit powers. Our numerical results indicate that when data flows are fixed, energy is routed from nodes with lower data loads to nodes with higher data loads; while in the more general problem, where data flows are optimized also, allocation of data and energy flows are performed in a balanced fashion.

3.8 Appendix

3.8.1 Derivation of (3.32)

Starting from (3.31), we have

$$\lambda = \frac{t_l}{2\sigma_l}\left[\frac{1}{2}\log\left(1+\frac{p_l}{\sigma_l}\right) - t_l\right]^{-2}\left(1+\frac{p_l}{\sigma_l}\right)^{-1} \tag{3.76}$$

We let $r_l \triangleq \frac{1}{2}\log\left(1+\frac{p_l}{\sigma_l}\right) - t_l$, then $1+\frac{p_l}{\sigma_l} = e^{2(r_l+t_l)}$. With these definitions, we rewrite (3.76):

$$\lambda = \frac{t_l}{2\sigma_l} r_l^{-2} e^{-2(r_l+t_l)} \tag{3.77}$$

Or equivalently,

$$r_l e^{r_l} = \sqrt{\frac{t_l e^{-2t_l}}{2\lambda\sigma_l}} \tag{3.78}$$

From here, $r_l = W(z_l)$ where $z_l \triangleq \sqrt{\frac{t_l e^{-2t_l}}{2\lambda\sigma_l}}$ and $W(\cdot)$ is the Lambert W function defined as the inverse function of $w \to we^w$ [75]. From the definition of r_l,

$$\frac{1}{2}\log\left(1+\frac{p_l}{\sigma_l}\right) - t_l = r_l = W(z_l) \tag{3.79}$$

and

$$p_l = \sigma_l\left(e^{2(W(z_l)+t_l)} - 1\right) \tag{3.80}$$

which is (3.32).

3.8.2 Derivation of (3.34)

From (3.32), we have

$$p_l = \sigma_l \left(e^{2(W(z_l)+t_l)} - 1 \right) \tag{3.81}$$

with $z_l = \sqrt{\frac{t_l e^{-2t_l}}{2\lambda\sigma_l}}$. Our aim is to find $\frac{\partial p_l}{\partial \sigma_l}$. To this end, define $v_l \triangleq e^{2(W(z_l)+t_l)} - 1$. Now we have,

$$\frac{\partial p_l}{\partial \sigma_l} = \left(e^{2(W(z_l)+t_l)} - 1 \right) + \sigma_l \frac{\partial v_l}{\partial z_l} \frac{\partial z_l}{\partial \sigma_l} \tag{3.82}$$

The first partial derivative on the right hand side of (3.82) is,

$$\frac{\partial v_l}{\partial z_l} = e^{2(W(z_l)+t_l)} 2 \frac{W(z_l)}{z_l(1+W(z_l))} \tag{3.83}$$

where we have used (3.33). The second partial derivative in (3.82) is,

$$\frac{\partial z_l}{\partial \sigma_l} = -\frac{1}{2} \sqrt{\frac{t_l e^{-2t_l}}{2\lambda\sigma_l}} \frac{1}{\sigma_l} = -\frac{1}{2} \frac{z_l}{\sigma_l} \tag{3.84}$$

Using (3.83) and (3.84) in (3.82), we have

$$\frac{\partial p_l}{\partial \sigma_l} = e^{2t_l} \frac{e^{2W(z_l)}}{1+W(z_l)} - 1 \tag{3.85}$$

which is (3.34).

3.8.3 Derivation of (3.35)

Starting from (3.32), we have

$$p_l + \sigma_l = \sigma_l e^{2(W(z_l)+t_l)} \tag{3.86}$$

with $z_l = \sqrt{\frac{t_l e^{-2t_l}}{2\lambda\sigma_l}}$. Our aim is to find $\frac{\partial p_l}{\partial t_l}$. Taking logarithm of (3.86), and differentiating both sides with respect to t_l, we have

$$\frac{1}{2}\frac{1}{\sigma_l + p_l}\frac{\partial p_l}{\partial t_l} = \frac{\partial W(z_l)}{\partial z_l}\frac{\partial z_l}{\partial t_l} + 1 \tag{3.87}$$

$\frac{\partial W(z_l)}{\partial z_l}$ is evaluated from (3.33) and $\frac{\partial z_l}{\partial t_l}$ is

$$\frac{\partial z_l}{\partial t_l} = \frac{1}{2}\sqrt{\frac{t_l e^{-2t_l}}{2\lambda\sigma_l}}\frac{1}{t_l} - \sqrt{\frac{t_l e^{-2t_l}}{2\lambda\sigma_l}} = z_l\left(\frac{1}{2t_l} - 1\right) \tag{3.88}$$

Using (3.33) and (3.88) in (3.87), we obtain

$$\frac{\partial p_l}{\partial t_l} = 2(\sigma_l + p_l)\left[\frac{W(z_l)}{1+W(z_l)}\left(\frac{1}{2t_l} - 1\right) + 1\right] \tag{3.89}$$

$$= \sigma_l e^{2(W(z_l)+t_l)}\frac{W(z_l) + 2t_l}{t_l(1+W(z_l))} \tag{3.90}$$

which is (3.35).

3.8.4 Proof of Lemma 3.8

Assume that sum powers at each slot $s_i \triangleq \sum_l b_{li}$ is given for each i. Consider the inner optimization in (3.58) for a fixed slot, say slot i. For convenience, we drop the slot index i, and denote s_i by s, and b_{li} by b_l. We define a function $x(s)$ as the minimization over b_l for fixed s as follows:

$$\begin{aligned} x(s) = \min_{b_l} \quad & \sum_l \frac{t_l}{\frac{1}{2}\log\left(e^{2t_l} + \frac{b_l}{\sigma_l}\right) - t_l} \\ \text{s.t.} \quad & \sum_l b_l = s, \quad b_l \geq 0, \quad \forall l \end{aligned} \tag{3.91}$$

which is the inner optimization in (3.58) for fixed i, and is also equivalent to:

$$\begin{aligned} x(s) = \min_{b_l} \quad & \sum_l \frac{t_l}{\frac{1}{2}\log\left(e^{2t_l} + \frac{b_l}{\sigma_l}\right) - t_l} \\ \text{s.t.} \quad & \sum_l b_l \leq s, \quad b_l \geq 0, \quad \forall l \end{aligned} \tag{3.92}$$

Now, we claim that $x(s)$ is non-increasing and convex in s. Since increasing s can only expand the feasible set, $x(s)$ is non-increasing in s. To prove the convexity: Let $s_1, s_2 \in \mathbf{R}^+$. Let $0 \leq \lambda \leq 1$ and $\bar{\lambda} = 1 - \lambda$. Let $\mathbf{b}_1$ be the solution of the problem with s_1, and $\mathbf{b}_2$ be the solution of the problem with s_2. Note that $\mathbf{b}_1$ and $\mathbf{b}_2$ exist and are unique due to convexity. The vector $\lambda\mathbf{b}_1 + \bar{\lambda}\mathbf{b}_2$ is feasible for the problem

with $\lambda s_1 + \bar{\lambda} s_2$ since the constraints are linear. Then,

$$x(\lambda s_1 + \bar{\lambda} s_2) \leq \sum_l \frac{t_l}{\frac{1}{2}\log\left(e^{2t_l} + \frac{\lambda b_{1l} + \bar{\lambda} b_{2l}}{\sigma_l}\right) - t_l} \tag{3.93}$$

$$\leq \sum_l \frac{\lambda t_l}{\frac{1}{2}\log\left(e^{2t_l} + \frac{b_{1l}}{\sigma_l}\right) - t_l} + \frac{\bar{\lambda} t_l}{\frac{1}{2}\log\left(e^{2t_l} + \frac{b_{2l}}{\sigma_l}\right) - t_l} \tag{3.94}$$

$$= \lambda x(s_1) + \bar{\lambda} x(s_2) \tag{3.95}$$

where (3.93) follows because the minimum value of the problem can be no larger than the objective value of any feasible point, (3.94) follows from the convexity of $\frac{1}{\log(a+x)}$, and (3.95) follows from the fact that $\mathbf{b}_1$ solves the problem with s_1 and $\mathbf{b}_2$ solves the problem with s_2. Now, the optimization problem in (3.58) can be written as:

$$\begin{aligned} \min_{s_i} \quad & \sum_{i=1}^{T} x(s_i) \\ \text{s.t.} \quad & \sum_{i=1}^{k} s_i \leq \sum_{i=1}^{k} G_i, \quad \forall i, \forall k \end{aligned} \tag{3.96}$$

The problem in (3.96) is in the same form as the problems in [5, eqn. (2)], [6, eqns. (6)-(8)] and [9, eqn. (15)] and is equivalent to the problem in [4, eqn. (3)], where a concave non-decreasing function of powers is maximized subject to energy harvesting constraints. In addition, [5, 6, 9] have additional finite battery constraints which we do not have here. References [4, 5] showed that the solution to this problem is invariant to the specific form of the function as long as it is convex (in minimization problems) or concave (in maximization problems). We follow the proof

in [9, Appendix B] and conclude that $\mathbf{s}$, the optimal solution of (3.96), is given by the single-link optimal transmit powers.

3.8.5 Proof of Lemma 3.9

We show that the conditions in (3.70)-(3.72) are equivalent to (3.62)-(3.64) therefore proving the necessity statement of the lemma.

1) Writing (3.62) for node n and the data links $l \in \mathcal{O}_d(n)$ connected to it

$$\frac{t_l}{2\sigma_l}\left[\frac{1}{2}\log\left(1+\frac{p_l}{\sigma_l}\right)-t_l\right]^{-2}\left(1+\frac{p_l}{\sigma_l}\right)^{-1}=\lambda_n-\beta_l\leq\lambda_n \tag{3.97}$$

Now, we claim that when $p_l > 0$, $\beta_l = 0$. Assume $p_l > 0$ and $\beta_l > 0$. From (3.68), this means that $p_l = \sigma_l(e^{2t_l}-1)$ and the delay at link l becomes $\frac{t_l}{0}$ which is unbounded for $t_l > 0$. Then, we must have $t_l = 0$, but this means $p_l = 0$, as otherwise power has been consumed on a link with zero flow. This is a contradiction to $p_l > 0$. Thus, $\beta_l = 0$ when $p_l > 0$ and (3.70) is satisfied with equality.

2) We choose any origin destination pair (n, d) and identify a path starting from node n and ending at destination node d, and in which all link powers and therefore flows are strictly positive. We denote this path by $\mathcal{F}_{n,d}$. We write the conditions (3.63) on links on this path and sum them to get

$$\begin{aligned}&\sum_{l\in\mathcal{F}_{n,d}}\frac{1}{2}\log\left(1+\frac{p_l}{\sigma_l}\right)\left[\frac{1}{2}\log\left(1+\frac{p_l}{\sigma_l}\right)-t_l\right]^{-2}\\&\quad=\sum_{l\in\mathcal{F}_{n,d}}\nu_{m(l)}-\nu_{n(l)}-2\beta_l\sigma_l e^{2t_l}+\gamma_l\end{aligned} \tag{3.98}$$

$$= \sum_{l \in \mathcal{F}_{n,d}} \nu_{m(l)} - \nu_{n(l)} \tag{3.99}$$

$$= \nu_d - \nu_n \tag{3.100}$$

$$= -\nu_n \tag{3.101}$$

where (3.99) follows from $\beta_l = \gamma_l = 0$ since $p_l > 0$, $t_l > 0$, (3.100) follows from telescoping the sum $\sum_{l \in \mathcal{F}_{n,d}} \nu_{n(l)} - \nu_{m(l)}$, and (3.101) follows from setting $\nu_d = 0$ since it is a destination node and there are no flow conservation constraints at that node. We let $\tilde{\nu}_n = -\nu_n$ and get (3.71).

3) For energy link q between nodes n and m, $k(q) = n$ and $z(q) = m$ in (3.64). From (3.64), we have $\lambda_n = \alpha_q \lambda_m + \theta_q \geq \alpha_q \lambda_m$ since $\theta_q \geq 0$. Then,

$$\frac{t_l}{2\sigma_l}\left[\frac{1}{2}\log\left(1+\frac{p_l}{\sigma_l}\right) - t_l\right]^{-2}\left(1+\frac{p_l}{\sigma_l}\right)^{-1}$$

$$= \lambda_n \tag{3.102}$$

$$\geq \alpha_q \lambda_m \tag{3.103}$$

$$= \alpha_q \frac{t_k}{2\sigma_k}\left[\frac{1}{2}\log\left(1+\frac{p_k}{\sigma_k}\right) - t_k\right]^{-2}\left(1+\frac{p_k}{\sigma_k}\right)^{-1} \tag{3.104}$$

where (3.102) and (3.104) are from using part 1 of Lemma 3.9 for node n and m, respectively. Equality is achieved when $y_q > 0$, since in this case $\theta_q = 0$ from (3.67).

CHAPTER 4

Cooperative Diamond Channel with Energy Harvesting Nodes

4.1 Introduction

In this chapter, we consider the cooperative energy harvesting diamond channel [68], see Fig. 4.1. We model the physical layer as a concatenation of a Gaussian broadcast channel and a Gaussian multiple access channel. Since the broadcast channel iss degraded, one of the relays has the message of the other relay. Therefore, the multiple access channel is an extended multiple access channel with common data [69], which we also call the cooperative multiple access channel. Our aim is to determine the optimum power and rate allocation policies of the users in order to maximize the end-to-end throughput of this system.

Prior work of particular relevance to our work in this chapter are [12–15, 76], where two-hop communication is considered with energy harvesting nodes for half- or full-duplex relay settings. Recently, in [61, 77], two-hop communication systems with two parallel relays are studied. In [77], two parallel half-duplex relays with various combinations of different transmission modes are considered. Due to the half-duplex nature of the relays, broadcast and multiple access operations are not

simultaneously possible. In [61], all four links of the broadcast and multiple access channels are restricted to be orthogonal, and no storage of data is allowed at the relays due to strict delay constraints. The setting in this chapter can be viewed as a generalization of [61] to general broadcast and multiple access channels, and general data storage at the relays.

In the setting of the diamond channel, see Fig. 4.1, when the transmission rates of the source in the broadcast side are fixed, the problem can be viewed as an energy harvesting multiple access channel where data packets as well as the harvested energies arrive at the transmitters intermittently over time. Of particular relevance to this specific problem, are references [10, 78, 79] where optimal scheduling problems on a multiple access channel are investigated. In [78], minimum energy scheduling problem over a multiple access channel where data packets arrive over time is solved. In [10], a multiple access channel with energy arrivals is considered but it is assumed that the users are infinitely backlogged, i.e., the data packets do not arrive over time. In [79], an energy harvesting multiple access channel with additional maximum power constraints on each user is considered. These previous works either consider data arrivals or energy arrivals but not both; in our current work, we need to consider both constraints due to the two-hop nature of the diamond channel.

In the first part of the chapter, in Section 4.3, we focus on the broadcast half of the diamond network. We first show that there exists an optimal source power allocation policy which is equal to the single-user optimal power policy for the source energy arrivals and does not depend on the relay energy arrivals. This

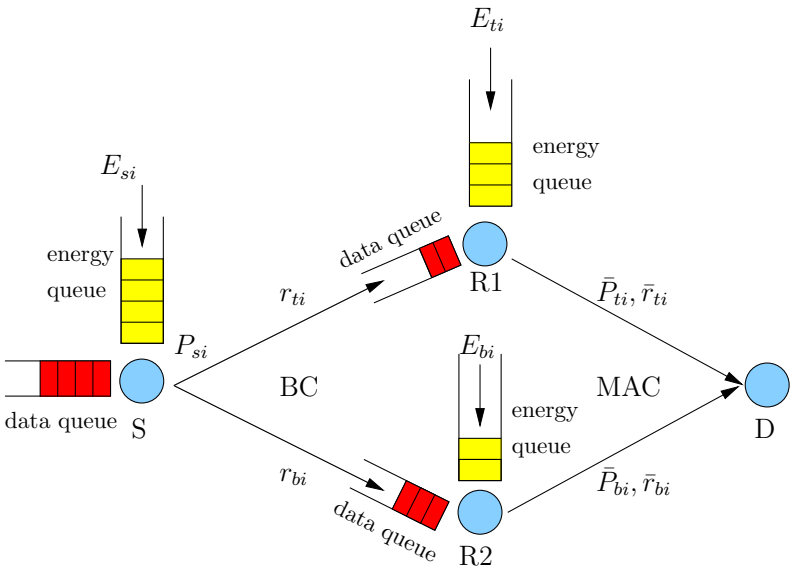

Figure 4.1: Cooperative diamond network with energy harvesting nodes.

is a generalization of [7, 9], which proved the optimality of a single-user power allocation for the capacity region of a broadcast channel; our work shows that the result remains the same even when the broadcast channel is concatenated with a multiple access channel. Our result is also a generalization of the *separation* result proved in [12, 13], which showed that, in a single relay channel, the source can optimize its transmit power irrespective of the relay's energy arrivals; our work shows that this result remains the same for the case of two relays forming a multiple access second hop. Next, we show that even though the total power can be selected as the single-user optimal power, the fraction of the power spent on each broadcast link depends on the energy arrivals of the relays. Specifically, we show that the optimal source rate allocation can be found by solving an optimal broadcasting problem with slot-dependent user priorities and these priorities can change only at instants when one of the relay data buffers is empty.

In the second part of the chapter, in Section 4.4, we turn our attention to the multiple access side of the diamond network. As mentioned before, this is a cooperative multiple access channel with common data. To take the full advantage of cooperation arising from common data, the relays need to use commonly generated codebooks. For simplicity of operation, the relays may choose to ignore the constructed common data, and operate the second hop as a regular multiple access channel. Therefore, we first consider a regular Gaussian multiple access channel for the second hop of the diamond channel. In this setting, first we note that when the transmission rates of the source in the broadcast side are fixed, the overall problem becomes a multiple access channel with both data and energy arrivals. Then, we show that this problem can be formulated in terms of data transmission rates only, instead of formulating over both transmission powers and data rates. In the multiple access channel with only energy arrivals, it was observed in [10], that the optimal sum rate is equal to the single-user optimal rate with both user energies merged. This may naturally suggest that, with the presence of the data causality constraints, the optimal sum rate is given by the single-user optimal rate with both data and energy causality constraints merged. In Section 4.4.1, we show that this suggestion is not entirely valid, but a majorization relationship exists between these two solutions. In Section 4.4.2, we solve the overall diamond channel problem with non-cooperative multiple access channel, using a dual decomposition method.

In the third part of the chapter, in Section 4.5, we recover the original setting of the diamond channel by focusing on the cooperative (extended) multiple access capacity region. With the extended multiple access capacity region, we find the

overall solution using a decomposition into inner and outer maximization problems. The outer problem consists of finding the optimal source transmission rates in the broadcast side. The inner problem consists of finding the optimal relay rate and power allocations when the transmission rates of the source in the broadcast side are fixed. We solve the overall problem by iterating between the two sides.

4.2 System Model

We consider the energy harvesting diamond channel shown in Fig. 4.1. The harvested energies are saved in the corresponding batteries. The physical layer is modeled as a concatenation of a broadcast channel and a multiple access channel. In the broadcast channel, relay 1 is the stronger receiver: the channel noises have variances $\sigma_1^2 \leq \sigma_2^2$. The Gaussian broadcast channel capacity region with transmitter power p is given by [44]

$$\mathcal{C}_{BC}(p) = \left\{ r_1 \leq f\left(\frac{\alpha p}{\sigma_1^2}\right), \quad r_2 \leq f\left(\frac{(1-\alpha)p}{\alpha p + \sigma_2^2}\right) \right\} \tag{4.1}$$

where α is the fraction of power spent for the message of user 1, and $f(x) \triangleq \frac{1}{2}\log(1+x)$. The function $g(r_1, r_2)$ is the minimum energy required to transmit at rates (r_1, r_2):

$$g(r_1, r_2) \triangleq \sigma_1^2 2^{2(r_1+r_2)} + (\sigma_2^2 - \sigma_1^2)2^{2r_2} - \sigma_2^2 \tag{4.2}$$

and is strictly convex in (r_1, r_2). Since relay 2 is degraded with respect to relay 1, relay 1 can decode the messages intended for relay 2. Therefore, the second hop is an extended multiple access channel with common data. The capacity region for this channel with transmitter powers (p_1, p_2) and Gaussian noise power σ_3^2 is given as [68, 69, 80]:

$$\mathcal{C}_{EMAC}(p_1, p_2) = \Big\{ r_1 \leq f((1-\beta)p_1/\sigma_3^2), \\ r_1 + r_2 \leq f\left((p_1 + p_2 + 2\sqrt{\beta p_1 p_2})/\sigma_3^2\right) \Big\} \tag{4.3}$$

If the presence of common data is ignored, the second hop becomes a regular Gaussian multiple access channel whose capacity region is given as [44]:

$$\mathcal{C}_{MAC}(p_1, p_2) = \Big\{ r_1 \leq f(p_1/\sigma_3^2),\ r_2 \leq f(p_2/\sigma_3^2), \\ r_1 + r_2 \leq f((p_1 + p_2)/\sigma_3^2) \Big\} \tag{4.4}$$

There are N equal length slots of duration τ seconds and $\tau = 1$ is assumed without loss of generality. We refer to relay 1 as the *top* and relay 2 as the *bottom* relay and use subscripts t and b to denote their parameters; subscript s denotes the source node's parameters. In slot i, the source, top and bottom relays harvest energy with amounts E_{si}, E_{ti}, E_{bi}, respectively. We denote the transmission power of the source as p_{si} and source rates to the top (bottom) relay as r_{ti} (r_{bi}), the transmission power of the top (bottom) relay to the destination as $\bar{p}_{ti}$ ($\bar{p}_{bi}$) and data rates of the top (bottom) relays to the destination as $\bar{r}_{ti}$ ($\bar{r}_{bi}$). We denote these power and rate

sequences with the vectors $\mathbf{p}_s, \bar{\mathbf{p}}_t, \bar{\mathbf{p}}_b, \mathbf{r}_t, \mathbf{r}_b, \bar{\mathbf{r}}_t, \bar{\mathbf{r}}_b$. The energy that has not yet been harvested cannot be used, leading to the following *energy causality constraints* at all transmitters:

$$\sum_{i=1}^{k} \bar{p}_{ti} \leq \sum_{i=1}^{k} E_{ti}, \quad \forall k \tag{4.5}$$

$$\sum_{i=1}^{k} \bar{p}_{bi} \leq \sum_{i=1}^{k} E_{bi}, \quad \forall k \tag{4.6}$$

$$\sum_{i=1}^{k} p_{si} \leq \sum_{i=1}^{k} E_{si}, \quad \forall k \tag{4.7}$$

The relays cannot forward data that has not yet arrived, leading to the following *data causality constraints* at the relays:

$$\sum_{i=1}^{k} \bar{r}_{ti} \leq \sum_{i=1}^{k} r_{ti}, \quad \forall k \tag{4.8}$$

$$\sum_{i=1}^{k} \bar{r}_{bi} \leq \sum_{i=1}^{k} r_{bi}, \quad \forall k \tag{4.9}$$

The rate allocations must be achievable for each channel:

$$(r_{ti}, r_{bi}) \in \mathcal{C}_{BC}(p_{si}), \quad \forall i \tag{4.10}$$

$$(\bar{r}_{ti}, \bar{r}_{bi}) \in \mathcal{C}_{EMAC}(\bar{p}_{ti}, \bar{p}_{bi}), \quad \forall i \tag{4.11}$$

where we will use $\mathcal{C}_{MAC}(\bar{p}_{ti}, \bar{p}_{bi})$ in (4.11), if we operate the second hop as a regular multiple access channel.

We aim to maximize the end-to-end throughput:

$$\max_{\mathbf{p}_s,\bar{\mathbf{p}}_t,\bar{\mathbf{p}}_b,\mathbf{r}_t,\mathbf{r}_b,\bar{\mathbf{r}}_t,\bar{\mathbf{r}}_b,\boldsymbol{\alpha}} \quad \sum_{i=1}^{N}\bar{r}_{ti}+\sum_{i=1}^{N}\bar{r}_{bi}$$

$$\text{s.t.} \quad (4.5)\text{-}(4.11) \tag{4.12}$$

In this chapter we will solve the problem in (4.12). We will separately focus on the broadcast and the multiple access sides of the problem in the following sections.

4.3 Broadcast Channel Side

First, we will focus on the broadcast side of the problem. We consider the source which is broadcasting data to the two relays, and focus on the source power (p_{si}) and rate (r_{ti}, r_{bi}) allocations. We first prove some properties of the optimal solution which hold regardless of the existence of the multiple access link.

Lemma 4.1 *Either the source energy or both of the relay energies must be consumed fully.*

Proof: The proof follows by contradiction. If any excess energy is left, then we can increase the rates, which contradicts optimality. ■

Lemma 4.2 *There exists an optimal source profile* $(\mathbf{p}_s^*, \mathbf{r}_t^*, \mathbf{r}_b^*)$ *that is on the boundary of the broadcast capacity region in each slot, i.e.,*

$$r_{ti}^* = f\left(\frac{\alpha_i p_{si}^*}{\sigma_1^2}\right), \quad r_{bi}^* = f\left(\frac{(1-\alpha_i)p_{si}^*}{\alpha p_{si}^* + \sigma_2^2}\right), \forall i. \tag{4.13}$$

Proof: In slots where the constraints $r_{ti}^* \leq f\left(\frac{\alpha_i p_{si}^*}{\sigma_1^2}\right)$ and $r_{bi}^* \leq f\left(\frac{(1-\alpha_i)p_{si}^*}{\alpha p_{si}^* + \sigma_2^2}\right)$ are satisfied with strict inequality, we can increase r_{ti}^* or r_{bi}^* without violating any feasibility constraints as we can always increase the right hand sides of the data feasibility constraints in (4.8) and (4.9). ■

Using Lemma 4.2 we can remove the broadcast capacity region constraints from the problem and let $p_{si} = g(r_{ti}, r_{bi})$. The corresponding energy causality constraints for the source node can now be written as:

$$\sum_{i=1}^{k} g(r_{ti}, r_{bi}) \leq \sum_{i=1}^{k} E_{si}, \quad \forall k \tag{4.14}$$

The optimization problem can now be written as:

$$\begin{aligned} \max_{\bar{\mathbf{p}}_t, \bar{\mathbf{p}}_b, \mathbf{r}_t, \mathbf{r}_b, \bar{\mathbf{r}}_t, \bar{\mathbf{r}}_b} \quad & \sum_{i=1}^{N} \bar{r}_{ti} + \sum_{i=1}^{N} \bar{r}_{bi} \\ \text{s.t.} \quad & \text{(4.5)-(4.6), (4.8)-(4.9), (4.11), (4.14)} \end{aligned} \tag{4.15}$$

The following theorem states a key structural property of the optimal policy, and is proved in Appendix 4.8.1.

Theorem 4.1 *There exists an optimal total source power sequence $g(r_{ti}^*, r_{bi}^*)$ which is the same as the single-user optimal transmit power sequence for the energy arrivals E_{si}.*

Theorem 4.1 tells us that there exists a solution to the problem in (4.15) in which $g(r_{ti}^*, r_{bi}^*) = P_i$, where P_is are the single-user optimal transmit powers for the en-

ergy arrivals E_{si}. This constraint can always be relaxed to $g(r_{ti}, r_{bi}) \leq P_i$. Using Theorem 4.1, the optimization problem becomes:

$$\begin{aligned} \max_{\bar{\mathbf{p}}_t, \bar{\mathbf{p}}_b, \mathbf{r}_t, \mathbf{r}_b, \bar{\mathbf{r}}_t, \bar{\mathbf{r}}_b} \quad & \sum_{i=1}^{N} \bar{r}_{ti} + \sum_{i=1}^{N} \bar{r}_{bi} \\ \text{s.t.} \quad & \text{(4.5)-(4.6), (4.8)-(4.9), (4.11), } g(r_{ti}, r_{bi}) \leq P_i \end{aligned} \tag{4.16}$$

We note that the single-user optimal transmit powers P_is can be found by the directional water filling algorithm in [6] or the staircase water filling algorithm in [54]. Theorem 4.1 generalizes the results of [7, 9] to the case of concatenated networks, and the results of [12, 13] to the case of multiple relays. While the source power does not depend on the energy arrival profile of the relays, the fraction of the total power spent on each broadcast link depends on the energy arrival profile of the relays. In the following lemmas, we show how to find the distribution of power over the broadcast links.

Lemma 4.3 *There exists a positive real vector* $\boldsymbol{\mu} \triangleq \{\mu_i\}_{i=1}^{N}, \mu_i \in [0, 1]$ *such that* (r_{ti}^*, r_{bi}^*) *simultaneously solves the problem in (4.16) and the following optimization problem:*

$$\begin{aligned} \max_{r_{ti}, r_{bi}} \quad & \sum_{i=1}^{N} \mu_i r_{ti} + \sum_{i=1}^{N} r_{bi} \\ \text{s.t.} \quad & g(r_{ti}, r_{bi}) \leq P_i \end{aligned} \tag{4.17}$$

Lemma 4.4 μ_i *can increase (decrease) only when the bottom (top) data buffer is*

empty.

The proofs of Lemma 4.3 and Lemma 4.4 are given in Appendix 4.8.2.

In a single-hop broadcasting problem as in [7–9], the capacity region can be traced by solving the following optimization problem: $\max_{r_{1i},r_{2i}} \mu_1 \sum_{i=1}^{N} r_{1i} + \mu_2 \sum_{i=1}^{N} r_{2i}$ for some $\mu_1, \mu_2 \in \mathbb{R}^+$. Here, μ_1, μ_2 are called *user priorities* and are constant throughout slots. Lemmas 4.3 and 4.4 show us that the existence of a multiple access layer affects the broadcast layer by introducing variable user priorities in time. The user priorities can change only when one of the data buffers is empty: the priority of the first user can increase only when the bottom data buffer is empty, and can decrease only when the top data buffer is empty. From [7], the solution to (4.17) is:

$$r_{ti} = \frac{1}{2}\log(1 + \min\{P_{ci}, P_i\}) \tag{4.18}$$

$$r_{bi} = \frac{1}{2}\log\left(1 + \frac{(P_i - P_{ci})^+}{P_{ci} + \sigma_2^2}\right) \tag{4.19}$$

where, if $\mu_i \geq 1$, all of the power is allocated to the top relay only. If $\mu_i < 1$, we define

$$P_{ci} \triangleq \left(\frac{\mu_i \sigma_2^2 - \sigma_1^2}{1 - \mu_i}\right)^+ \tag{4.20}$$

In other words, given (μ_i, P_i), the rate pairs (r_{ti}, r_{bi}) can uniquely be determined from (4.18) and (4.19). We denote the unique rate pairs found from (4.18) and (4.19) for fixed (μ_i, P_i) by $r_{ti}(\mu_i, P_i)$ and $r_{bi}(\mu_i, P_i)$. Let us define the function $z(\boldsymbol{\mu})$

which is a maximization over $(\bar{\mathbf{p}}_t, \bar{\mathbf{p}}_b, \bar{\mathbf{r}}_t, \bar{\mathbf{r}}_b)$ for fixed $\boldsymbol{\mu}$:

$$\begin{aligned} z(\boldsymbol{\mu}) = \max_{\bar{\mathbf{p}}_t, \bar{\mathbf{p}}_b, \bar{\mathbf{r}}_t, \bar{\mathbf{r}}_b} \quad & \sum_{i=1}^{N} \bar{r}_{ti} + \sum_{i=1}^{N} \bar{r}_{bi} \\ \text{s.t.} \quad & \sum_{i=1}^{k} \bar{r}_{ti} \leq \sum_{i=1}^{k} r_{ti}(\mu_i, P_i), \quad \forall k \\ & \sum_{i=1}^{k} \bar{r}_{bi} \leq \sum_{i=1}^{k} r_{bi}(\mu_i, P_i), \quad \forall k \\ & \text{(4.5)-(4.6), (4.11)} \end{aligned} \tag{4.21}$$

Then, the original problem in (4.12) is equivalent to:

$$\max_{\boldsymbol{\mu} \in [0,1]^N} z(\boldsymbol{\mu}) \tag{4.22}$$

4.4 Non-Cooperative Multiple Access Channel Side

In this section, we consider the regular multiple access channel by ignoring the presence of common data. We note that the problem in (4.21) is a throughput maximization problem in an energy harvesting multiple access channel with data arrivals as shown in Fig. 4.2. For notational convenience, we denote $d_{ti} = r_{ti}(\mu_i, P_i), d_{bi} = r_{bi}(\mu_i, P_i)$. When $\boldsymbol{\mu}$ is fixed, the data arrivals to the multiple access side are fixed and the data causality constraints can be written as

$$\sum_{i=1}^{k} \bar{r}_{ti} \leq \sum_{i=1}^{k} d_{ti}, \quad \forall k \tag{4.23}$$

$$\sum_{i=1}^{k} \bar{r}_{bi} \leq \sum_{i=1}^{k} d_{bi}, \quad \forall k \tag{4.24}$$

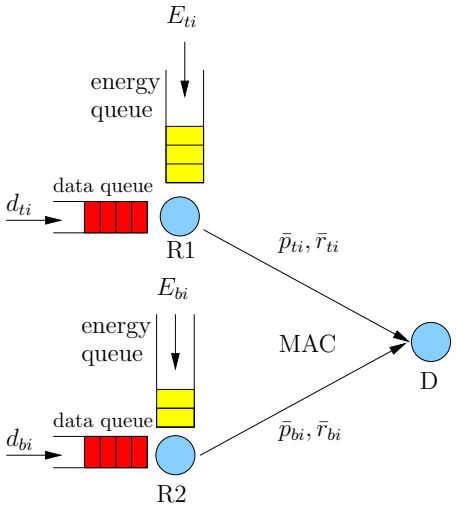

Figure 4.2: Multiple access channel with energy and data arrivals.

We start this section by reformulating the problem in terms of the rates only. We consider the following energy causality constraints on the rates:

$$\sum_{i=1}^{k} \sigma_3^2(2^{2\bar{r}_{ti}} - 1) \leq \sum_{i=1}^{k} E_{ti}, \quad \forall k \tag{4.25}$$

$$\sum_{i=1}^{k} \sigma_3^2(2^{2\bar{r}_{bi}} - 1) \leq \sum_{i=1}^{k} E_{bi}, \quad \forall k \tag{4.26}$$

$$\sum_{i=1}^{k} \sigma_3^2(2^{2(\bar{r}_{ti}+\bar{r}_{bi})} - 1) \leq \sum_{i=1}^{k} E_{ti} + E_{bi}, \quad \forall k \tag{4.27}$$

and the corresponding throughput maximization problem:

$$\begin{aligned} \max_{\bar{r}_{ti}, \bar{r}_{bi}} \quad & \sum_{i=1}^{N} \bar{r}_{ti} + \sum_{i=1}^{N} \bar{r}_{bi} \\ \text{s.t.} \quad & (4.23)\text{-}(4.27) \end{aligned} \tag{4.28}$$

The following lemma, proved in Appendix 4.8.3, shows that this is an equivalent

representation for the problem in (4.21).

Lemma 4.5 *The problems in (4.21) and (4.28) are equivalent.*

We solve the problem in (4.28) in the remainder of this section. We denote the optimal solution to (4.28) by $(\bar{r}^*_{ti}, \bar{r}^*_{bi})$. We have the following lemma.

Lemma 4.6 *The optimal sum rate for relays is non-decreasing in time, i.e.,* $\bar{r}^*_{ti} + \bar{r}^*_{bi} \leq \bar{r}^*_{t,i+1} + \bar{r}^*_{b,i+1}, \forall i$.

Proof: The proof follows by contradiction. Assume that there is a slot k such that $\bar{r}^*_{tk} + \bar{r}^*_{bk} > \bar{r}^*_{t,k+1} + \bar{r}^*_{b,k+1}$. We will show that this policy cannot be optimal. There can be three cases, case 1: $\bar{r}^*_{tk} > \bar{r}^*_{t,k+1}, \bar{r}^*_{bk} \leq \bar{r}^*_{b,k+1}$, case 2: $\bar{r}^*_{bk} > \bar{r}^*_{b,k+1}, \bar{r}^*_{tk} \leq \bar{r}^*_{t,k+1}$ and case 3: $\bar{r}^*_{bk} > \bar{r}^*_{b,k+1}, \bar{r}^*_{tk} > \bar{r}^*_{t,k+1}$. Assume that the first case happens. Consider the modified policy $\hat{r}_{tk} = \hat{r}_{t,k+1} = \frac{\bar{r}^*_{tk} + \bar{r}^*_{t,k+1}}{2}$. This modified policy is feasible and transmits the same amount of data as $\bar{r}^*_{ti}, \bar{r}^*_{bi}$, but due to the convexity of the functions $2^{2(\bar{r}_{ti} + \bar{r}_{bi})}$ and $2^{2\bar{r}_{ti}}$, consumes less energy. This additional energy can be used to transmit more data and therefore the policy $(\bar{r}^*_{ti}, \bar{r}^*_{bi})$ cannot be optimal. For the second case, we set $\hat{r}_{bk} = \hat{r}_{b,k+1} = \frac{\bar{r}^*_{bk} + \bar{r}^*_{b,k+1}}{2}$ and for the third case we modify both $\bar{r}^*_{tk}, \bar{r}^*_{t,k+1}$ and $\bar{r}^*_{bk}, \bar{r}^*_{b,k+1}$ to reach a similar contradiction. ■

4.4.1 Relaxed Problem and Majorization

Without the data causality constraints of (4.23) and (4.24) it was observed in [10], that the optimal sum rate is equal to the single-user optimal rate with the energies merged as $E_{ti} + E_{bi}$. This may naturally suggest that, with the presence of the data

causality constraints, the optimal sum rate is given by the single-user optimal rate with both data and energy causality constraints. In this section, we show that this suggestion is not entirely valid, but a majorization relationship exists between these two solutions. Consider the following problem:

$$\begin{aligned} \max_{q_i} \quad & \sum_{i=1}^{N} q_i \\ \text{s.t.} \quad & \sum_{i=1}^{k} \sigma_3^2(2^{2q_i}-1) \leq \sum_{i=1}^{k} E_{ti} + E_{bi}, \quad \forall k \\ & \sum_{i=1}^{k} q_i \leq \sum_{i=1}^{k} d_{ti} + d_{bi}, \quad \forall k \end{aligned} \tag{4.29}$$

This problem can be solved using the geometric approach in [4] or the directional waterfilling with both data and energy arrivals in [6]. We note that the problem in (4.29) is a relaxed version of (4.28) where the energy arrivals and data arrivals are merged to a single-user. I.e., we sum up (4.23) and (4.24) to obtain a single data arrival constraint and remove (4.25) and (4.26). We denote the solution to (4.29) by q_i^*. Now, we show two weak majorization results whose proofs are provided in Appendix 4.8.4 and 4.8.5 respectively.

Lemma 4.7 *We must have* $\sum_{i=1}^{k} \bar{r}_{ti}^* + \bar{r}_{bi}^* \leq \sum_{i=1}^{k} q_i^*, \forall k$.

Lemma 4.8 *If at any slot* k*, we have* $\sum_{i=1}^{k} \bar{r}_{ti}^* + \bar{r}_{bi}^* = \sum_{i=1}^{k} q_i^*$*, then* $\sum_{i=1}^{k} 2^{2(\bar{r}_{ti}^* + \bar{r}_{bi}^*)} \geq \sum_{i=1}^{k} 2^{2q_i^*}$*. If, in addition, we have* $\sigma_3^2 \left(\sum_{i=1}^{k} 2^{2q_i^*} - 1 \right) = \sum_{i=1}^{k} E_{ti} + E_{bi}$*, then we must have* $\bar{r}_{ti}^* + \bar{r}_{bi}^* = q_i^*$ *for* $i = 1, \ldots, k$.

In some special instances of the problem, Lemmas 4.7 and 4.8 can be utilized, by enforcing the constraint $\bar{r}_{ti} + \bar{r}_{bi} = q_i^*, \forall i$, replacing $\bar{r}_{bi} = q_i^* - \bar{r}_{ti}$ and solving a

single-user problem.

4.4.2 Iterative Solution

In this section, we will solve the overall problem by utilizing a dual decomposition method. After applying Lemma 4.5, the problem in (4.16) is equivalent to:

$$\begin{aligned} \max_{\bar{r}_{ti},\bar{r}_{bi},r_{ti},r_{bi}} \quad & \sum_{i=1}^{N} \bar{r}_{ti} + \sum_{i=1}^{N} \bar{r}_{bi} \\ \text{s.t.} \quad & (4.8),\ (4.9),\ (4.25)\text{-}(4.27), g(r_{ti}, r_{bi}) \leq P_i \end{aligned} \tag{4.30}$$

Defining a new variable as $w_i = \bar{r}_{ti} + \bar{r}_{bi}$, we formulate the following equivalent optimization problem:

$$\begin{aligned} \max_{\bar{r}_{ti},\bar{r}_{bi},r_{ti},r_{bi},w_i} \quad & \sum_{i=1}^{N} w_i \\ \text{s.t.} \quad & (4.8),\ (4.9),\ (4.25),\ (4.26), g(r_{ti}, r_{bi}) \leq P_i \\ & \sum_{i=1}^{k} \sigma_3^2 (2^{2w_i} - 1) \leq \sum_{i=1}^{k} E_{ti} + E_{bi}, \quad \forall k \\ & w_i = \bar{r}_{ti} + \bar{r}_{bi}, \quad \forall i \end{aligned} \tag{4.31}$$

which can be relaxed to:

$$\begin{aligned} \max_{\bar{r}_{ti},\bar{r}_{bi},r_{ti},r_{bi},w_i} \quad & \sum_{i=1}^{N} w_i \\ \text{s.t.} \quad & (4.8),\ (4.9),\ (4.25),\ (4.26), g(r_{ti}, r_{bi}) \leq P_i \end{aligned}$$

$$\sum_{i=1}^{k} \sigma_3^2 \left(2^{2w_i} - 1\right) \leq \sum_{i=1}^{k} E_{ti} + E_{bi}, \quad \forall k$$

$$w_i \leq \bar{r}_{ti} + \bar{r}_{bi}, \quad \forall i \tag{4.32}$$

since at slots where the last inequality is not satisfied with equality, $\bar{r}_{ti}$ and $\bar{r}_{bi}$ can be decreased until equality is satisfied without changing the throughput. The problem in (4.32) is convex since the objective function is linear and the constraints are convex. Define the following sets:

$$\mathcal{R}_s = \{(r_{ti}, r_{bi}) \in (\mathbb{R}^+ \times \mathbb{R}^+) : g(r_{ti}, r_{bi}) \leq P_i, \, \forall i\} \tag{4.33}$$

$$\mathcal{R}_t = \{\bar{r}_{ti} \in \mathbb{R}^+ : \sum_{i=1}^{k} \sigma_3^2 (2^{2\bar{r}_{ti}} - 1) \leq \sum_{i=1}^{k} E_{ti}, \, \forall k\} \tag{4.34}$$

$$\mathcal{R}_b = \{\bar{r}_{bi} \in \mathbb{R}^+ : \sum_{i=1}^{k} \sigma_3^2 (2^{2\bar{r}_{bi}} - 1) \leq \sum_{i=1}^{k} E_{bi}, \, \forall k\} \tag{4.35}$$

$$\mathcal{R}_w = \{w_i \in \mathbb{R}^+ : \sum_{i=1}^{k} \sigma_3^2 (2^{2w_i} - 1) \leq \sum_{i=1}^{k} E_{ti} + E_{bi}, \, \forall k\} \tag{4.36}$$

Now, we write the partial Lagrangian function for the problem in (4.32) corresponding to the constraints (4.8), (4.9) and $w_i \leq \bar{r}_{ti} + \bar{r}_{bi}$ as follows:

$$\begin{aligned} \mathcal{L} = & \sum_{i=1}^{N} w_i + \sum_{k=1}^{N} \lambda_{1k} \left(\sum_{i=1}^{k} r_{ti} - \sum_{i=1}^{k} \bar{r}_{ti} \right) \\ & + \sum_{k=1}^{N} \lambda_{2k} \left(\sum_{i=1}^{k} r_{bi} - \sum_{i=1}^{k} \bar{r}_{bi} \right) + \sum_{i=1}^{N} \nu_i \left(\bar{r}_{ti} + \bar{r}_{bi} - w_i \right) \end{aligned} \tag{4.37}$$

Now, the dual function is [70]:

$$\mathcal{K}(\boldsymbol{\lambda}_1, \boldsymbol{\lambda}_2, \boldsymbol{\nu}) = \max_{(r_{ti}, r_{bi}) \in \mathcal{R}_s, \bar{r}_{ti} \in \mathcal{R}_t, \bar{r}_{bi} \in \mathcal{R}_b, w_i \in \mathcal{R}_w} \mathcal{L}(\mathbf{r}_t, \mathbf{r}_b, \bar{\mathbf{r}}_t, \bar{\mathbf{r}}_b, \mathbf{w}) \tag{4.38}$$

$$\begin{aligned} &= \max_{(r_{ti}, r_{bi}) \in \mathcal{R}_s} \left[\sum_{i=1}^{N} r_{ti} \sum_{k=i}^{N} \lambda_{1k} + \sum_{i=1}^{N} r_{bi} \sum_{k=i}^{N} \lambda_{2k} \right] \\ &\quad + \max_{\bar{r}_{ti} \in \mathcal{R}_t} \left[\sum_{i=1}^{N} \bar{r}_{ti} \left(\nu_i - \sum_{k=i}^{N} \lambda_{1k} \right) \right] \\ &\quad + \max_{\bar{r}_{bi} \in \mathcal{R}_b} \left[\sum_{i=1}^{N} \bar{r}_{bi} \left(\nu_i - \sum_{k=i}^{N} \lambda_{2k} \right) \right] \\ &\quad + \max_{w_i \in \mathcal{R}_w} \sum_{i=1}^{N} (1 - \nu_i) w_i \end{aligned} \tag{4.39}$$

Denote the collection of Lagrange multiplier vectors as $\boldsymbol{\gamma} \triangleq (\boldsymbol{\lambda}_1, \boldsymbol{\lambda}_2, \boldsymbol{\nu})$. For fixed $\boldsymbol{\gamma}$, we define the following subproblems:

$$\mathcal{K}_1(\boldsymbol{\gamma}) = \max_{(r_{ti}, r_{bi}) \in \mathcal{R}_s} \sum_{i=1}^{N} r_{ti} \sum_{k=i}^{N} \lambda_{1k} + \sum_{i=1}^{N} r_{bi} \sum_{k=i}^{N} \lambda_{2k} \tag{4.40}$$

$$\mathcal{K}_2(\boldsymbol{\gamma}) = \max_{\bar{r}_{ti} \in \mathcal{R}_t} \sum_{i=1}^{N} \bar{r}_{ti} \left(\nu_i - \sum_{k=i}^{N} \lambda_{1k} \right) \tag{4.41}$$

$$\mathcal{K}_3(\boldsymbol{\gamma}) = \max_{\bar{r}_{bi} \in \mathcal{R}_b} \sum_{i=1}^{N} \bar{r}_{bi} \left(\nu_i - \sum_{k=i}^{N} \lambda_{2k} \right) \tag{4.42}$$

$$\mathcal{K}_4(\boldsymbol{\gamma}) = \max_{w_i \in \mathcal{R}_w} \sum_{i=1}^{N} (1 - \nu_i) w_i \tag{4.43}$$

Slater's condition holds for the problem in (4.30) [70]. Therefore, there is no duality gap and the optimal values of the dual problem and the primal problem are

the same. This implies that (4.30) is equivalent to the following problem:

$$\min_{\boldsymbol{\gamma} \geq \mathbf{0}} \quad \mathcal{K}(\boldsymbol{\gamma}) \tag{4.44}$$

or equivalently:

$$\min_{\boldsymbol{\gamma} \geq \mathbf{0}} \quad \mathcal{H}(\boldsymbol{\gamma}) \tag{4.45}$$

where $\mathcal{H} \triangleq \mathcal{K}_1 + \mathcal{K}_2 + \mathcal{K}_3 + \mathcal{K}_4$. We observe that for fixed $\boldsymbol{\gamma}$ we can solve the subproblems independently. We solve the problem in (4.45) by separately solving the outer minimization and inner maximization problems.

4.4.2.1 Inner Maximization

Here, we focus on the inner problems (4.40)-(4.43). We start by analyzing (4.40). We define $a_i = \sum_{k=i}^{N} \lambda_{1k}$ and $b_i = \sum_{k=i}^{N} \lambda_{2k}$. Then (4.40) becomes:

$$\begin{aligned} \max_{r_{ti}, r_{bi}} \quad & \sum_{i=1}^{N} a_i r_{ti} + \sum_{i=1}^{N} b_i r_{bi} \\ \text{s.t.} \quad & g(r_{ti}, r_{bi}) \leq P_i \end{aligned} \tag{4.46}$$

Since the constraint set depends only on index i, (4.46) is solved individually for each i as follows:

$$\max_{r_{ti}, r_{bi}} \quad a_i r_{ti} + b_i r_{bi}$$

$$\text{s.t.} \quad g(r_{ti}, r_{bi}) \leq P_i \tag{4.47}$$

The problem in (4.47) is a single-user throughphut maximization problem in a broadcast channel setting as in [7] with user priorities as a_i and b_i. Therefore, the solution to (4.47) is given by $r_{ti}(a_i/b_i, P_i)$ and $r_{bi}(a_i/b_i, P_i)$ with the definitions as given in (4.18)-(4.20).

Now, we examine (4.41). We define $c_i \triangleq \nu_i - \sum_{k=i}^{N} \lambda_{1k}$ and with this definition (4.41) becomes:

$$\begin{aligned} \max_{\bar{r}_{ti}} \quad & \sum_{i=1}^{N} c_i \bar{r}_{ti} \\ \text{s.t.} \quad & \sum_{i=1}^{k} \sigma_3^2 (2^{2\bar{r}_{ti}} - 1) \leq \sum_{i=1}^{k} E_{ti}, \quad \forall k \end{aligned} \tag{4.48}$$

We reformulate the problem in (4.48) in terms of powers as:

$$\begin{aligned} \max_{\bar{p}_{ti}} \quad & \sum_{i=1}^{N} \frac{c_i}{2} \log\left(1 + \frac{\bar{p}_{ti}}{\sigma_3^2}\right) \\ \text{s.t.} \quad & \sum_{i=1}^{k} \bar{p}_{ti} \leq \sum_{i=1}^{k} E_{ti}, \quad \forall k \end{aligned} \tag{4.49}$$

The problem in (4.48) is a convex optimization problem and by a Lagrangian analysis similar to [6] we obtain:

$$\bar{p}_{ti} = \left(\frac{c_i}{\sum_{k=i}^{N} \pi_k} - 1\right)^+ = c_i \left(\frac{1}{\sum_{k=i}^{N} \pi_k} - \frac{1}{c_i}\right)^+ \tag{4.50}$$

where π_k is the Lagrange multiplier corresponding to the energy causality constraint

at slot k in (4.49). The solution to (4.50) is given by directional waterfilling on rectangles of width c_i and base level $1/c_i$ as explained in [81, Fig. 2]. In slots where $c_i < 0$, no power should be allocated and those slots can be treated as if they are not there.

The problems in (4.42) and (4.43) have the same structure and are solved similarly. In (4.42), the fading levels are $d_i \triangleq \nu_i - \sum_{k=i}^{N} \lambda_{2k}$ and energy arrivals are E_{bi} and in (4.43), the fading levels are $(1-\nu_i)$ and energy arrivals are $E_{ti} + E_{bi}$. If the fading levels are negative in any slot, those slots can be skipped. Denote the solutions to $\mathcal{K}_1(\boldsymbol{\gamma})$ by $(r_{ti}^*(\boldsymbol{\gamma}), r_{bi}^*(\boldsymbol{\gamma}))$ and the solutions to $\mathcal{K}_2(\boldsymbol{\gamma}), \mathcal{K}_3(\boldsymbol{\gamma}), \mathcal{K}_4(\boldsymbol{\gamma})$ by $\bar{r}_{ti}^*(\boldsymbol{\gamma}), \bar{r}_{bi}^*(\boldsymbol{\gamma})$ and $w_i^*(\boldsymbol{\gamma})$, respectively.

4.4.2.2 Outer Minimiziation

The outer minimization problem is the problem of finding optimal $\boldsymbol{\gamma}$ in (4.45). For this problem we will use the normalized subgradient method, which is defined as

$$\boldsymbol{\gamma}^{l+1} = \left(\boldsymbol{\gamma}^l - \zeta_l \frac{\boldsymbol{v}^l}{\|\boldsymbol{v}^l\|} \right)^+ \tag{4.51}$$

where $\boldsymbol{\gamma}^{l+1}$ is the lth iterate, $\boldsymbol{v}^l$ is any subgradient of h at $\boldsymbol{\gamma}^l$ and $\zeta_l > 0$ is the lth step size. The $(+)$ operator is used to enforce the constraints that $\boldsymbol{\gamma} \geq \mathbf{0}$. For completeness, first we define the subgradient of a function: $\boldsymbol{v}$ is a subgradient of $\mathcal{H}$ at $\boldsymbol{x}$ if [70, Eq. (6.20)]

$$\mathcal{H}(\boldsymbol{y}) \geq \mathcal{H}(\boldsymbol{x}) + \boldsymbol{v}^{\mathsf{T}}(\boldsymbol{y} - \boldsymbol{x}), \quad \forall \boldsymbol{y} \tag{4.52}$$

Now, we show that a subgradient for $\mathcal{H}(\boldsymbol{\gamma})$ is readily available once the inner maximization problems are solved. The following lemma is proved in Appendix 4.8.6.

Lemma 4.9 *The vector* $\left[\left(\sum_{i=1}^{k} r_{ti}^{*}(\boldsymbol{\gamma}^l) - \sum_{i=1}^{k} \bar{r}_{ti}^{*}(\boldsymbol{\gamma}^l) \right), \left(\sum_{i=1}^{k} r_{bi}^{*}(\boldsymbol{\gamma}^l) - \sum_{i=1}^{k} \bar{r}_{bi}^{*}(\boldsymbol{\gamma}^l) \right), \left(\bar{r}_{ti}^{*}(\boldsymbol{\gamma}^l) + \bar{r}_{bi}^{*}(\boldsymbol{\gamma}^l) - w_i^{*}(\boldsymbol{\gamma}^{(l)}) \right) \right]_{k=1}^{N}$ *is a subgradient for* $\mathcal{H}(\boldsymbol{\gamma})$ *at* $\boldsymbol{\gamma}^l$.

We note that the subgradient method is not a descent method, i.e., the iterations at every step do not necessarily decrease the objective value. Therefore, it is necessary to keep track of the best point found so far. At each step, we set:

$$\mathcal{H}_{\text{best}}^{l} = \min\{\mathcal{H}_{\text{best}}^{l-1}, \mathcal{H}(\boldsymbol{\gamma}^l)\} \tag{4.53}$$

We denote $\boldsymbol{\gamma}_{\text{best}}^{l}$ as the argument of $\mathcal{H}_{\text{best}}^{l}$. It can be shown that for appropriately selected ζ_l, $\mathcal{H}_{\text{best}}^{l} \to \mathcal{H}^*$ [82, Section 6.3]. Furthermore, if the step size ζ_l is chosen such that $\sum_{l=1}^{\infty} \zeta_l = \infty$, $\sum_{l=1}^{\infty} \zeta_l^2 < \infty$, then $\boldsymbol{\gamma}_{\text{best}}^{l} \to \boldsymbol{\gamma}^*$ [83, Proposition 5.1]. Once the optimal $\boldsymbol{\gamma}^*$ is found, $w_i^{*}(\boldsymbol{\gamma}^*)$ is the optimal sum rate and we can find $r_{ti}^{*}(\boldsymbol{\gamma}^*), r_{bi}^{*}(\boldsymbol{\gamma}^*)$ as the optimal source rates and $\bar{r}_{ti}^{*}(\boldsymbol{\gamma}^*), \bar{r}_{bi}^{*}(\boldsymbol{\gamma}^*)$ as the optimal relay rates. If $\bar{r}_{tk}^{*}(\boldsymbol{\gamma}^*) + \bar{r}_{bk}^{*}(\boldsymbol{\gamma}^*) > w_k^{*}(\boldsymbol{\gamma}^*)$ for some slot k then we can decrease first or second user rates until equality is achieved.

4.5 Cooperative (Extended) Multiple Access Region

In this section, consider an extended multiple access capacity region for the second hop of the diamond channel. We note that the statement of Theorem 4.1 still holds when the multiple access region of (4.3) is used instead of (4.4). However,

the statement of Lemma 4.5 and the discussions in Section 4.4 do not hold and it is not clear how to formulate the multiple access side using rate expressions only. Therefore, here we keep the expressions in terms of both power and rate allocations. Using the approach followed before, we have that the original problem in (4.12) is equivalent to:

$$\max_{\boldsymbol{\mu}\in[0,1]^N} z(\boldsymbol{\mu}) \tag{4.54}$$

where $z(\boldsymbol{\mu})$ is defined as in (4.21). We solve the problem in (4.54) in this section.

4.5.1 Inner Maximization

In this section, we focus on the inner problem in (4.21) for fixed $\boldsymbol{\mu}$. We define the new variables $\bar{p}_{1ti} = (1-\beta_i)\bar{p}_{ti}$ and $\bar{p}_{2ti} = \beta_i \bar{p}_{ti}$ and rewrite (4.21) as:

$$\begin{aligned}
\max \quad & \sum_{i=1}^{N} \bar{r}_{ti} + \sum_{i=1}^{N} \bar{r}_{bi} \\
\text{s.t.} \quad & \sum_{i=1}^{k} \bar{r}_{ti} \leq \sum_{i=1}^{k} r_{ti}(\mu_i, P_i),\ \sum_{i=1}^{k} \bar{r}_{bi} \leq \sum_{i=1}^{k} r_{bi}(\mu_i, P_i) \\
& \sum_{i=1}^{k} \bar{p}_{1ti} + \bar{p}_{2ti} \leq \sum_{i=1}^{k} E_{ti},\ \sum_{i=1}^{k} \bar{p}_{bi} \leq \sum_{i=1}^{k} E_{bi} \\
& \bar{r}_{ti} \leq f(\bar{p}_{1ti}/\sigma_3^2) \\
& \bar{r}_{ti} + \bar{r}_{bi} \leq f\big((\bar{p}_{1ti} + \bar{p}_{2ti} + \bar{p}_{bi} + 2\sqrt{\bar{p}_{2ti}\bar{p}_{bi}})/\sigma_3^2\big)
\end{aligned} \tag{4.55}$$

We denote the vector triple $\boldsymbol{\mathcal{P}} = (\bar{\mathbf{p}}_{1t}, \bar{\mathbf{p}}_{2t}, \bar{\mathbf{p}}_b)$ and define the function $y(\boldsymbol{\mathcal{P}})$ as maximization over $(\bar{\mathbf{r}}_t, \bar{\mathbf{r}}_b)$ for fixed $\boldsymbol{\mathcal{P}}$:

$$\begin{aligned} y(\boldsymbol{\mathcal{P}}) \triangleq \max_{(\bar{\mathbf{r}}_t, \bar{\mathbf{r}}_b)} \quad & \sum_{i=1}^{N} \bar{r}_{ti} + \sum_{i=1}^{N} \bar{r}_{bi} \\ \text{s.t.} \quad & \sum_{i=1}^{k} \bar{r}_{ti} \leq \sum_{i=1}^{k} r_{ti}(\mu_i, P_i), \sum_{i=1}^{k} \bar{r}_{bi} \leq \sum_{i=1}^{k} r_{bi}(\mu_i, P_i) \\ & \bar{r}_{ti} \leq f(\bar{p}_{1ti}/\sigma_3^2) \\ & \bar{r}_{ti} + \bar{r}_{bi} \leq f\big((\bar{p}_{1ti} + \bar{p}_{2ti} + \bar{p}_{bi} + 2\sqrt{\bar{p}_{2ti}\bar{p}_{bi}})/\sigma_3^2\big) \end{aligned} \tag{4.56}$$

For fixed $\boldsymbol{\mathcal{P}}$, (4.56) is a linear program, and $y(\boldsymbol{\mathcal{P}})$ can be determined efficiently. We next note the following fact.

Lemma 4.10 *$y(\boldsymbol{\mathcal{P}})$ is non-decreasing and concave in $\boldsymbol{\mathcal{P}}$.*

Proof: Since increasing the powers can only expand the feasible region, y is non-decreasing in its arguments. To prove the concavity: Let $\boldsymbol{\mathcal{P}} = (\bar{\mathbf{p}}_{1t}, \bar{\mathbf{p}}_{2t}, \bar{\mathbf{p}}_b)$ and $\boldsymbol{\mathcal{Q}} = (\bar{\mathbf{q}}_{1t}, \bar{\mathbf{q}}_{2t}, \bar{\mathbf{q}}_b)$ be two power vectors. Let $\lambda = 1 - \bar{\lambda} \in [0, 1]$. Let $(\bar{\mathbf{r}}_t, \bar{\mathbf{r}}_b)$ solve $y(\boldsymbol{\mathcal{P}})$ and $(\bar{\mathbf{s}}_t, \bar{\mathbf{s}}_b)$ solve $y(\boldsymbol{\mathcal{Q}})$. Now, we show that $(\lambda\bar{\mathbf{r}}_t + \bar{\lambda}\bar{\mathbf{s}}_t, \lambda\bar{\mathbf{r}}_b + \bar{\lambda}\bar{\mathbf{s}}_b)$ is feasible for the problem $y(\lambda\boldsymbol{\mathcal{P}} + \bar{\lambda}\boldsymbol{\mathcal{Q}})$. The first two constraints in (4.56) are linear, thus, their linear combinations are feasible. The third constraint is convex because f is concave. The last constraint is convex because f is concave, non-decreasing, and $\sqrt{\bar{p}_{2ti}\bar{p}_{bi}}$ is concave. Thus, $(\lambda\bar{\mathbf{r}}_t + \bar{\lambda}\bar{\mathbf{s}}_t, \lambda\bar{\mathbf{r}}_b + \bar{\lambda}\bar{\mathbf{s}}_b)$ is feasible for $y(\lambda\boldsymbol{\mathcal{P}} + \bar{\lambda}\boldsymbol{\mathcal{Q}})$. Now,

$$y(\lambda\boldsymbol{\mathcal{P}} + \bar{\lambda}\boldsymbol{\mathcal{Q}}) \geq \sum_{i=1}^{N} \lambda\bar{r}_{ti} + \bar{\lambda}\bar{s}_{ti} + \lambda\bar{r}_{bi} + \bar{\lambda}\bar{s}_{bi} \tag{4.57}$$

$$= \lambda y(\boldsymbol{\mathcal{P}}) + \bar{\lambda} y(\boldsymbol{\mathcal{Q}}) \tag{4.58}$$

where (4.57) follows because the maximum value of the problem can be no smaller than the objective value of any feasible point, and (4.58) follows from the fact that $(\bar{\mathbf{r}}_t, \bar{\mathbf{r}}_b)$ solves $y(\boldsymbol{\mathcal{P}})$ and $(\bar{\mathbf{s}}_t, \bar{\mathbf{s}}_b)$ solves $y(\boldsymbol{\mathcal{Q}})$. ■

The problem in (4.55) can equivalently be written as:

$$\begin{aligned} \max_{\bar{\mathbf{p}}_{1t}, \bar{\mathbf{p}}_{2t}, \bar{\mathbf{p}}_b} \quad & y(\bar{\mathbf{p}}_{1t}, \bar{\mathbf{p}}_{2t}, \bar{\mathbf{p}}_b) \\ \text{s.t.} \quad & \sum_{i=1}^{k} \bar{p}_{1ti} + \bar{p}_{2ti} \leq \sum_{i=1}^{k} E_{ti}, \quad \forall k \\ & \sum_{i=1}^{k} \bar{p}_{bi} \leq \sum_{i=1}^{k} E_{bi}, \quad \forall k \end{aligned} \tag{4.59}$$

The problem in (4.59) is convex as it involves maximizing a concave function over a feasible set with linear constraints. This can be performed efficiently by iterating over feasible $(\bar{\mathbf{p}}_{1t}, \bar{\mathbf{p}}_{2t}, \bar{\mathbf{p}}_b)$ such that every iteration increases the objective function, for example, using the method described in [61, Section III.B]. Due to convexity, the convergence to an optimal solution is guaranteed. Once $(\bar{\mathbf{p}}^*_{1t}, \bar{\mathbf{p}}^*_{2t}, \bar{\mathbf{p}}^*_b)$ is found, $z(\boldsymbol{\mu}) = y(\bar{\mathbf{p}}^*_{1t}, \bar{\mathbf{p}}^*_{2t}, \bar{\mathbf{p}}^*_b)$.

4.5.2 Outer Maximization

The outer maximization problem is the problem of finding the optimal $\boldsymbol{\mu}$ in (4.54). For this purpose, we use the block coordinate descent method on the vector $\boldsymbol{\mu}$. First,

we fix $(\mu_1, \ldots, \mu_{N-1})$ and solve the following problem

$$\max_{\mu_N \in [0,1]} z(\mu_1, \mu_2, \ldots, \mu_{N-1}, \mu_N) \tag{4.60}$$

which can be done using a one-dimensional search on $\mu_N \in [0, 1]$. Then, using this newly found μ_N, we fix $(\mu_1, \ldots, \mu_{N-2}, \mu_N)$ and maximize over μ_{N-1}. We cyclically iterate through each μ_i, one at a time, maximizing the objective function with respect to that μ_i. By construction, the iterations $z(\boldsymbol{\mu}^{(k)})$ is a monotone increasing sequence and is bounded because the optimal value of problem (4.12) is bounded, which guarantees convergence. The iterations converge to an optimal point due to the convexity of the original problem. We can utilize Lemma 4.4 to search over $\boldsymbol{\mu}$ space more efficiently. Using this procedure, we reduced an N dimensional search for $\boldsymbol{\mu}$ to N one dimensional searches for each individual μ_i. For large N, this search can be computationally demanding, however numerically we observed quick convergence.

4.6 Numerical Results

In this section, we provide numerical examples and illustrate the resulting optimal policies. We consider band-limited AWGN broadcast and multiple-access channels. The bandwidth is $B_W = 1$ MHz and the noise power spectral density is $N_0 = 10^{-19}$ W/Hz. We assume that the path loss between the source and relay 1 (h_{sr1}) is 123dB, source and relay 2 (h_{sr2}) is 127dB and the path loss between relays and destination are assumed to be same ($h_{r1d} = h_{r2d}$) and 130dB. With these definitions, equations

(4.1) and (4.2) become:

$$r_1 \leq B_W \log_2\left(1+\frac{\alpha P h_{sr1}}{N_0 B_W}\right) = \log_2\left(1+\frac{\alpha P}{0.2}\right) \text{Mbps} \tag{4.61}$$

$$r_2 \leq B_W \log_2\left(1+\frac{(1-\alpha) P h_{sr2}}{\alpha P h_{sr2} + N_0 B_W}\right) = \log_2\left(1+\frac{(1-\alpha) P}{\alpha P + 0.6}\right) \text{Mbps} \tag{4.62}$$

$$g(r_1, r_2) = 0.2 * 2^{(r_1+r_2)} + (0.6-0.2) * 2^{r_2} - 0.6 \text{ W} \tag{4.63}$$

The extended multiple access capacity region described in (4.3) becomes:

$$r_1 \leq B_W \log_2\left(1+\frac{(1-\beta) h_{r1d} P_1}{N_0 B_W}\right) = \log_2\left(1+(1-\beta) P_1\right) \text{Mbps} \tag{4.64}$$

$$\begin{aligned} r_1 + r_2 &\leq B_W \log_2\left[1+(N_0 B_W)^{-1}\left(h_{r1d} P_1 + h_{r2d} P_2 + 2\sqrt{\beta h_{r1d} P_1 h_{r2d} P_2}\right)\right] \\ &= \log_2\left(1+P_1+P_2+2\sqrt{\beta P_1 P_2}\right) \text{Mbps} \end{aligned} \tag{4.65}$$

Similarly the non-cooperative multiple access capacity region described in (4.4) becomes

$$r_1 \leq B_W \log_2\left(1+\frac{h_{r1d} P_1}{N_0 B_W}\right) = \log_2\left(1+P_1\right) \text{Mbps} \tag{4.66}$$

$$r_2 \leq B_W \log_2\left(1+\frac{h_{r2d} P_2}{N_0 B_W}\right) = \log_2\left(1+P_2\right) \text{Mbps} \tag{4.67}$$

$$r_1 + r_2 \leq B_W \log_2\left(1+\frac{h_{r1d} P_1 + h_{r2d} P_2}{N_0 B_W}\right) = \log_2\left(1+P_1+P_2\right) \text{Mbps} \tag{4.68}$$

4.6.1 Deterministic Energy Arrivals

In this subsection, we consider deterministic energy arrivals, and focus on the offline problem studied in this chapter. We study a 3 slot scenario with the following energy

arrivals, $\mathbf{E}_s = [5, 20, 9]$ J, $\mathbf{E}_t = [4, 6, 5]$ J, $\mathbf{E}_b = [6, 10, 4]$ J.

First, we investigate the non-cooperative Gaussian multiple access scenario, disregarding the possible cooperation between the top and bottom relays. The evolution of our subgradient descent based algorithm is shown in Fig. 4.3. The step size is taken as $\zeta_k = \frac{1.3}{k}$ and the initial points are taken as $\boldsymbol{\lambda}_1^0 = [3.4, 1, 1], \boldsymbol{\lambda}_2^0 = [2.8, 1.1, 1.4], \boldsymbol{\nu}^0 = [10, 4, 3]$. The plot shows the percentage error between the best iteration so far and the optimal value of the problem in (4.12). The algorithm converges after around 10^4 steps to reasonable accuracy. The resulting Lagrange multipliers are found as $\boldsymbol{\lambda}_1 = [3.04, 0.04, 0.4] \times 10^{-3}, \boldsymbol{\lambda}_2 = [4.29, 0, 0] \times 10^{-3}, \boldsymbol{\nu} = [4.51, 4.29, 4.26] \times 10^{-3}$. The optimal rates are then found as $\mathbf{r}_t = [1.55, 1.18, 1.14]$ Mbits, $\mathbf{r}_b = [0.69, 1.7, 1.72]$ Mbits, $\bar{\mathbf{r}}_t = [1.16, 1.34, 1.35]$ Mbits, $\bar{\mathbf{r}}_b = [1.4, 1.73, 0]$ Mbits, $\mathbf{w} = [1.72, 1.87, 1.87]$ Mbits. We observe that by setting $\bar{\mathbf{r}}_b = \mathbf{w} - \bar{\mathbf{r}}_t = [0.56, 0.53, 0.52]$ Mbits we can get $w_i = \bar{r}_{ti} + \bar{r}_{bi}, \forall i$ and this set of rates is the optimal solution. The feasibility of this solution can be verified. Due to the non-uniqueness of the solution, there may exist multiple $\bar{r}_{ti}^*, \bar{r}_{bi}^*$ pairs that yield the optimal sum rate however the optimal sum rate $\bar{r}_{ti}^* + \bar{r}_{bi}^*$ is unique. The optimal sum throughput in this case is calculated as $\sum_{i=1}^N \bar{r}_{ti} + \sum_{i=1}^N \bar{r}_{bi} = 5.46$ Mbits. The optimal user priorities for the source are calculated as $\boldsymbol{\mu}_1 = [0.81, 0.72, 0.71]$.

Second, we investigate the extended multiple access scenario. The optimal user priorities for the source are found as $\boldsymbol{\mu}_2 = [0.83, 0.43, 0.43]$. The optimal rates are then found as $\mathbf{r}_t = [0.74, 0.07, 0.07]$ Mbits, $\mathbf{r}_b = [1.27, 2.3, 2.3]$ Mbits, $\bar{\mathbf{r}}_t = [0.74, 0.07, 0.07]$ Mbits, $\bar{\mathbf{r}}_b = [1.27, 2.3, 2.3]$ Mbits, $\bar{\mathbf{p}}_{1t} = [1.8, 0.1, 0.1]$ W,

$\bar{\mathbf{p}}_{2t} = [2.2, 5.39, 5.39]$ W, $\bar{\mathbf{p}}_b = [4.82, 7.58, 7.58]$ W. We note that $\bar{\mathbf{p}}_{2t}$ is much larger

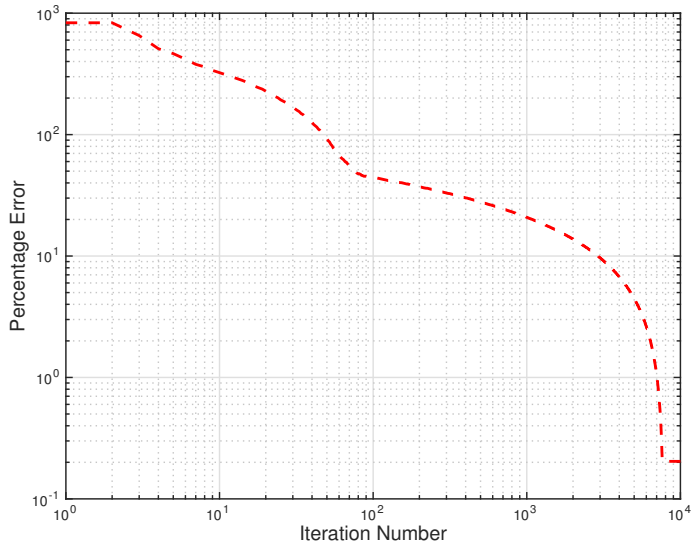

Figure 4.3: Percentage error between the best iteration so far and the optimal value vs iteration number k.

than $\bar{\mathbf{p}}_{1t}$ which means that relay 1 has spent a significant portion of its power on the cooperative communication rather than forwarding its own data. The optimal sum throughput in this case is calculated as $\sum_{i=1}^{N} \bar{r}_{ti} + \sum_{i=1}^{N} \bar{r}_{bi} = 6.76$ Mbits which is higher than in the non-cooperative case.

Finally, we examine the maximum departure region and the optimal trajectories for the broadcast side of this diamond channel for the non-cooperative and cooperative Gaussian multiple access channel second hops. Without the existence of relays, for the two user Gaussian broadcast channel, to maximize the sum rate we need to set $\boldsymbol{\mu} = [1, 1, 1]$ and $r_{bi} = 0, \forall i$, i.e., all the power must be allocated to the stronger user[7]. The existence of the multiple access layer changes this structure. We sketch the maximum departure region and trajectories to reach the optimal point in Fig. 4.4. When there is no multiple access layer, all the power is allocated

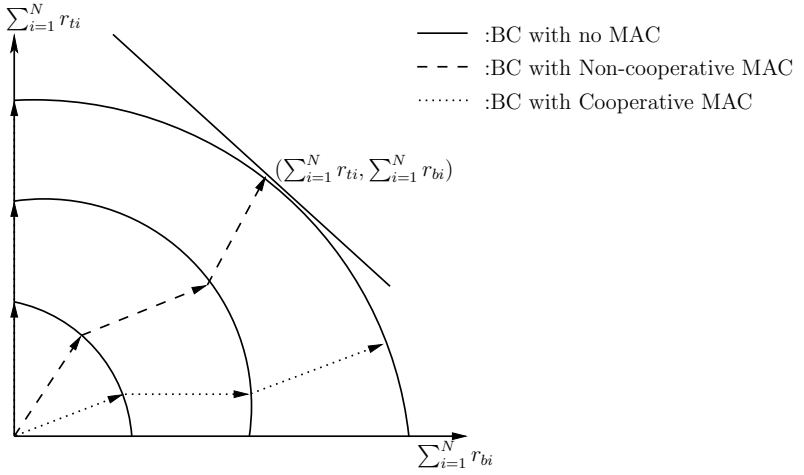

Figure 4.4: Maximum departure region and trajectories to reach the optimal point for BC with no MAC, BC with non-cooperative MAC and BC with cooperative MAC.

to the first user. In the case of non-cooperative multiple access layer, the rates to both of the relays follow a balanced pattern. In the case of cooperative multiple access layer, the weaker relay gets more data than the stronger relay due to the possibility of cooperation.

4.6.2 Stochastic Energy Arrivals

In this subsection, we consider stochastic energy arrivals and we compare the performance of the offline optimal policy with that of a suboptimal online policy. These policies are inspired by the optimal offline policy while they require partial or no offline knowledge of the energy arrivals. We have shown that a partial separation holds between the broadcast and the multiple access parts of the problem, therefore the online policies we consider will be of separation based. We denote the amount of energy in the batteries of the source, top relay and bottom relay as B_s, B_t, B_b and

the data buffers of the top and bottom relays as D_t, D_b. The presented online algorithms are of best-effort type [6, 84], where the transmitters aim to keep a constant power if feasible, or transmit with the currently available power otherwise.

4.6.2.1 Source Power and Rate Allocation

This policy determines the source power p_{si} and rate (r_{ti}, r_{bi}) allocations. We choose a policy that transmits with constant power equal to the average recharge rate of the source battery, if there is enough energy, otherwise it uses all of the battery energy, i.e., $p_s = \min\{\mathbb{E}[E_s], B_s\}$. First, we define a constant C which depends only on the average recharge rates of the top and bottom relays, as follows:

$$C = \begin{cases} \frac{\log_2(1+\mathbb{E}[E_t])}{\log_2(1+\mathbb{E}[E_b])}, & \text{if regular MAC} \\ \\ \frac{\log_2(1+\mathbb{E}[E_b])}{\log_2(1+\mathbb{E}[E_b]+\mathbb{E}[E_t])}, & \text{if cooperative MAC} \end{cases} \tag{4.69}$$

The reasoning behind the choice of C is as follows. For the regular MAC, the top relay can transmit at most an average rate of $\log_2(1 + \mathbb{E}[E_t])$, considering its own energy arrivals. Similarly, the bottom relay can transmit at most an average rate of $\log_2(1 + \mathbb{E}[E_b])$. Therefore, we have $\frac{\bar{r}_t}{\bar{r}_b} \sim \frac{\log_2(1+\mathbb{E}[E_t])}{\log_2(1+\mathbb{E}[E_b])}$. We choose the source rate division to be exactly equal to this quantity. For the cooperative MAC, we use a constant β policy and set $\beta = 1 - \frac{\mathbb{E}[E_b]}{\mathbb{E}[E_t]}$. Then, from (4.64) we have $\bar{r}_t \sim \log_2(1 + \mathbb{E}[E_b])$ and from (4.65) $\bar{r}_b \sim \log_2(1 + \mathbb{E}[E_b] + \mathbb{E}[E_t])$. We choose the source rate division to be exactly equal to the ratio of two rates. From (4.61) and (4.62),

we choose the power share α^* to satisfy the following equation:

$$C = \frac{\log_2\left(1 + \frac{\alpha\mathbb{E}[E_s]}{0.2}\right)}{\log_2\left(1 + \frac{(1-\alpha)\mathbb{E}[E_s]}{\alpha\mathbb{E}[E_s]+0.6}\right)} \tag{4.70}$$

4.6.2.2 Top and Bottom Relay Power and Rate Allocation

This policy determines the top and bottom relay power (p_{ti}, p_{bi}) and rate $(\bar{r}_{ti}, \bar{r}_{bi})$ allocations. We note that the policy for the relays must depend on the data arrivals from the source. For the regular MAC, the online policy is determined as follows. We set the top relay power allocation as the average recharge rate of the top relay battery if there is enough energy and data, otherwise it uses either all of the battery energy or transmits at a rate that transmits all of the available data. We set $p_t = \min\{\mathbb{E}[E_t], B_t, 2^{D_t-1}\}, r_t = \log_2(1+p_t)$. Similarly we set $p_b = \min\{\mathbb{E}[E_b], B_b, 2^{D_b-1}\}, r_b = \log_2(1+p_b)$. If the constraint $r_t + r_b \leq \log_2(1+p_t+p_b)$ is not satisfied, then we decrease r_b, p_b until equality is satisfied.

For the cooperative MAC, additional to p_t, p_b we need to determine β given in (4.65). We set $p_t = \min\{\mathbb{E}[E_t], B_t, 2^{D_t-1}\}, r_t = \log_2(1+p_t)$. We use a constant β policy and set $\beta = 1 - \frac{\mathbb{E}[E_b]}{\mathbb{E}[E_t]}$. Now, we set $p_b = \min\{\mathbb{E}[E_b], B_b\}$ and $r_b = \log_2(1+p_t+p_b+2\sqrt{\beta p_t p_b}) - r_t$. If $r_b > D_b$, then r_b, p_b are decreased until equality is satisfied.

4.6.2.3 Simulations

In the simulations, we consider Bernoulli energy arrival processes. The source energy arrivals are $E_{si} = 0$ with probability 0.5 and $E_{si} = 2\xi$ with probability 0.5 where ξ is

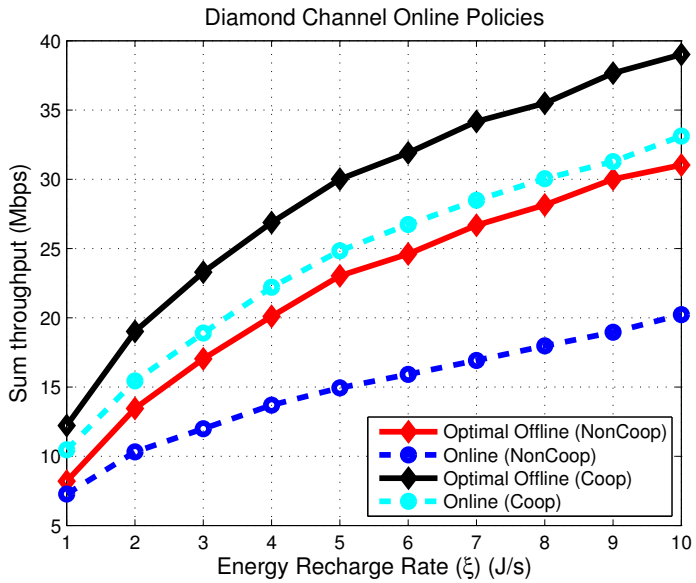

Figure 4.5: Average sum throughput versus average recharge rate for offline and online policies.

the average recharge rate, and we denote this process by $\text{Ber}(0.5, \xi)$. We assume that $E_{ti} \sim \text{Ber}(0.5, 0.5\xi)$ and $E_{bi} \sim \text{Ber}(0.5, 0.3\xi)$. We perform simulations for a deadline of 10 slots. The performance metric of the policies is the average sum throughput over 100 realizations of the stochastic energy arrival process. We plot our results in Fig. 4.5. We observe that the sum throughput increases with increasing energy recharge rate.

4.7 Concluding Remarks

In this chapter, we considered the energy harvesting diamond channel where the physical layer is modeled as a concatenation of a broadcast channel and a multiple access channel. In the first part of the chapter, we focused on the broadcast half of the diamond network. We first showed that there exists an optimal source power

allocation policy which is equal to the single-user optimal power policy for the source energy arrivals and does not depend on the relay energy arrivals. Next, we showed that even though the total power can be selected as the single-user optimal power, the fraction of the power spent on each broadcast link depends on the energy arrivals of the relays. In the second part of the chapter, we turned our attention to the multiple access side of the diamond network. This is a cooperative multiple access channel with common data. Initially, we ignored the possible cooperation between the relays and assumed a regular Gaussian multiple access channel with non-cooperating users. In this setting, first we showed that when the transmission rates of the source in the broadcast side are fixed, the overall problem becomes a multiple access channel with both data and energy arrivals. We showed that this problem can be formulated in terms of data transmission rates only, instead of formulating over both transmission powers and data rates. We solved the overall diamond channel problem with non-cooperative multiple access channel using a dual decomposition method. In the last part of the chapter, we considered the cooperative (extended) multiple access capacity region for the second hop. With the extended multiple access capacity region, we found the overall solution using a decomposition into inner and outer maximization problems.

4.8 Appendix

4.8.1 Proof of Theorem 4.1

In this proof, we are only interested in (r_{ti}^*, r_{bi}^*). Therefore, to find the necessary optimality conditions, we write the Lagrangian function of the problem in (4.15) as:

$$\begin{aligned}\mathcal{L} = &- \sum_{i=1}^{N} \bar{r}_{ti} - \sum_{i=1}^{N} \bar{r}_{bi} + \sum_{k=1}^{N} \lambda_{1k} \left(\sum_{i=1}^{k} \bar{r}_{ti} - \sum_{i=1}^{k} r_{ti} \right) + \sum_{k=1}^{N} \lambda_{2k} \left(\sum_{i=1}^{k} \bar{r}_{bi} - \sum_{i=1}^{k} r_{bi} \right) \\ &+ \sum_{k=1}^{N} \gamma_k \left(\sum_{i=1}^{k} g(r_{ti}, r_{bi}) - \sum_{i=1}^{k} E_{si} \right) - \sum_{i=1}^{N} \theta_{1i} r_{ti} - \sum_{i=1}^{N} \theta_{2i} r_{bi} + \text{ other terms}\end{aligned} \tag{4.71}$$

where other terms include the Lagrange multipliers for the other constraints but they are not needed in the proof and are omitted for the sake of brevity. The complementary slackness conditions for these Lagrange multipliers are:

$$\lambda_{1k} \left(\sum_{i=1}^{k} \bar{r}_{ti} - \sum_{i=1}^{k} r_{ti} \right) = \lambda_{2k} \left(\sum_{i=1}^{k} \bar{r}_{bi} - \sum_{i=1}^{k} r_{bi} \right) = 0 \tag{4.72}$$

$$\gamma_k \left(\sum_{i=1}^{k} g(r_{ti}, r_{bi}) - \sum_{i=1}^{k} E_{si} \right) = 0 \tag{4.73}$$

$$\theta_{1i} r_{ti} = \theta_{2i} r_{bi} = 0, \qquad \lambda_{1k}, \lambda_{2k}, \gamma_k \geq 0 \tag{4.74}$$

Taking the derivatives of $\mathcal{L}$ with respect to r_{ti} and r_{bi}:

$$- \sum_{k=i}^{N} \lambda_{1k} + \left(\sum_{k=i}^{N} \gamma_k \right) \sigma_1^2 2^{2(r_{ti}+r_{bi})} - \theta_{1i} = 0 \tag{4.75}$$

$$-\sum_{k=i}^{N}\lambda_{2k}+\left(\sum_{k=i}^{N}\gamma_k\right)\left(g(r_{ti},r_{bi})+\sigma_2^2\right)-\theta_{2i}=0 \tag{4.76}$$

From (4.75) and (4.76), we get:

$$g(r_{ti},r_{bi})=\frac{\theta_{2i}+\sum_{k=i}^{N}\lambda_{2k}}{\sum_{k=i}^{N}\gamma_k}-\sigma_2^2 \tag{4.77}$$

$$2^{2(r_{ti}+r_{bi})}=\frac{\theta_{1i}+\sum_{k=i}^{N}\lambda_{1k}}{\sigma_1^2\sum_{k=i}^{N}\gamma_k} \tag{4.78}$$

Lemma 4.11 *When the optimal total source power $g(r_{ti}^*, r_{bi}^*)$ increases, the energy buffer must be empty.*

Proof: We will show that if $g(r_{ti}, r_{bi}) < g(r_{t,i+1}, r_{b,i+1})$ then $\gamma_i > 0$. First, assume $r_{b,i+1} > 0$ which implies from (4.74) that $\theta_{2,i+1} = 0$. Then, from (4.77), $g(r_{ti}, r_{bi}) < g(r_{t,i+1}, r_{b,i+1})$ is only possible if $\gamma_i > 0$. Next, assume $r_{b,i+1} = 0$ which implies that $r_{t,i+1} > 0$ otherwise $g(r_{t,i+1}, r_{b,i+1}) = 0$ which cannot be optimal. When $r_{b,i+1} = 0$, $g(r_{ti}, r_{bi}) < g(r_{t,i+1}, r_{b,i+1})$ is equivalent to $2^{2(r_{ti}+r_{bi})} < 2^{2(r_{t,i+1}+r_{b,i+1})}$, and from (4.78) and $\theta_{1,i+1} = 0$, we must have $\gamma_i > 0$. ■

Next, we show that the total source power cannot strictly decrease over the slots.

Lemma 4.12 *The total source power must be non-decreasing, i.e., $g(r_{ti}^*, r_{bi}^*) \leq g(r_{t,i+1}^*, r_{b,i+1}^*)$, $\forall i$.*

Proof: We will prove this statement by contradiction. Specifically, we assume a policy in which there is a slot k such that $g(r_{tk}^*, r_{bk}^*) > g(r_{t,k+1}^*, r_{b,k+1}^*)$. We will show

that this policy cannot be optimal.

We first show that if $g(r_{tk}, r_{bk}) > g(r_{t,k+1}, r_{b,k+1})$ then $\lambda_{1k} = \lambda_{2k} = 0$ cannot happen. First, assume $r_{bk} > 0$ which implies from (4.74) that $\theta_{2k} = 0$. Then, from (4.77), $g(r_{tk}, r_{bk}) > g(r_{t,k+1}, r_{b,k+1})$ is only possible if $\lambda_{2k} > 0$. Next, assume $r_{bk} = 0$ which implies that $r_{tk} > 0$ otherwise $g(r_{tk}, r_{bk}) = 0$ which cannot be optimal. When $r_{bk} = 0$, $g(r_{tk}, r_{bk}) > g(r_{t,k+1}, r_{b,k+1})$ is equivalent to $2^{2(r_{tk}+r_{bk})} > 2^{2(r_{t,k+1}+r_{b,k+1})}$, and from (4.78) and $\theta_{1k} = 0$, we have $\lambda_{1k} > 0$.

Now, for $g(r^*_{tk}, r^*_{bk}) > g(r^*_{t,k+1}, r^*_{b,k+1})$ to happen, we need to have either $r^*_{tk} > r^*_{t,k+1}, r^*_{bk} \leq r^*_{b,k+1}$ or $r^*_{bk} > r^*_{b,k+1}, r^*_{tk} \leq r^*_{t,k+1}$ or $r^*_{tk} > r^*_{t,k+1}, r^*_{bk} > r^*_{b,k+1}$. We will examine these cases separately.

Case 1: $r^*_{tk} > r^*_{t,k+1}, r^*_{bk} \leq r^*_{b,k+1}$: We must have $r^*_{tk} > 0$ which implies $\theta_{1k} = 0$. In this case, for $g(r^*_{tk}, r^*_{bk}) > g(r^*_{t,k+1}, r^*_{b,k+1})$, we must also have $r^*_{tk} + r^*_{bk} > r^*_{t,k+1} + r^*_{b,k+1}$. This implies from (4.78) that $\lambda_{1k} > 0$ and $\sum_{i=1}^{k} \bar{r}^*_{ti} = \sum_{i=1}^{k} r^*_{ti}$. From the data causality constraints at the $(k-1)$st slot and $\sum_{i=1}^{k} \bar{r}^*_{ti} = \sum_{i=1}^{k} r^*_{ti}$, we must have $\bar{r}_{tk} \geq r_{tk}$. Similarly, from data causality at the $(k+1)$st slot and $\sum_{i=1}^{k} \bar{r}^*_{ti} = \sum_{i=1}^{k} r^*_{ti}$, we must have $\bar{r}_{t,k+1} \leq r_{t,k+1}$. This implies that we must have $\bar{r}_{tk} \geq r_{tk} > r_{t,k+1} \geq \bar{r}_{t,k+1}$, thus $\bar{r}_{tk} > \bar{r}_{t,k+1}$. Now, consider the following modified policy for some $\delta > 0$, $\hat{r}_{tk} = r^*_{tk} - \delta, \hat{r}_{t,,k+1} = r^*_{t,k+1} + \delta, \hat{r}_{tk} = \bar{r}^*_{tk} - \delta, \hat{r}_{t,k+1} = \bar{r}^*_{t,k+1} + \delta$. Data causality constraints are trivially satisfied. Energy causality at the top node can be satisfied by letting $\hat{P}_{tk} = \bar{p}_{tk} - \epsilon$ and $\hat{P}_{t,k+1} = \bar{p}_{t,k+1} + \epsilon$ because there exists $\epsilon > 0$ such that $\bar{r}^*_{tk} \leq f\left((\bar{p}_{tk} - \epsilon)/\sigma_3^2\right)$ and $\bar{r}^*_{t,k+1} \leq f\left((\bar{p}_{t,k+1} + \epsilon)/\sigma_3^2\right)$. Energy causality at the source node is satisfied since at slot k we have $g(r^*_{tk} - \delta, r^*_{bk}) < g(r^*_{tk}, r^*_{bk})$ and at slot $k+1$ we have $g(r^*_{tk} - \delta, r^*_{bk}) + g(r^*_{t,k+1} + \delta, r^*_{b,k+1}) < g(r^*_{tk}, r^*_{bk}) + g(r^*_{t,k+1}, r^*_{b,k+1})$

due to joint convexity of $g(\cdot,\cdot)$ and $r^*_{tk} + r^*_{bk} > r^*_{t,k+1} + r^*_{b,k+1}$. This means that the modified policy is feasible, forwards the same amount of data, and consumes strictly less energy than the original one. This additional energy can be used to increase r^*_{bk} and r^*_{tk} which causes the data buffers at the top and bottom relays to be non-empty. This modified policy cannot be optimal because it does not satisfy the fact that if $g(r_{tk}, r_{bk})$ strictly decreases in time, then both λ_{1k} and λ_{2k} cannot be zero, as proved at the beginning above. This also means the original policy cannot be optimal because its throughput is equal to the throughput of a sub-optimal policy.

Case 2: $r^*_{bk} > r^*_{b,k+1}, r^*_{tk} \leq r^*_{t,k+1}$: We must have $r^*_{bk} > 0$, therefore $\theta_{2k} = 0$. From $\lambda_{2k} > 0$, we must have that the bottom data buffer is empty, which implies $\sum_{i=1}^{k} \bar{r}^*_{bi} = \sum_{i=1}^{k} r^*_{bi}$. From this point on, the proof follows exactly as in **Case 1** but with modifications to $r^*_{bk}, \bar{r}^*_{bk}, \bar{p}_{bk}$ instead of to $r^*_{tk}, r^*_{tk}, \bar{p}_{tk}$, and we conclude that this case cannot happen.

Case 3: $r^*_{bk} > r^*_{b,k+1}, r^*_{tk} > r^*_{t,k+1}$: This case follows the same line of reasoning as the previous cases and by modifying both r^*_{tk}, r^*_{bk} we reach the same conclusion.

To summarize, since none of the above cases can be true, we have $g(r^*_{ti}, r^*_{bi}) \leq g(r^*_{t,i+1}, r^*_{b,i+1}), \forall i$. ■

We can always impose the constraint $\sum_{i=1}^{N} g(r^*_{ti}, r^*_{bi}) = \sum_{i=1}^{N} E_{si}$ on the problem in (4.15) because this does not change the optimal value. From Lemma 4.12, the total source power must be non-decreasing, and from Lemma 4.11, the total source power can only increase when the energy buffer is empty. The source power policy that satisfies these properties is the unique single-user optimal power policy

[4, 6].

4.8.2 Proof of Lemma 4.3

Assume (r_{ti}^*, r_{bi}^*) solves the problem in (4.16). Carrying out a similar analysis as in Appendix 4.8.1, the KKT conditions are

$$-\sum_{k=i}^{N} \lambda_{1k} + \gamma_k \sigma_1^2 2^{2(r_{ti}+r_{bi})} - \theta_{1i} = 0 \tag{4.79}$$

$$-\sum_{k=i}^{N} \lambda_{2k} + \gamma_k (g(r_{ti}, r_{bi}) + \sigma_2^2) - \theta_{2i} = 0 \tag{4.80}$$

where γ_k is the Lagrange multiplier for the constraint $g(r_{ti}, r_{bi}) \leq P_i$. Now, we examine the following optimization problem for some $\boldsymbol{\mu}_1, \boldsymbol{\mu}_2 \in \mathbb{R}^N$.

$$\max_{r_{ti}, r_{bi} \geq 0} \quad \sum_{i=1}^{N} \mu_{1i} r_{ti} + \sum_{i=1}^{N} \mu_{2i} r_{bi} \tag{4.81}$$

$$\text{s.t.} \quad g(r_{ti}, r_{bi}) \leq P_i \tag{4.82}$$

Since the constraint set depends only on the current slot i, this problem is separable into N local optimization problems which are given as

$$\max_{r_{ti}, r_{bi} \geq 0} \quad \mu_{1i} r_{ti} + \mu_{2i} r_{bi} \tag{4.83}$$

$$\text{s.t.} \quad g(r_{ti}, r_{bi}) \leq P_i \tag{4.84}$$

The problem in (4.84) is convex and is solved in [7]. Following [7, Eqn. (13)] the KKT conditions are

$$-\mu_1 + \eta_k \sigma_1^2 2^{2(r_{ti}+r_{bi})} - \omega_{1i} = 0 \tag{4.85}$$

$$-\mu_2 + \eta_k (g(r_{ti}, r_{bi}) + \sigma_2^2) - \omega_{2i} = 0 \tag{4.86}$$

with the complementary slackness conditions as

$$\omega_{1i} r_{ti} = \omega_{2i} r_{bi} = \eta_i \left(g(r_{ti}, r_{bi}) - P_i \right) = 0, \quad \forall i \tag{4.87}$$

We require the same (r_{ti}^*, r_{bi}^*) pair to solve both of these problems. When $r_{ti}^* = 0$ we set $\mu_{1i} = 0$, otherwise from (4.79), (4.85) we have $\mu_{1i} = (\sum_{k=i}^{N} \lambda_{1k})\eta_k/\gamma_k$. Similarly, when $r_{bi}^* = 0$ we set $\mu_{2i} = 0$ otherwise from (4.80), (4.86) we have $\mu_{2i} = (\sum_{k=i}^{N} \lambda_{2k})\eta_k/\gamma_k$. Note that $\eta_k, \gamma_k > 0$ because the energy causality constraints will always be satisfied with equality at every slot. Now we define

$$\mu_i \triangleq \min \left\{ \frac{\mu_{1i}}{\mu_{2i}}, 1 \right\} = \min \left\{ \frac{\sum_{k=i}^{N} \lambda_{1k}}{\sum_{k=i}^{N} \lambda_{2k}}, 1 \right\} \tag{4.88}$$

With this definition, the problems (4.82) and (4.17) are equivalent and have the same solution as (4.16). This proves Lemma 4.3. We observe from (4.88) that if $\mu_i > \mu_{i+1}$ then $\lambda_{1k} > 0$ which implies the top data buffer is empty. Similarly, if $\mu_i < \mu_{i+1}$ then $\lambda_{2k} > 0$ which implies the bottom data buffer is empty. This proves Lemma 4.4.

4.8.3 Proof of Lemma 4.5

Denote the feasible set and the optimal value of the problem in (4.21) by $(\mathcal{F}_1, T_1)$ and that of the problem in (4.28) by $(\mathcal{F}_2, T_2)$. First, we show $T_1 \leq T_2$. For any $(\bar{p}_{ti}, \bar{p}_{bi}, \bar{r}_{ti}, \bar{r}_{bi}) \in \mathcal{F}_1$, from (4.11) we have

$$\bar{p}_{ti} \geq \sigma_3^2 \left(2^{2\bar{r}_{ti}} - 1\right), \quad \bar{p}_{bi} \geq \sigma_3^2 \left(2^{2\bar{r}_{bi}} - 1\right), \tag{4.89}$$

$$\bar{p}_{ti} + \bar{p}_{bi} \geq \sigma_3^2 \left(2^{2(\bar{r}_{ti}+\bar{r}_{bi})} - 1\right) \tag{4.90}$$

These constraints imply

$$\sum_{i=1}^{k} \bar{p}_{ti} \geq \sigma_3^2 \left(\sum_{i=1}^{k} 2^{2\bar{r}_{ti}} - 1\right), \quad \forall k \tag{4.91}$$

$$\sum_{i=1}^{k} \bar{p}_{bi} \geq \sigma_3^2 \left(\sum_{i=1}^{k} 2^{2\bar{r}_{bi}} - 1\right), \quad \forall k \tag{4.92}$$

$$\sum_{i=1}^{k} \bar{p}_{ti} + \bar{p}_{bi} \geq \sigma_3^2 \left(\sum_{i=1}^{k} 2^{2(\bar{r}_{ti}+\bar{r}_{bi})} - 1\right), \quad \forall k \tag{4.93}$$

Together with (4.5) and (4.6), (4.91)-(4.93) imply

$$\sigma_3^2 \left(\sum_{i=1}^{k} 2^{2\bar{r}_{ti}} - 1\right) \leq \sum_{i=1}^{k} E_{ti}, \quad \forall k \tag{4.94}$$

$$\sigma_3^2 \left(\sum_{i=1}^{k} 2^{2\bar{r}_{bi}} - 1\right) \leq \sum_{i=1}^{k} E_{bi}, \quad \forall k \tag{4.95}$$

$$\sigma_3^2 \left(\sum_{i=1}^{k} 2^{2(\bar{r}_{ti}+\bar{r}_{bi})} - 1\right) \leq \sum_{i=1}^{k} E_{ti} + E_{bi}, \quad \forall k \tag{4.96}$$

This means $(\bar{r}_{ti}, \bar{r}_{bi}) \in \mathcal{F}_2$ and therefore $T_1 \leq T_2$.

Now, we show $T_2 \leq T_1$. For any $(\bar{r}_{ti}, \bar{r}_{bi}) \in \mathcal{F}_2$, we will find $\bar{p}_{ti}, \bar{p}_{bi}$ such that $(\bar{p}_{ti}, \bar{p}_{bi}, \bar{r}_{ti}, \bar{r}_{bi}) \in \mathcal{F}_1$. To accomplish this, we solve the feasibility problem

$$\begin{aligned}
\max_{\bar{p}_{ti}, \bar{p}_{bi}} \quad & 1 \\
\text{s.t.} \quad & \bar{p}_{ti} \geq \sigma_3^2 \left(2^{2\bar{r}_{ti}} - 1\right), \quad \forall i \\
& \bar{p}_{bi} \geq \sigma_3^2 \left(2^{2\bar{r}_{bi}} - 1\right), \quad \forall i \\
& \bar{p}_{ti} + \bar{p}_{bi} \geq \sigma_3^2 \left(2^{2(\bar{r}_{ti} + \bar{r}_{bi})} - 1\right), \quad \forall i \\
& \sum_{i=1}^{k} \bar{p}_{ti} \leq \sum_{i=1}^{k} E_{ti}, \sum_{i=1}^{k} \bar{p}_{bi} \leq \sum_{i=1}^{k} E_{bi}, \quad \forall k
\end{aligned} \tag{4.97}$$

We can let $\bar{p}_{ti} + \bar{p}_{bi} = \sigma_3^2 \left(2^{2(\bar{r}_{ti} + \bar{r}_{bi})} - 1\right), \forall i$ without changing the optimal value of the feasibility problem. Now, we have the following set of inequalities to be satisfied:

$$\bar{p}_{ti} \geq \sigma_3^2 \left(2^{2\bar{r}_{ti}} - 1\right), \quad \forall i \tag{4.98}$$

$$\bar{p}_{ti} \leq \sigma_3^2 \left(2^{2(\bar{r}_{ti} + \bar{r}_{bi})} - 2^{2\bar{r}_{bi}}\right), \quad \forall i \tag{4.99}$$

$$\sum_{i=1}^{k} \bar{p}_{ti} \leq \sum_{i=1}^{k} E_{ti}, \quad \forall k \tag{4.100}$$

$$\sum_{i=1}^{k} \bar{p}_{ti} \geq \sum_{i=1}^{k} \left[\sigma_3^2 \left(2^{2(\bar{r}_{ti} + \bar{r}_{bi})} - 1\right) - E_{bi}\right], \quad \forall k \tag{4.101}$$

We note that this set of inequalities is consistent by showing every lower bound is no larger than every upper bound. (4.98) is consistent with (4.99) since $2^{2(x+y)} - 2^{2y} \geq 2^{2x} - 1, \forall x, y \geq 0$. (4.98) is consistent with (4.100) since $\bar{r}_{ti}$ satisfies (4.94). (4.99) is consistent with (4.101) since $\bar{r}_{bi}$ satisfies (4.95) and finally (4.100) is consistent with

(4.101) since $\bar{r}_{ti}, \bar{r}_{bi}$ satisfy (4.96). We also have $\bar{p}_{ti} \geq 0$ which is consistent with both (4.99) and (4.100) since these lower bounds are non-negative. This feasibility problem then has a solution and there exists $\bar{p}_{ti}, \bar{p}_{bi}$ that solve (4.97). This means there exists $(\bar{p}_{ti}, \bar{p}_{bi}, \bar{r}_{ti}, \bar{r}_{bi}) \in \mathcal{F}_1$ and therefore $T_2 \leq T_1$, proving the lemma.

4.8.4 Proof of Lemma 4.7

The statement is true for $k = N$ because the optimal value of problem (4.29) is at least as large as that of (4.28) since any profile that is feasible for (4.28) is also feasible for (4.29). We will show that if the statement holds for slot k, i.e., $\sum_{i=1}^{k} \bar{r}_{ti}^* + \bar{r}_{bi}^* \leq \sum_{i=1}^{k} q_i^*$, then it also holds for slot $k-1$. By induction this will imply that it is true for all k. Assume on the contrary that $\sum_{i=1}^{k-1} \bar{r}_{ti}^* + \bar{r}_{bi}^* > \sum_{i=1}^{k-1} q_i^*$. Together with $\sum_{i=1}^{k} \bar{r}_{ti}^* + \bar{r}_{bi}^* \leq \sum_{i=1}^{k} q_i^*$, this implies $\bar{r}_{tk}^* + \bar{r}_{bk}^* < q_k^*$.

Now, we claim that we must have $\sum_{i=1}^{k-1} 2^{2(\bar{r}_{ti}^* + \bar{r}_{bi}^*)} > \sum_{i=1}^{k-1} 2^{2q_i^*}$. This is true because otherwise, up to slot $k-1$, the profile $\bar{r}_{ti}^* + \bar{r}_{bi}^*$ sends more data than q_i^* and in view of the energy constraints in (4.29) leads to a more relaxed feasible set. This means that the profile q_i^* can be replaced with $\bar{r}_{ti}^* + \bar{r}_{bi}^*$ for slots 1 to $k-1$ and for the remaining slots $k, \ldots, N$ more data can be transmitted because there is more energy left. This contradicts the optimality of q_i^*, therefore we must have $\sum_{i=1}^{k-1} 2^{2(\bar{r}_{ti}^* + \bar{r}_{bi}^*)} > \sum_{i=1}^{k-1} 2^{2q_i^*}$.

Note that this also means $\sigma_3^2 \left(\sum_{i=1}^{k-1} 2^{2q_i^*} - 1 \right) < \sum_{i=1}^{k-1} E_{ti} + E_{bi}$ because otherwise $\bar{r}_{ti}^* + \bar{r}_{bi}^*$ cannot be energy feasible. From the assumption, we have $\sum_{i=1}^{k-1} \bar{r}_{ti}^* + \bar{r}_{bi}^* > \sum_{i=1}^{k-1} q_i^*$, which implies $\sum_{i=1}^{k-1} q_i^* < \sum_{i=1}^{k-1} d_{ti} + d_{bi}$ because otherwise $\bar{r}_{ti}^* + \bar{r}_{bi}^*$ can-

not be data feasible. These collectively mean that slot $k-1$ cannot be an energy or data exhausting slot for q_i^* and therefore $q_{k-1}^* = q_k^*$. From this fact and $\bar{r}_{ti}^* + \bar{r}_{bi}^*$ is non-decreasing, we have $\bar{r}_{t,k-1}^* + \bar{r}_{b,k-1}^* \leq \bar{r}_{tk}^* + \bar{r}_{bk}^* < q_k^* = q_{k-1}^*$ which implies $\bar{r}_{t,k-1}^* + \bar{r}_{b,k-1}^* < q_{k-1}^*$. Together with $\sum_{i=1}^{k-1} \bar{r}_{ti}^* + \bar{r}_{bi}^* > \sum_{i=1}^{k-1} q_i^*$, this implies $\sum_{i=1}^{k-2} \bar{r}_{ti}^* + \bar{r}_{bi}^* > \sum_{i=1}^{k-2} q_i^*$. Following the same reasoning as before, we have that $k-2$ is a non energy and data exhausting slot for q_i^* and therefore $q_{k-2}^* = q_{k-1}^*$. We apply the same argument to reach the conclusion that $q_1^* = q_2^* = \cdots = q_k^*$ and $\bar{r}_{ti}^* + \bar{r}_{bi}^* < q_i^*, \forall i \leq k$. This contradicts the assumption $\sum_{i=1}^{k-1} \bar{r}_{ti}^* + \bar{r}_{bi}^* > \sum_{i=1}^{k-1} q_i^*$.

4.8.5 Proof of Lemma 4.8

The proof follows from majorization theory. We know that $\bar{r}_{ti}^* + \bar{r}_{bi}^*$ and q_i^* are non-decreasing in i, so they are ordered vectors. From Lemma 4.7, we have $\sum_{i=1}^{l} \bar{r}_{ti}^* + \bar{r}_{bi}^* \leq \sum_{i=1}^{l} q_i^* \ \forall l < k$ and if in addition we have $\sum_{i=1}^{k} \bar{r}_{ti}^* + \bar{r}_{bi}^* = \sum_{i=1}^{k} q_i^*$, then the vector q_i^* is majorized by the vector $\bar{r}_{ti}^* + \bar{r}_{bi}^*$. This means $\sum_{i=1}^{k} g(\bar{r}_{ti}^* + \bar{r}_{bi}^*) \geq \sum_{i=1}^{k} g(q_i^*)$ for any convex, increasing g and in particular for $g = 2^x$ [71, Section I.3.C1B]. Furthermore, if we have $\sigma_3^2 \left(\sum_{i=1}^{k} 2^{2q_i^*} - 1 \right) = \sum_{i=1}^{k} E_{ti} + E_{bi}$, then we have $\sigma_3^2 \left(\sum_{i=1}^{k} 2^{2(\bar{r}_{ti}^* + \bar{r}_{bi}^*)} - 1 \right) \geq \sum_{i=1}^{k} E_{ti} + E_{bi}$. From energy feasibility of $\bar{r}_{ti}^* + \bar{r}_{bi}^*$ we also have $\sigma_3^2 \left(\sum_{i=1}^{k} 2^{2(\bar{r}_{ti}^* + \bar{r}_{bi}^*)} - 1 \right) \leq \sum_{i=1}^{k} E_{ti} + E_{bi}$. These two constraints are feasible if and only if $\sigma_3^2 \left(\sum_{i=1}^{k} 2^{2(\bar{r}_{ti}^* + \bar{r}_{bi}^*)} - 1 \right) = \sum_{i=1}^{k} E_{ti} + E_{bi} = \sigma_3^2 \left(\sum_{i=1}^{k} 2^{2q_i^*} - 1 \right)$. From the strict convexity of 2^x and therefore strict Schur-convexity of $\sum 2^x$ we must have $\bar{r}_{ti}^* + \bar{r}_{bi}^* = q_i^*, \forall i \leq k$.

4.8.6 Proof of Lemma 4.9

Similar to the discussion that follows [82, Section 6.1, Eq. (1.1)] we have:

$$\begin{aligned}
\mathcal{H}(\boldsymbol{\gamma}) \geq & \sum_{i=1}^{N} w_i^*(\boldsymbol{\gamma}^{(l)}) - \sum_{k=1}^{N} \lambda_{1k} \left(\sum_{i=1}^{k} \bar{r}_{ti}^*(\boldsymbol{\gamma}^l) - \sum_{i=1}^{k} r_{ti}^*(\boldsymbol{\gamma}^l) \right) \\
& - \sum_{k=1}^{N} \lambda_{2k} \left(\sum_{i=1}^{k} \bar{r}_{bi}^*(\boldsymbol{\gamma}^l) - \sum_{i=1}^{k} r_{bi}^*(\boldsymbol{\gamma}^l) \right) \\
& - \sum_{i=1}^{N} \nu_i \left(w_i^*(\boldsymbol{\gamma}^{(l)}) - \bar{r}_{ti}^*(\boldsymbol{\gamma}^l) - \bar{r}_{bi}^*(\boldsymbol{\gamma}^l) \right) \qquad (4.102) \\
= & \sum_{i=1}^{N} w_i^*(\boldsymbol{\gamma}^{(l)}) - \sum_{k=1}^{N} \lambda_{1k}^l \left(\sum_{i=1}^{k} \bar{r}_{ti}^*(\boldsymbol{\gamma}^l) - \sum_{i=1}^{k} r_{ti}^*(\boldsymbol{\gamma}^l) \right) \\
& - \sum_{k=1}^{N} \lambda_{2k}^l \left(\sum_{i=1}^{k} \bar{r}_{bi}^*(\boldsymbol{\gamma}^l) - \sum_{i=1}^{k} r_{bi}^*(\boldsymbol{\gamma}^l) \right) \\
& - \sum_{i=1}^{N} {\nu_i}^l \left(w_i^*(\boldsymbol{\gamma}^{(l)}) - \bar{r}_{ti}^*(\boldsymbol{\gamma}^l) - \bar{r}_{bi}^*(\boldsymbol{\gamma}^l) \right) \\
& + \sum_{k=1}^{N} (\lambda_{1k}^l - \lambda_{1k}) \left(\sum_{i=1}^{k} \bar{r}_{ti}^*(\boldsymbol{\gamma}^l) - \sum_{i=1}^{k} r_{ti}^*(\boldsymbol{\gamma}^l) \right) \\
& + \sum_{k=1}^{N} (\lambda_{2k}^l - \lambda_{2k}) \left(\sum_{i=1}^{k} \bar{r}_{bi}^*(\boldsymbol{\gamma}^l) - \sum_{i=1}^{k} r_{bi}^*(\boldsymbol{\gamma}^l) \right) \\
& + \sum_{i=1}^{N} ({\nu_i}^l - \nu_i) \left(w_i^*(\boldsymbol{\gamma}^{(l)}) - \bar{r}_{ti}^*(\boldsymbol{\gamma}^l) - \bar{r}_{bi}^*(\boldsymbol{\gamma}^l) \right) \qquad (4.103) \\
= & \mathcal{H}(\boldsymbol{\gamma}^l) + \boldsymbol{v}^{\mathsf{T}}(\boldsymbol{\gamma} - \boldsymbol{\gamma}^l) \qquad (4.104)
\end{aligned}$$

where the inequality follows from the fact that $(r_{ti}^*(\boldsymbol{\gamma}^l), r_{bi}^*(\boldsymbol{\gamma}^l)) \in \mathcal{R}_s$ so feasible for $\mathcal{K}_1(\boldsymbol{\gamma})$ but may not solve $\mathcal{K}_1(\boldsymbol{\gamma})$, $\bar{r}_{ti}^*(\boldsymbol{\gamma}^l) \in \mathcal{R}_t$ but may not solve $\mathcal{K}_2(\boldsymbol{\gamma})$, $\bar{r}_{bi}^*(\boldsymbol{\gamma}^l) \in \mathcal{R}_b$ but may not solve $\mathcal{K}_3(\boldsymbol{\gamma})$, and $w_i^*(\boldsymbol{\gamma}^{(l)}) \in \mathcal{R}_w$ but may not solve $\mathcal{K}_4(\boldsymbol{\gamma})$. The expression for $\boldsymbol{v}^{\mathsf{T}}$ is given in the statement of the lemma.

CHAPTER 5

Energy and Data Cooperative Multiple Access Channel with Data Arrivals

5.1 Introduction

In this chapter, we consider the two-user cooperative Gaussian multiple access channel, see Fig. 5.1.In the first part of this chapter, we consider a cooperative MAC with both energy and data arrivals as shown in Fig. 5.1(a). In the second part of this chapter, we consider a cooperative MAC with both energy and data cooperation as shown in Fig. 5.1(b). We use this system model to investigate interactions of data and energy cooperation, and study their joint optimization.

In the first part of the chapter, in Section 5.3, we consider the data arrival scenario. While most of the offline optimization literature so far has focused on throughput maximization under the assumption of infinitely back-logged data queues, in many applications, data may arrive intermittently at the nodes just like energy. Two prominent examples of such scenarios are: multi-hop networks and sensor networks. In multi-hop networks, each hop forwards the data that has arrived from the previous hop, therefore, data is not always available and arrives intermittently

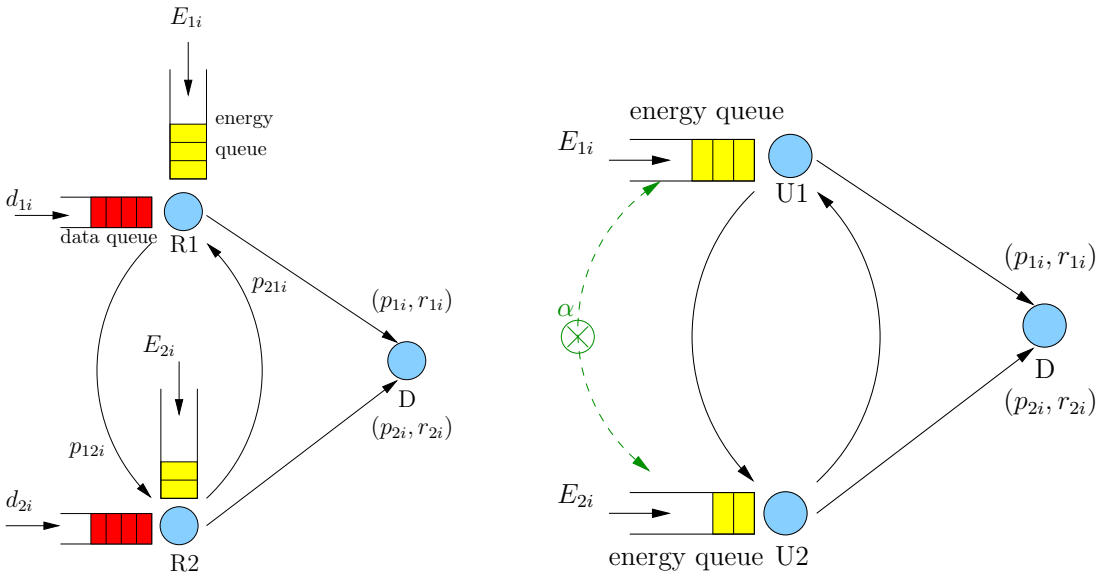

(a) Cooperative MAC with energy and data arrivals.

(b) Cooperative MAC with joint energy and data cooperation

Figure 5.1: Cooperative MAC system models.

depending on the energy arrivals and achievable rates of the previous hops; an example of such scenario is investigated in a diamond network in Chapter 4. In sensor networks, sensor nodes make measurements of an event of interest, therefore, data to send becomes available as the event occurs intermittently. We first show that there exists an optimal rate and power allocation which is on the achievable rate region boundary of the cooperative MAC at every slot, instead of being strictly inside the achievable rate region. Then, we formulate the problem in terms of data rates only, rather than both transmission powers and data rates. Although this new problem is non-convex, we show that strong duality holds. As a result, we are able to employ a successive convex approximation technique in which non-convex constraints are approximated by suitable convex functions. Using this approximation, we solve the problem using an iterative algorithm which iterates between inner and outer

maximization problems.

In the second part of the chapter, in Section 5.4, we consider the energy cooperative scenario. In this case, in addition to data cooperation being implemented at the physical layer by decoding and forwarding the overhead data, energy cooperation is implemented at the battery level by forwarding energy between users by using wireless energy transfer. By such a formulation, we investigate the interaction between data and energy cooperation, their relative effectiveness, and the direction, timing and amount of energy exchange in coordination with data cooperation. We first show that in this scenario, the cooperative powers in all slots must be non-zero for both users. Then, we derive a one-to-one relation between the optimal transmission rates and the optimal transmission powers. Next, we show that data cooperation always precedes energy cooperation. In other words, excess energy must first be used to increase cooperative powers and then to further assist the other user by means of direct energy transfer. We determine necessary conditions for energy transfer to take place. We then propose an algorithm which solves the offline energy transfer and power allocation problem iteratively based on these conditions.

5.2 System Model and Problem Formulation

We consider an energy harvesting cooperative MAC with intermittent data arrivals, as shown in Fig. 5.1(a) and bidirectional energy cooperation as shown in Fig 5.1(b). The harvested energies are saved in the corresponding batteries. There are N equal length slots. We use subscripts 1 and 2 to denote the parameters of users 1 and

2. In slot i, there are energy and data arrivals to both users with amounts E_{1i}, E_{2i} and d_{1i}, d_{2i}, respectively. Energy transfers from user 1 (2) to user 2 (1) are denoted by δ_{1i} (δ_{2i}). Energy transfer efficiency is $0 \leq \alpha < 1$: when user 1 (2) transfers δ_{1i} (δ_{2i}) Joules of energy to user 2 (1), $\alpha\delta_{1i}$ ($\alpha\delta_{2i}$) Joules of energy enters the energy queue of user 2 (1). We denote the transmission powers, energy transfers and data rates of users 1 and 2 as $p_{12i}, p_{U1i}, d_{1i}, r_{1i}$ and $p_{21i}, p_{U2i}, d_{2i}, r_{2i}$, respectively. We use boldface letters to denote vectors of these variables. When there is wireless energy transfer, this is done by two separate orthogonal energy transfer units whose coupling frequencies are set differently [33]. Finally, data transmission and energy transfer channels are orthogonal, i.e., energy transfer does not create interference to data communication.

The physical layer is a cooperative Gaussian MAC with unit-variance Gaussian noises at the users and $\sigma^2 > 1$ variance Gaussian noise at the receiver. We employ the delay constrained cooperation model proposed in [85]. The users cooperate in a slot by slot basis, by first exchanging information and then beamforming, to send the established common information, in each given slot. The specifics of the encoding and decoding policy can be found in [85, Section II]. The achievable rate region with transmitter sub-powers $p_{12i}, p_{21i}, p_{U1i}, p_{U2i}$ at each slot i is given as [85, 86]:

$$\mathcal{C}(p_{12i}, p_{21i}, p_{U1i}, p_{U2i}) = \left\{ r_{1i} \leq f(1 + p_{12i}), r_{2i} \leq f(1 + p_{21i}), r_{1i} + r_{2i} \leq f(s_i/\sigma^2) \right\} \tag{5.1}$$

where $f(x) = \frac{1}{2}\log(x)$, $p_{1i} = p_{12i} + p_{U1i}$, $p_{2i} = p_{21i} + p_{U2i}$ and

$$s_i = \sigma^2 + p_{1i} + p_{2i} + 2\sqrt{p_{U1i}p_{U2i}} \tag{5.2}$$

The operational meaning of the sub-powers will be important to us: p_{12i} and p_{21i} denote the powers used in slot i to build up common information at the cooperative partner, while p_{U1i} and p_{U2i} are cooperative powers used for jointly conveying the common information to the receiver.

Energy arrivals as well as energy transfers occur at the beginning of each slot. Hence, the net energy available for user $\ell \in \{1, 2\}$ in each slot $k \in \{1, \ldots, N\}$ is given by $\sum_{i=1}^{k}(E_{\ell i} - \delta_{\ell i} + \alpha\delta_{mi})$ where m is the other user. The energy that has not arrived yet cannot be used for data transmission or energy transfer, leading to the following *energy causality constraints*:

$$\sum_{i=1}^{k} p_{1i} \leq \sum_{i=1}^{k}(E_{1i} - \delta_{1i} + \alpha\delta_{2i}), \quad \forall k \tag{5.3}$$

$$\sum_{i=1}^{k} p_{2i} \leq \sum_{i=1}^{k}(E_{2i} - \delta_{2i} + \alpha\delta_{1i}), \quad \forall k \tag{5.4}$$

When there is no energy cooperation, these constraints simplify as:

$$\sum_{i=1}^{k} p_{1i} \leq \sum_{i=1}^{k} E_{1i}, \quad \forall k \tag{5.5}$$

$$\sum_{i=1}^{k} p_{2i} \leq \sum_{i=1}^{k} E_{2i}, \quad \forall k \tag{5.6}$$

The data that has not arrived yet cannot be transmitted, leading to the following

data causality constraints:

$$\sum_{i=1}^{k} r_{1i} \leq \sum_{i=1}^{k} d_{1i}, \quad \forall k \tag{5.7}$$

$$\sum_{i=1}^{k} r_{2i} \leq \sum_{i=1}^{k} d_{2i}, \quad \forall k \tag{5.8}$$

The rate allocations must be achievable for the cooperative MAC in each slot:

$$(r_{1i}, r_{2i}) \in \mathcal{C}(p_{12i}, p_{21i}, p_{U1i}, p_{U2i}), \quad \forall i \tag{5.9}$$

For notational convenience, we denote the sub-power and rate sequences and energy transfer sequences by the vectors $\mathbf{p}_{12}, \mathbf{p}_{21}, \mathbf{p}_{U1}, \mathbf{p}_{U2}, \mathbf{r}_1, \mathbf{r}_2, \boldsymbol{\delta}_1, \boldsymbol{\delta}_2$.

In the first half of this chapter, we investigate the data arrival scenario with no energy transfer. The departure region maximization problem can be stated as a weighted sum rate maximization for given priorities $0 \leq \mu_1, \mu_2 \leq 1$, due to the convexity of the departure region:

$$\begin{aligned} \max_{\mathbf{p}_{12},\mathbf{p}_{21},\mathbf{p}_{U1},\mathbf{p}_{U2},\mathbf{r}_1,\mathbf{r}_2 \geq \mathbf{0}} \quad & \mu_1 \sum_{i=1}^{N} r_{1i} + \mu_2 \sum_{i=1}^{N} r_{2i} \\ \text{s.t.} \quad & (5.5)\text{-}(5.9) \end{aligned} \tag{5.10}$$

In the second half of the chapter, we investigate the energy cooperative scenario with no data arrivals. Then, the departure region maximization problem can be

stated as:

$$\max_{\mathbf{p}_{12},\mathbf{p}_{21},\mathbf{p}_{U1},\mathbf{p}_{U2},\mathbf{r}_1,\mathbf{r}_2,\boldsymbol{\delta}_1,\boldsymbol{\delta}_2\geq\mathbf{0}} \quad \mu_1\sum_{i=1}^{N} r_{1i}+\mu_2\sum_{i=1}^{N} r_{2i}$$

$$\text{s.t.} \quad \text{(5.3)-(5.4), (5.9)} \tag{5.11}$$

5.3 Intermittent Data Arrivals Scenario

In this section, we focus on the scenario with intermittent data arrivals. The system model is shown in Fig. 5.1(a). We solve the problem in (5.10). First, we prove some properties of the optimal solution.

Lemma 5.1 *There exists an optimal profile that satisfies the following property,*

$$r_{1i}=f(1+p_{12i}), \quad r_{2i}=f(1+p_{21i}), \quad \forall i \tag{5.12}$$

Proof: We will prove this lemma by showing that for any policy that does not satisfy the above property, there exists another policy that satisfies it and achieves the same weighted sum rate. Assume there exists an optimal policy and slot i such that $r_{1i} < f(1+p_{12i})$. Now consider the modified policy, $q_{12i}=p_{12i}-\epsilon$, $q_{U1i}=p_{U1i}+\epsilon$ while keeping the remaining variables fixed. In this modified policy, $q_{1i}=q_{12i}+q_{U1i}=p_{12i}+p_{U1i}=p_{1i}$, therefore the new policy spends the same amount of energy as the previous one and is energy feasible. It is easy to check that this modification increases s_i and (r_{1i},r_{2i}) still belongs to the set $\mathcal{C}(q_{12i},p_{21i},q_{U1i},p_{U2i})$. Since we have not changed the rates, the data causality constraints are still feasible.

By repeating this process we will reach a profile where $r_{1i} = f(1 + p_{12i})$. By using similar arguments for r_{2i} and modifying p_{21i} and p_{U2i} we will reach a profile where $r_{2i} = f(1 + p_{21i})$. Since we have not changed the rates, the weighted sum rate is the same and the policy is still optimal. This proves the lemma. ■

With Lemma 5.1 and enforcing the constraints in (5.12) the sum rate constraints in (5.1) become:

$$f(1 + p_{12i}) + f(1 + p_{21i}) \leq f(s_i/\sigma^2), \quad \forall i \tag{5.13}$$

In addition to the rate-power relationships dictated by Lemma 5.1, we further introduce the auxiliary rate variables, r_{U1i}, r_{U2i}, and perform the variable changes, $r_{U1i} = f(1 + p_{U1i}), r_{U2i} = f(1 + p_{U2i})$. Then $s_i = \sigma^2 + 2^{2r_{1i}} + 2^{2r_{U1i}} + 2^{2r_{2i}} + 2^{2r_{U2i}} + 2\sqrt{(2^{2r_{U1i}} - 1)(2^{2r_{U2i}} - 1)} - 4$. We formulate the problem only in terms of rates as,

$$\begin{aligned}
\max_{\mathbf{r}_1, \mathbf{r}_2, \mathbf{r}_{U1}, \mathbf{r}_{U2}} \quad & \sum_{i=1}^{N} \mu_1 r_{1i} + \mu_2 r_{2i} \\
\text{s.t.} \quad & \sum_{i=1}^{k} 2^{2r_{1i}} + 2^{2r_{U1i}} \leq \sum_{i=1}^{k} (E_{1i} + 2), \ \forall k && (5.14) \\
& \sum_{i=1}^{k} 2^{2r_{2i}} + 2^{2r_{U2i}} \leq \sum_{i=1}^{k} (E_{2i} + 2), \ \forall k && (5.15) \\
& \sum_{i=1}^{k} r_{1i} \leq \sum_{i=1}^{k} d_{1i}, \quad \forall k && (5.16) \\
& \sum_{i=1}^{k} r_{2i} \leq \sum_{i=1}^{k} d_{2i}, \quad \forall k && (5.17) \\
& r_{1i} + r_{2i} \leq f(s_i/\sigma^2), \quad \forall i && (5.18)
\end{aligned}$$

The problem in (5.18) is a non-convex optimization problem due to the last set of constraints $r_{1i} + r_{2i} \leq f(s_i/\sigma^2)$, $\forall i$. We use the successive convex approximation technique to approximate the constraints in (5.18) as explained in [87]. We use the first order Taylor expansion to the function $f(s_i/\sigma^2)$ around the point $\mathbf{R}^n \triangleq (\mathbf{r}_1^n, \mathbf{r}_2^n, \mathbf{r}_{U1}^n, \mathbf{r}_{U2}^n)$ for iteration $n+1$, by

$$f(s_i/\sigma^2) \simeq C_i^n + \alpha_{1i}^n(r_{1i} - r_{1i}^n) + \alpha_{2i}^n(r_{2i} - r_{2i}^n) + \beta_{1i}^n(r_{U1i} - r_{U1i}^n) + \beta_{2i}^n(r_{U2i} - r_{U2i}^n) \tag{5.19}$$

where the values of the coefficients are given in Appendix 5.7.1 and depend only on the solution of the previous iteration n. With this approximation the problem in (5.18) becomes

$$\begin{aligned} \max_{\mathbf{r}_1,\mathbf{r}_2,\mathbf{r}_{U1},\mathbf{r}_{U2}} \quad & \sum_{i=1}^{N} \mu_1 r_{1i} + \mu_2 r_{2i} \\ \text{s.t.} \quad & \text{(5.14)-(5.17)} \\ & (1-\alpha_{1i}^n) r_{1i} + (1-\alpha_{2i}^n) r_{2i} - \beta_{1i}^k r_{U1i} - \beta_{2i}^n r_{U2i} \leq D_i^n, \quad \forall i \end{aligned} \tag{5.20}$$

where $D_i^n \triangleq C_i^n - \alpha_{1i}^n r_{1i}^n - \alpha_{2i}^n r_{2i}^n - \beta_{1i}^n r_{U1i}^n - \beta_{2i}^n r_{U2i}^n$ and is a constant for this optimization problem. At iteration $n+1$, we evaluate the coefficients in (5.19) using the optimal rate allocations at iteration n, we solve the problem in (5.20) using these coefficients and we update the initial point as $\mathbf{R}^{n+1} = \mathbf{R}^*(n)$ where $\mathbf{R}^*(n)$ denotes the optimal values of the variables when (5.20) is solved. Now we show that this procedure stops at an optimal solution to the problem in (5.18). To achieve this,

we first show that strong duality holds for (5.18). The proof is given in Appendix 5.7.2.

Lemma 5.2 *Strong duality holds for the problem in (5.18).*

Now we show that the procedure converges to an optimal solution and the proof is in Appendix 5.7.3.

Lemma 5.3 $\mathbf{R}^n \rightarrow \mathbf{R}^*$ *where* $\mathbf{R}^*$ *solves (5.18).*

In the next section, we solve the problem in (5.20) for fixed n.

5.3.1 Solution for Approximate Problems

In this sub-section, we solve the approximate problems for iteration $n+1$. For notational convenience we drop the superscript n from the last constraints in (5.20) noting that they depend only on the solution of the problem at the previous iteration n. Therefore the coefficients $\alpha_{1i}^n, \alpha_{2i}^n, \beta_{1i}^n, \beta_{2i}^n$ are essentially constants for the problem at step $n+1$.

Lemma 5.4 *There exists an optimal solution in which* $(1-\alpha_{1i})r_{1i} + (1-\alpha_{2i})r_{2i} - \beta_{1i}r_{U1i} - \beta_{2i}r_{U2i} = D_i, \quad \forall i.$

Proof: Assume there exists a profile where $(1-\alpha_{1i})r_{1i} + (1-\alpha_{2i})r_{2i} - \beta_{1i}r_{U1i} - \beta_{2i}r_{U2i} < D_i$ for some slot i. Then we can decrease, r_{U1i} or r_{U2i} to achieve equality.

■

Invoking Lemma 5.4, the problem becomes,

$$\begin{aligned} \max_{\mathbf{r}_1,\mathbf{r}_2,\mathbf{r}_{U1},\mathbf{r}_{U2}} \quad & \sum_{i=1}^{N} \mu_1 r_{1i} + \mu_2 r_{2i} \\ \text{s.t.} \quad & (5.14)\text{-}(5.17) \\ & (1-\alpha_{1i})r_{1i} + (1-\alpha_{2i})r_{2i} - \beta_{1i} r_{U1i} - \beta_{2i} r_{U2i} = D_i, \quad \forall i \end{aligned} \tag{5.21}$$

We solve the problem in (5.21) using a primal decomposition. We add a new optimization variable $\mathbf{t} \in \mathbb{R}^N$ and equivalently formulate (5.21) as follows:

$$\begin{aligned} \max_{\mathbf{r}_1,\mathbf{r}_2,\mathbf{r}_{U1},\mathbf{r}_{U2},\mathbf{t}} \quad & \sum_{i=1}^{N} \mu_1 r_{1i} + \mu_2 r_{2i} \\ \text{s.t.} \quad & (5.14)\text{-}(5.17) \\ & (1-\alpha_{1i})r_{1i} - \beta_{1i} r_{U1i} = D_i + t_i & (5.22) \\ & (1-\alpha_{2i})r_{2i} - \beta_{2i} r_{U2i} = -t_i, \quad \forall i & (5.23) \end{aligned}$$

Let us define the function $z(\mathbf{t})$ which is a maximization over $(\mathbf{r}_1, \mathbf{r}_2, \mathbf{r}_{U1}, \mathbf{r}_{U2})$ for fixed $\mathbf{t}$:

$$\begin{aligned} z(\mathbf{t}) = \max_{\mathbf{r}_1,\mathbf{r}_2,\mathbf{r}_{U1},\mathbf{r}_{U2}} \quad & \sum_{i=1}^{N} \mu_1 r_{1i} + \mu_2 r_{2i} \\ \text{s.t.} \quad & (5.14)\text{-}(5.17),\ (5.22),\ (5.23) \end{aligned} \tag{5.24}$$

Then the original problem in (5.21) is equivalent to

$$\max_{\mathbf{t}} z(\mathbf{t}) \tag{5.25}$$

We solve (5.25) by separately solving the outer and inner maximization problems.

5.3.1.1 Inner Maximization

In this section, we focus on the inner problem in (5.24) for fixed $\mathbf{t}$. Note that when $\mathbf{t}$ is fixed, the variables $(\mathbf{r}_1, \mathbf{r}_{U1})$ and $(\mathbf{r}_2, \mathbf{r}_{U2})$ are decoupled and (5.24) can be separated into two sub-problems. We define $z_1(\mathbf{t})$ and $z_2(\mathbf{t})$ as

$$\begin{aligned}
z_1(\mathbf{t}) = \max_{\mathbf{r}_1, \mathbf{r}_{U1}} \quad & \sum_{i=1}^{N} \mu_1 r_{1i} \\
\text{s.t.} \quad & \sum_{i=1}^{k} 2^{2r_{1i}} + 2^{2r_{U1i}} \leq \sum_{i=1}^{k} (E_{1i} + 2) && (5.26) \\
& \sum_{i=1}^{k} r_{1i} \leq \sum_{i=1}^{k} d_{1i}, \quad \forall k && (5.27) \\
& (1 - \alpha_{1i}) r_{1i} - \beta_{1i} r_{U1i} = D_i + t_i, \quad \forall i && (5.28) \\
z_2(\mathbf{t}) = \max_{\mathbf{r}_2, \mathbf{r}_{U2}} \quad & \sum_{i=1}^{N} \mu_2 r_{2i} \\
\text{s.t.} \quad & \sum_{i=1}^{k} 2^{2r_{2i}} + 2^{2r_{U2i}} \leq \sum_{i=1}^{k} (E_{2i} + 2) && (5.29) \\
& \sum_{i=1}^{k} r_{2i} \leq \sum_{i=1}^{k} d_{2i}, \quad \forall k && (5.30) \\
& (1 - \alpha_{2i}) r_{2i} - \beta_{2i} r_{U2i} = -t_i, \quad \forall i && (5.31)
\end{aligned}$$

and note that $z(\mathbf{t}) = z_1(\mathbf{t}) + z_2(\mathbf{t})$. First we concentrate on solving z_1. Let $w_{1i} = (1-\alpha_{1i})/\beta_{1i}, v_{1i} = 2^{-2(D_i+t_i)/\beta_{1i}}$. Using the equality constraints in (5.28) we get,

$$\begin{aligned} \max_{\mathbf{r}_1} \quad & \sum_{i=1}^{N} \mu_1 r_{1i} \\ \text{s.t.} \quad & \sum_{i=1}^{k} 2^{2r_{1i}} + v_{1i} 2^{2w_{1i} r_{1i}} \leq \sum_{i=1}^{k} (E_{1i} + 2) \qquad (5.32) \\ & \sum_{i=1}^{k} r_{1i} \leq \sum_{i=1}^{k} d_{1i}, \quad \forall k \qquad (5.33) \end{aligned}$$

This is a single-user problem with data arrivals d_{1i}, energy arrivals E_{1i} and a modified energy consumption function $m(r_{1i}) = 2^{2r_{1i}} + v_{1i}2^{2w_{1i}r_{1i}}$. In order to solve it: first, we perform directional waterfilling on the data arrivals d_{1i}. Second, we perform directional waterfilling on the energy arrivals E_{1i} with the understanding that $m'(r_{1i})$ is a generalized water level and the quantity to be kept constant over the slots. Then, we take the minimum of the two solutions ensuring that any unused data or energy must be carried over to the future slots.

Now we solve z_2. Let $w_{2i} = (1-\alpha_{2i})/\beta_{2i}$ and $v_{2i} = 2^{t_i/\beta_{2i}}$. Using the equality constraints of (5.31) we get,

$$\begin{aligned} \max_{\mathbf{r}_2} \quad & \sum_{i=1}^{N} \mu_2 r_{2i} \\ \text{s.t.} \quad & \sum_{i=1}^{k} 2^{2r_{2i}} + v_{2i} 2^{2w_{2i} r_{1i}} \leq \sum_{i=1}^{k} (E_{2i} + 2) \qquad (5.34) \\ & \sum_{i=1}^{k} r_{2i} \leq \sum_{i=1}^{k} d_{2i}, \quad \forall k \qquad (5.35) \end{aligned}$$

This problem is solved similarly as in the case of z_1.

5.3.1.2 Outer Maximization

The outer maximization problem is that of finding optimal $\mathbf{t}$ in (5.25). The equality constraints in (5.22) and (5.23) impose some feasibility constraints on $\mathbf{t}$. Then the problem is equivalent to

$$\begin{aligned} \max_{\mathbf{t}} \quad & z(\mathbf{t}) \\ \text{s.t.} \quad & z_1(\mathbf{t}), z_2(\mathbf{t}) \text{ are feasible} \end{aligned} \tag{5.36}$$

It can be shown that $z(\mathbf{t})$ is concave in $\mathbf{t}$. Solving this problem can be performed efficiently by iterating over feasible $\mathbf{t}$ such that every iteration increases the objective function, for example, using the method described in [61, Section III.B]. Due to convexity, the convergence to an optimal solution is guaranteed. The overall solution algorithm is given in Algorithm 4. The solution to outer maximization problem is in lines 2 to 16.

5.4 Energy Cooperation Scenario

In this section, we focus on the scenario with energy cooperation as well as data cooperation. The system model is shown in Fig. 5.1(b). We solve the problem in (5.11). First, we state the necessary conditions for the optimal profile. These conditions lead to interesting interpretations regarding the nature of energy exchange, including its direction, timing and physical relation to data cooperation. We relax

Algorithm 4 Algorithm to solve (5.18)

Initialize

Find initial feasible $\mathbf{R}^0 \triangleq (\mathbf{r}_1^0, \mathbf{r}_2^0, \mathbf{r}_{U1}^0, \mathbf{r}_{U2}^0)$

Define function to find z(t)

function SolveZ($\alpha_{1i}^n, \alpha_{2i}^n, \beta_{1i}^n, \beta_{2i}^n, D_i^n$) ▷ Solves z
    Set $\mathbf{u} \leftarrow \mathbf{0}, \mathbf{t}_1 \leftarrow \mathbf{u}, \mathbf{t}_2 \leftarrow \mathbf{u}$
    Solve $z_1(\mathbf{u}), z_2(\mathbf{u})$ as explained after (5.33) and (5.35)
    $z(\mathbf{u}) \leftarrow z_1(\mathbf{u}) + z_2(\mathbf{u})$
    for $i = 1 : N$ **do**
        $t_{1i} \leftarrow u_i + \epsilon, t_{2i} \leftarrow u_i - \epsilon$
        Solve $z_1(\mathbf{t}_1), z_2(\mathbf{t}_1), z_1(\mathbf{t}_2), z_2(\mathbf{t}_2)$
        $z(\mathbf{t}_1) \leftarrow z_1(\mathbf{t}_1) + z_2(\mathbf{t}_1), z(\mathbf{t}_2) \leftarrow z_1(\mathbf{t}_2) + z_2(\mathbf{t}_2)$
        if $[z(\mathbf{t}_1) > z(\mathbf{u})]$ **then** $\mathbf{u} \leftarrow \mathbf{t}_1$
        else if $[z(\mathbf{t}_2) > z(\mathbf{u})]$ **then** $\mathbf{u} \leftarrow \mathbf{t}_2$
        end if
    end for
    Go to (6) until convergence
    return last found optimal $(\mathbf{r}_1, \mathbf{r}_2, \mathbf{r}_{U1}, \mathbf{r}_{U2})$
end function

Main Algorithm

repeat
    Find $A_i^n, \alpha_{1i}^n, \alpha_{2i}^n, \beta_{1i}^n, \beta_{2i}^n, C_i^n$ from (5.75) - (5.80)
    $D_i^n \leftarrow C_i^n - \alpha_{1i}^n r_{1i}^n - \alpha_{2i}^n r_{2i}^n - \beta_{1i}^n r_{U1i}^n - \beta_{2i}^n r_{U2i}^n$
    $\mathbf{R}^{n+1} \leftarrow$ SolveZ($\alpha_{1i}^n, \alpha_{2i}^n, \beta_{1i}^n, \beta_{2i}^n, D_i^n$)
    $n \leftarrow n + 1$
until convergence

the equality in (5.2) to reformulate (5.10) as follows.

$$\begin{aligned}
\max \quad & \mu_1 \sum_{i=1}^{N} r_{1i} + \mu_2 \sum_{i=1}^{N} r_{2i} \\
\text{s.t.} \quad & \sum_{i=1}^{k} p_{12i} + p_{U1i} \leq \sum_{i=1}^{k} E_{1i} - \delta_{1i} + \alpha\delta_{2i}, \quad \forall k && (5.37) \\
& \sum_{i=1}^{k} p_{21i} + p_{U2i} \leq \sum_{i=1}^{k} E_{2i} - \delta_{2i} + \alpha\delta_{1i}, \quad \forall k && (5.38) \\
& r_{1i} \leq f(1 + p_{12i}), \quad \forall i && (5.39) \\
& r_{2i} \leq f(1 + p_{21i}), \quad \forall i && (5.40) \\
& r_{1i} + r_{2i} \leq f(s_i/\sigma^2), \quad \forall i && (5.41) \\
& s_i \leq \sigma^2 + p_{12i} + p_{U1i} + p_{21i} + p_{U2i} + 2\sqrt{p_{U1i}p_{U2i}}, \quad \forall i && (5.42) \\
& \mathbf{p}_{12}, \mathbf{p}_{21}, \mathbf{p}_{U1}, \mathbf{p}_{U2}, \mathbf{d}_1, \mathbf{d}_2, \mathbf{r}_1, \mathbf{r}_2, \mathbf{s} \geq \mathbf{0} && (5.43)
\end{aligned}$$

The problem in (5.43) is a convex optimization problem, however it is non-differentiable due to the term $\sqrt{p_{U1i}p_{U2i}}$ when $p_{U1i} = 0$ or $p_{U2i} = 0$. Now, we show that in the optimal solution, the cooperative powers p_{U1i}, p_{U2i} are non-zero at all slots. The proof is given in Appendix 5.7.4.

Lemma 5.5 *The cooperative powers are strictly positive at all slots, i.e.,* $p_{U1i} > 0, p_{U2i} > 0, \forall i$.

Utilizing Lemma 5.5, the functions $\sqrt{p_{U1i}p_{U2i}}$ are now differentiable. Then, the KKT optimality conditions are found as:

$$-\mu_1 + \theta_{1i} + \theta_{3i} - \gamma_{5i} = 0, \quad \forall i \qquad (5.44)$$

$$-\mu_2 + \theta_{2i} + \theta_{3i} - \gamma_{6i} = 0, \quad \forall i \tag{5.45}$$

$$\sum_{k=i}^{N} \lambda_{1k} - \frac{\theta_{1i}}{(1+p_{12i})} - \beta_i - \gamma_{1i} = 0, \quad \forall i \tag{5.46}$$

$$\sum_{k=i}^{N} \lambda_{2k} - \frac{\theta_{2i}}{(1+p_{21i})} - \beta_i - \gamma_{2i} = 0, \quad \forall i \tag{5.47}$$

$$\sum_{k=i}^{N} \lambda_{1k} - \beta_i \left(1 + \frac{\sqrt{p_{U2i}}}{\sqrt{p_{U1i}}}\right) - \gamma_{3i} = 0, \quad \forall i \tag{5.48}$$

$$\sum_{k=i}^{N} \lambda_{2k} - \beta_i \left(1 + \frac{\sqrt{p_{U1i}}}{\sqrt{p_{U2i}}}\right) - \gamma_{4i} = 0, \quad \forall i \tag{5.49}$$

$$\sum_{k=i}^{N} \lambda_{1k} - \alpha \sum_{k=i}^{N} \lambda_{2k} - \gamma_{7i} = 0, \quad \forall i \tag{5.50}$$

$$\sum_{k=i}^{N} \lambda_{2k} - \alpha \sum_{k=i}^{N} \lambda_{1k} - \gamma_{8i} = 0, \quad \forall i \tag{5.51}$$

$$-\frac{\theta_{3i}}{\sigma^2 + s_i} + \beta_i - \gamma_{9i} = 0, \quad \forall i \tag{5.52}$$

with complementary slackness conditions:

$$\lambda_{1k} \left(\sum_{i=1}^{k} p_{12i} + p_{U1i} - E_{1i} + \delta_{1i} - \alpha\delta_{2i} \right) = 0, \quad \forall k \tag{5.53}$$

$$\lambda_{2k} \left(\sum_{i=1}^{k} p_{21i} + p_{U2i} - E_{2i} + \delta_{2i} - \alpha\delta_{1i} \right) = 0, \quad \forall k \tag{5.54}$$

$$\theta_{1i} \left(r_{1i} - f(1+p_{12i}) \right) = 0, \quad \forall i \tag{5.55}$$

$$\theta_{2i} \left(r_{2i} - f(1+p_{21i}) \right) = 0, \quad \forall i \tag{5.56}$$

$$\theta_{3i} \left(r_{1i} + r_{2i} - f(s_i/\sigma^2) \right) = 0, \quad \forall i \tag{5.57}$$

$$\beta_i (s_i - \sigma^2 - p_{12i} - p_{U1i} - p_{21i} - p_{U2i} - 2\sqrt{p_{U1i}p_{U2i}}) = 0, \quad \forall i \tag{5.58}$$

$$\gamma_{1i}p_{12i} = \gamma_{2i}p_{21i} = \gamma_{3i}p_{U1i} = \gamma_{4i}p_{U2i} = 0, \quad \forall i \tag{5.59}$$

$$\gamma_{5i}r_{1i} = \gamma_{6i}r_{2i} = \gamma_{7i}\delta_{1i} = \gamma_{8i}\delta_{2i} = \gamma_{9i}s_i = 0, \quad \forall i \tag{5.60}$$

From Lemma 5.5, $\gamma_{3i} = \gamma_{4i} = 0, \forall i$. Now, we investigate the optimal Lagrange multipliers in the following two lemmas.

Lemma 5.6 *We have* $\beta_i > 0, \forall i$.

Proof: Assume $\beta_i = 0$. From (5.52), $\theta_{3i} = 0$, from (5.44), $\theta_{1i} = \mu_1 + \gamma_{5i} > 0$ and from (5.45), $\theta_{2i} = \mu_2 + \gamma_{6i} > 0$, which imply from (5.60) $r_{1i} = r_{2i} = 0$, which cannot be optimal. ■

We note that Lemma 5.6 further means, from (5.48) and (5.49), that $\sum_{k=i}^{N} \lambda_{1k} > 0, \sum_{k=i}^{N} \lambda_{2k} > 0, \forall i$.

Lemma 5.7 *We have* $\gamma_{9i} = 0, \forall i$.

Proof: Assume $\gamma_{9i} > 0$ for some i. This implies $s_i = 0$ and from (5.41), $r_{1i} = r_{2i} = 0$, which cannot be optimal. ■

Using the structure of the optimal Lagrange multipliers, the following lemma shows the properties of the optimal solution.

Lemma 5.8 *The optimal profile must satisfy:*

1. $s_i = \sigma^2 + p_{12i} + p_{U1i} + p_{21i} + p_{U2i} + 2\sqrt{p_{U1i}p_{U2i}}, \forall i$.
2. $r_{1i} + r_{2i} = f(s_i/\sigma^2), \forall i$
3. $r_{1i} = f(1 + p_{12i}), r_{2i} = f(1 + p_{12i}), \forall i$

Proof: We prove the lemma as follows:

1) Follows from Lemma 5.6 and (5.58).

2) From Lemma 5.7 and (5.52), we have $\theta_{3i} = \beta_i(\sigma^2 + s_i)$. Since $\beta_i > 0$ from Lemma 5.6, $\theta_{3i} > 0$ which implies $r_{1i} + r_{2i} = f(s_i/\sigma^2)$ from (5.57).

3) If $p_{12i} = 0$, then we must have $r_{1i} = 0$ and $r_{1i} = f(1+p_{12i})$ is satisfied. If $p_{12i} > 0$, then $\gamma_{1i} = 0$ from (5.59). From (5.46) and (5.48), $\theta_{1i} = \beta_i\sqrt{p_{U2i}/p_{U1i}}(1 + p_{12i}) > 0$. From (5.55), $r_{1i} = f(1 + p_{12i})$. Similarly, if $p_{21i} = 0$, then we must have $r_{2i} = 0$ and $r_{2i} = f(1 + p_{21i})$. If $p_{21i} > 0$, then $\gamma_{2i} = 0$ from (5.59). From (5.47) and (5.49), $\theta_{2i} = \beta_i\sqrt{p_{U1i}/p_{U2i}}(1 + p_{21i}) > 0$. From (5.56), $r_{2i} = f(1 + p_{21i})$. ■

Lemma 5.8 shows that there is a one-to-one correspondence between the transmission rates and transmission powers. Furthermore, the transmission powers should satisfy

$$f(1 + p_{12i}) + f(1 + p_{21i}) = f(s_i/\sigma^2), \quad \forall i. \tag{5.61}$$

Now, we show that, data cooperation always precedes energy cooperation. In other words, a user with excess energy to be invested in cooperation in a given slot, must first invest more energy for data cooperation than its partner; only then can it invest energy for direct energy cooperation.

Lemma 5.9 *The optimal profile satisfies the following:*

1. *If* $\delta_{2i} > 0$ *then* $p_{U2i} > p_{U1i}$.

2. *If* $\delta_{1i} > 0$ *then* $p_{U1i} > p_{U2i}$.

Proof: We start with the first item. If $\delta_{2i} > 0$, then from (5.60), we have $\gamma_{8i} = 0$. From (5.51), we have $\sum_{k=i}^{N} \lambda_{2k} = \alpha \sum_{k=i}^{N} \lambda_{1k}$. This implies from (5.48) and (5.49),

$$\beta_i \left(1 + \frac{\sqrt{p_{U1i}}}{\sqrt{p_{U2i}}}\right) = \alpha\beta_i \left(1 + \frac{\sqrt{p_{U2i}}}{\sqrt{p_{U1i}}}\right) \tag{5.62}$$

Since $\beta_i > 0$ and $\alpha < 1$, (5.62) implies:

$$\left(1 + \frac{\sqrt{p_{U1i}}}{\sqrt{p_{U2i}}}\right) < \left(1 + \frac{\sqrt{p_{U2i}}}{\sqrt{p_{U1i}}}\right) \tag{5.63}$$

which implies $p_{U2i} > p_{U1i}$. The second item is proved similarly. ■

Now, we show that if, in a given slot, a user with high priority transfers energy to a user with lower priority, the user with higher priority must already be transmitting at a higher data rate in that slot than the user with lower priority.

Lemma 5.10 *The optimal profile satisfies the following:*

1. *For $\mu_2 \geq \mu_1$, if $\delta_{2i} > 0$, then $r_{2i} \geq r_{1i}$.*

2. *For $\mu_1 \geq \mu_2$, if $\delta_{1i} > 0$, then $r_{1i} \geq r_{2i}$.*

Proof: We start with the first item. Assume $\mu_1 \geq \mu_2$ and $\delta_{2i} > 0$. If $p_{12i} = 0$, then $r_{1i} = 0$ and the statement holds trivially. We will assume $p_{12i} > 0$. From (5.60), $\gamma_{8i} = 0$. From (5.51), $\sum_{k=i}^{N} \lambda_{2k} < \sum_{k=i}^{N} \lambda_{1k}$. From (5.46) and (5.47), this implies

$$\frac{\theta_{2i}}{(1 + p_{21i})} + \beta_i + \gamma_{2i} < \frac{\theta_{1i}}{(1 + p_{12i})} + \beta_i + \gamma_{1i} = \frac{\theta_{1i}}{(1 + p_{12i})} + \beta_i \tag{5.64}$$

where the equality follows since $p_{12i} > 0$ implies $\gamma_{1i} = 0$. Then we have,

$$\frac{\theta_{2i}}{(1+p_{21i})} < \frac{\theta_{1i}}{(1+p_{12i})} \tag{5.65}$$

From (5.44) and (5.45) we have,

$$\theta_{1i} = \mu_1 + \gamma_{5i} - \theta_{3i} = \mu_1 - \theta_{3i} \tag{5.66}$$

$$\theta_{2i} = \mu_2 + \gamma_{6i} - \theta_{3i} \geq \mu_2 - \theta_{3i} \tag{5.67}$$

where (5.66) follows from $r_{1i} > 0 = f(1 + p_{12i}) > 0$, therefore $\gamma_{5i} = 0$. Since $\mu_2 \geq \mu_1$, we have $\theta_{2i} \geq \theta_{1i}$. Together with (5.65), this implies we have $p_{21i} > p_{12i}$ and therefore $r_{2i} > r_{1i}$. The second item is proved similarly. ■

5.4.1 Procrastinating Policies

In this sub-section, we show the existence of *procrastinating policies* that solve this problem. Procrastinating policies are introduced in [88] and they have the property that any energy transferred at slot i, must be immediately consumed by the receiving party at slot i. We formalize this definition below.

Definition 5.1 *A policy is called procrastinating if it satisfies the following property:*

$$p_{12i} + p_{U1i} \geq \alpha\delta_{2i}, \quad p_{21i} + p_{U2i} \geq \alpha\delta_{1i}, \quad \forall i \tag{5.68}$$

Lemma 5.11 *There exists a procrastinating policy that solves the problem in (5.10).*

The proof of Lemma 5.11 follows from similar arguments as in [88, Lemma 1].

We split the energy transfers δ_{1i}, δ_{2i} into two components $\pi_{1i} \geq 0, \pi_{2i} \geq 0$ and $\nu_{1i} \geq 0, \nu_{2i} \geq 0$ as follows:

$$\delta_{1i} = \pi_{1i} + \nu_{1i}, \quad \delta_{2i} = \pi_{2i} + \nu_{2i}, \quad \forall i \tag{5.69}$$

In this decomposion π_{1i}, π_{2i} represent the portion of energy transfer that is consumed in the *direct* transmission, i.e., to increase p_{12i}, p_{21i}. Similarly, ν_{1i}, ν_{2i} represent the portion of energy transfer that is consumed in the *cooperative* transmission, i.e., to increase p_{U1i}, p_{U2i}. Any procrastinating policy can now be written as

$$p_{12i} \geq \alpha\pi_{2i}, \quad p_{U1i} \geq \alpha\nu_{2i}, \quad \forall i \tag{5.70}$$

$$p_{21i} \geq \alpha\pi_{1i}, \quad p_{U2i} \geq \alpha\nu_{1i}, \quad \forall i \tag{5.71}$$

Lemma 5.12 *The optimal profile satisfies the following properties,*

1. *For $\mu_2 \geq \mu_1$, if $\pi_{2i} > 0$ then $p_{21i} > 0$.*

2. *For $\mu_1 \geq \mu_2$, if $\pi_{1i} > 0$, then $p_{12i} > 0$.*

Proof: We start with the first item. If $\pi_{2i} > 0$ then $\delta_{2i} > 0$ and from Lemma 5.10 we have $r_{2i} \geq r_{1i}$ which implies $p_{21i} \geq p_{12i}$. From procrastinating policies, we have that this transferred energy must be used immediately in direct power, therefore $p_{12i} > 0$, which implies $p_{21i} > 0$. The second item is proved similarly. ■

Lemma 5.12 shows that if any direct energy is transferred from a user with high priority to a user with low priority, then the sending party must be consuming at least some amount in direct transmission.

5.4.2 Algorithmic Solution

While we have shown several important properties of the optimal solution, we still need to solve the problem to obtain the transmit scheduling and energy transfer policy. We do this using an algorithmic approach based on the KKT conditions given earlier. We determine the conditions under which energy transfer occurs. Then, we develop an algorithm to compute the optimal energy transfer and power allocation policy. Now, we show that energy transfers are never bidirectional, i.e., in any slot energy transfer happens only in a single direction.

Lemma 5.13 *In the optimal profile if* $\delta_{1i} > 0$ *then* $\delta_{2i} = 0$ *and if* $\delta_{2i} > 0$ *then* $\delta_{1i} = 0$*, i.e.* $\delta_{1i}\delta_{2i} = 0$, $\forall i$.

Proof: Assume for some slot i, $\delta_{1i} > 0, \delta_{2i} > 0$. Then, from (5.60), $\gamma_{7i} = \gamma_{8i} = 0$, and from (5.50) and (5.51), $\sum_{k=i}^{N} \lambda_{1k} = \alpha \sum_{k=i}^{N} \lambda_{2k} = \alpha(\alpha \sum_{k=i}^{N} \lambda_{1k})$ which cannot happen unless $\alpha = 1$. ■

Lemma 5.14 *If* $\alpha < \frac{\sum_{k=i}^{N} \lambda_{1k}}{\sum_{k=i}^{N} \lambda_{2k}} < \frac{1}{\alpha}$*, there is no energy transfer in either direction at slot i, i.e.,* $\delta_{1i} = \delta_{2i} = 0$.

Proof: Let $\alpha < \frac{\sum_{k=i}^{N} \lambda_{1k}}{\sum_{k=i}^{N} \lambda_{2k}} < \frac{1}{\alpha}$, or equivalently $\sum_{k=i}^{N} \lambda_{1k} > \alpha \sum_{k=i}^{N} \lambda_{2k}$ and $\sum_{k=i}^{N} \lambda_{2k} > \alpha \sum_{k=i}^{N} \lambda_{1k}$. From (5.50) and (5.51), $\gamma_{7i} > 0, \gamma_{8i} > 0$ and from (5.60) $\delta_{1i} = \delta_{2i} = 0$.

■

Lemma 5.15 *A power allocation policy which yields* $\frac{\sum_{k=i}^{N}\lambda_{1k}}{\sum_{k=i}^{N}\lambda_{2k}} < \alpha$ *or* $\frac{\sum_{k=i}^{N}\lambda_{1k}}{\sum_{k=i}^{N}\lambda_{2k}} > \frac{1}{\alpha}$ *is strictly suboptimal.*

Proof: Follows from (5.50), (5.51) and $\gamma_{7i} \geq 0, \gamma_{8i} \geq 0$. ■

Lemma 5.16 *In a given slot* $i \in 1, \ldots, N$, *user* $\ell \in \{1, 2\}$ *transfers energy to user* $m \in \{1, 2\}, m \neq \ell$, *i.e.,* $\delta_{li} > 0$, *if* $\frac{\sum_{k=i}^{N}\lambda_{\ell k}}{\sum_{k=i}^{N}\lambda_{mk}} = \alpha$.

Proof: If $\delta_{1i} > 0$ then from (5.60) we have $\gamma_{7i} = 0$. If $\delta_{2i} > 0$ then from (5.60) we have $\gamma_{8i} = 0$. The result then follows from (5.50) and (5.51). ■

Lemmas 5.14, 5.15 and 5.16 have the following physical interpretation: the ratio of the generalized water levels $v_{\ell i} \triangleq \left(\sum_{k=i}^{N}\lambda_{\ell k}\right)^{-1}$, $\ell \in \{1, 2\}$, determines whether or not there should be energy cooperation in each given slot. In particular, for slot i in which the generalized water level ratio $v_{\ell i}/v_{mi}$ without energy transfer is below the energy transfer efficiency α, energy should be transferred from user m to user ℓ, until the ratio is exactly equal to α. If there is not much discrepancy between the water levels, i.e., the ratio is between α and $1/\alpha$, then there should be no energy transfer.

Note that, the KKT conditions pertaining to the energy transfer policy do not explicitly depend on the powers, and the KKT conditions pertaining to the optimal power distribution policy do not explicitly depend on the energy transfer variables. Since these two sets of conditions are coupled only through the generalized

Algorithm 5 Optimal energy and data cooperation algorithm

Initialize

for $i = 1 : N$ **do**
  $p_{1i} \leftarrow E_{1i}, p_{2i} \leftarrow E_{2i}$
  Determine subpowers $p_{12i}, p_{U1i}, p_{21i}, p_{U2i}$
  Determine water levels $\sum_{k=i}^{N} \lambda_{1k}, \sum_{k=i}^{N} \lambda_{2k}$ from (5.46), (5.47)
end for

Main Algorithm

repeat
  for $i = 1 : N$ **do**
If $\sum_{k=i}^{N} \lambda_{1k} < \alpha \sum_{k=i}^{N} \lambda_{2k}$, transfer energy from user 1 to user 2
If $\sum_{k=i}^{N} \lambda_{2k} < \alpha \sum_{k=i}^{N} \lambda_{1k}$, transfer energy from user 2 to user 1
      Determine new subpowers $p_{12i}, p_{U1i}, p_{21i}, p_{U2i}$
      Determine new water levels
  end for
until
$\sum_{k=i}^{N} \lambda_{1k} = \alpha \sum_{k=i}^{N} \lambda_{2k}$ or $\sum_{k=i}^{N} \lambda_{2k} = \alpha \sum_{k=i}^{N} \lambda_{1k}$

water levels, it is possible to develop an iterative algorithm that iterates over power distribution and energy transfer steps, updating the generalized water levels in each energy transfer step based on Lemmas 5.14, 5.15 and 5.16. Such an algorithm, that provably converges, is given in Algorithm 5.

5.5 Numerical Results

In this section, we provide numerical examples and illustrate the resulting optimal policies. We consider band-limited AWGN broadcast and multiple-access channels. The bandwidth is $B_W = 1$ MHz and the noise power spectral density is $N_0 = 10^{-19}$ W/Hz. We assume that the path loss between user 1 to user 2 (h_{12}) and user 2 to user 1 (h_{21}) are assumed to be same ($h_{12} = h_{21}$) and 130dB. The path loss between user 1 to destination (h_{1d}) and user 2 to destination (h_{2d}) are assumed to be same

$(h_{1d} = h_{2d})$ and 133dB. With these definitions, equations (5.1) and (5.2) become:

$$r_{1i} \leq B_W \log_2 \left(1 + \frac{h_{12} p_{12i}}{N_0 B_W}\right) = \log_2 \left(1 + p_{12i}\right) \text{Mbps} \tag{5.72}$$

$$r_{2i} \leq B_W \log_2 \left(1 + \frac{h_{21} p_{21i}}{N_0 B_W}\right) = \log_2 \left(1 + p_{21i}\right) \text{Mbps} \tag{5.73}$$

$$\begin{aligned} r_{1i} + r_{2i} &\leq B_W \log_2 \left[1 + (N_0 B_W)^{-1} \left(h_{1d} p_{1i} + h_{2d} p_{2i} + 2\sqrt{h_{1d} p_{U1i} h_{2d} p_{U2i}}\right)\right] \\ &= \log_2 \left(1 + \frac{p_{12i} + p_{21i} + 2\sqrt{p_{U1i} p_{U2i}}}{2}\right) \text{Mbps} \end{aligned} \tag{5.74}$$

5.5.1 Intermittent Data Arrivals Scenario

We demonstrate numerically that user cooperation improves the achievable departure region of a MAC, under data and energy arrival constraints. In Fig. 5.2 we plot the achievable departure region of the proposed cooperative MAC model with energy and data arrival constraints. The energy and data arrivals are chosen as $\mathbf{E}_1 = [5, 0, 5, 0, 0, 0, 0, 10, 0, 0]$ mJ, $\mathbf{E}_2 = [5, 0, 0, 0, 0, 10, 0, 0, 5, 0]$ mJ, $\mathbf{d}_1 = [1.4, 1.4, 0, 1.4, 0, 7, 14, 0, 14, 0] \times 10^{-1}$ Mbits, $\mathbf{d}_2 = [7, 2.8, 0, 14, 0, 0, 1.4, 2.8, 0, 0] \times 10^{-1}$ Mbits. The transmission deadline is chosen as 10 seconds. The existence of data arrivals in the cooperative MAC has an impact on the departure region and this effect is more apparent in the single user rates. We also observe that cooperation has enhanced the departure region when we compare the ordinary MAC and cooperative MAC both with data and energy arrrivals.

Additionally, we plot the data departure curves for both users in Fig. 5.3 in the case of sum rate maximization, i.e., $\mu_1 = \mu_2 = 1$. We see that the possibility of user cooperation allows for higher data rates to be sustained using the same amount

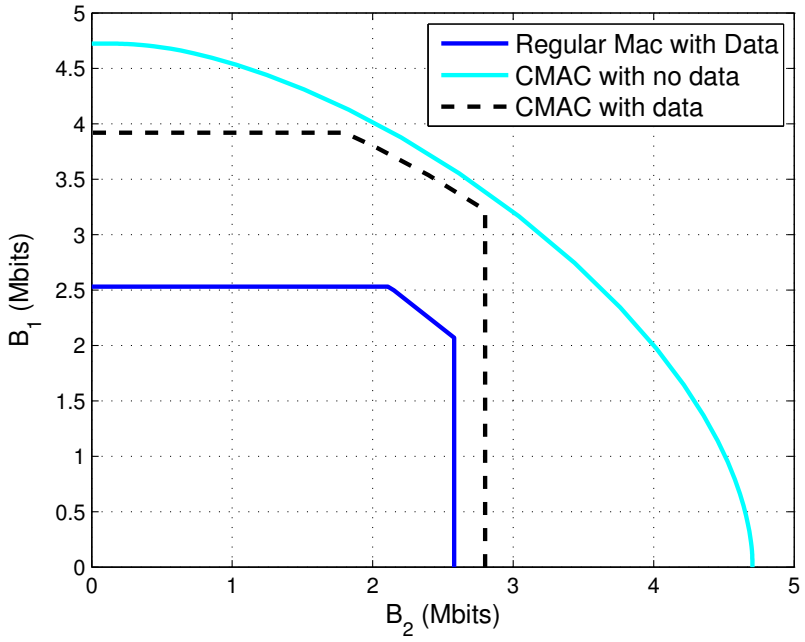

Figure 5.2: Departure regions of cooperative MAC with and without data arrivals vs the capacity region of regular MAC with data arrivals.

of energy.

5.5.2 Energy Cooperation Scenario

We demonstrate here that energy and data cooperation improve the achievable departure region of a MAC. In Fig. 5.4 we plot the achievable departure region of the proposed cooperative MAC model with energy and data cooperation. For comparison, we also plot the departure region of a cooperative MAC channel with only data cooperation which was studied in [85]. We use the channel parameters as described before.

The energy arrivals are $\mathbf{E}_1 = [5, 0, 5, 0, 0, 0, 0, 10, 0, 0]$ mJ, $\mathbf{E}_2 = [5, 0, 0, 0, 0, 10, 0, 0, 5, 0]$ mJ, with energy transfer efficiency of $\alpha = 0.6$ and the transmission

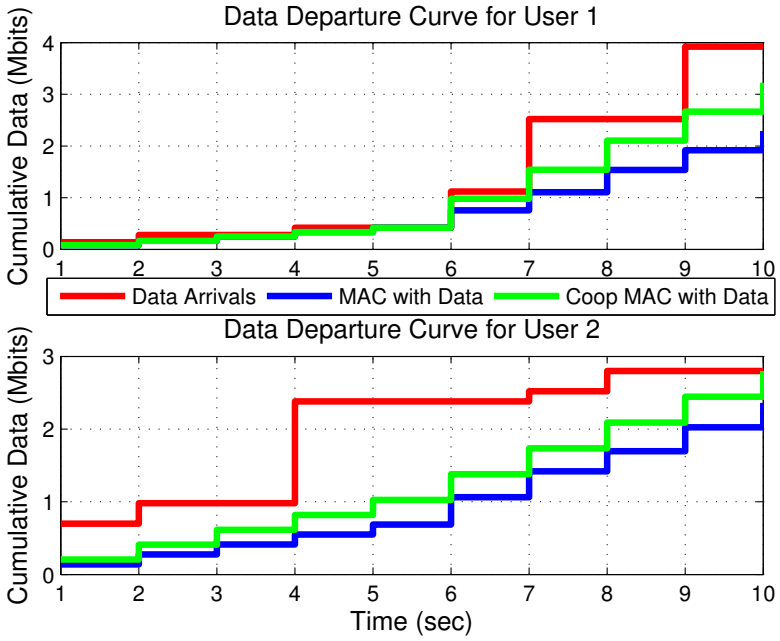

Figure 5.3: Data departure curves for both users in the case of $\mu_1 = \mu_2 = 1$.

deadline is chosen as 10 seconds. Energy cooperation together with data cooperation has enhanced the departure region of the MAC. It is interesting that this effect is more pronounced in single user optimal points rather than sum rate optimal point. At the sum rate optimal point, $\sum_{i=1}^{N} r_{1i} + r_{2i}$ is optimized and the discrepancies in the energy arrival patterns are negated due to the powers appearing as a summation term.

Now, we investigate the case when user priorities are fixed at $\mu_1 = 0.6, \mu_2 = 1$. In Figs. 5.5 and 5.6 we plot the energy usage curve, where we plot the cumulative energy consumption for each user. We separately plot the energy used for direct power components, p_{12}, p_{21} and the cooperative power components, p_{U1}, p_{U2}. We also compare the effect of energy cooperation. From Fig. 5.5 we see that with energy cooperation, user 1 has transferred considerable amount of energy to user

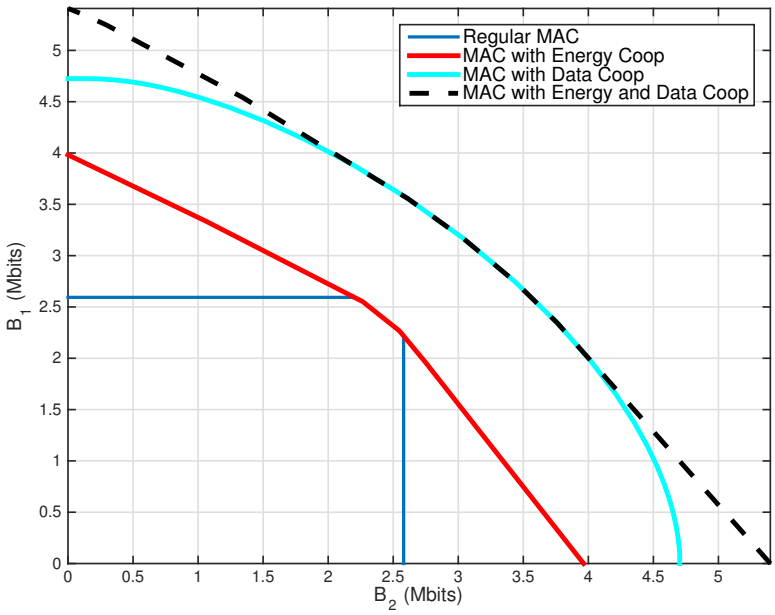

Figure 5.4: Departure regions of regular MAC, MAC with energy cooperation, MAC with data cooperation and MAC with energy and data cooperation

2 and set its direct powers to zero. This means that user 1 no longer transmits any independent data, but has become a dedicated relay for user 2. From Fig. 5.6 we see that with energy cooperation, the direct power of user 2 has exceeded the available energy at slot 5. The cooperative powers p_{U2} did not change with energy cooperation and therefore all the transferred energy from user 1 has been consumed in direct transmission.

5.6 Concluding Remarks

In the first part of the chapter, we considered a cooperative MAC with intermittent data and energy arrivals. We found the optimal offline power and rate allocation policy that maximize the departure region. We first showed that there exists an

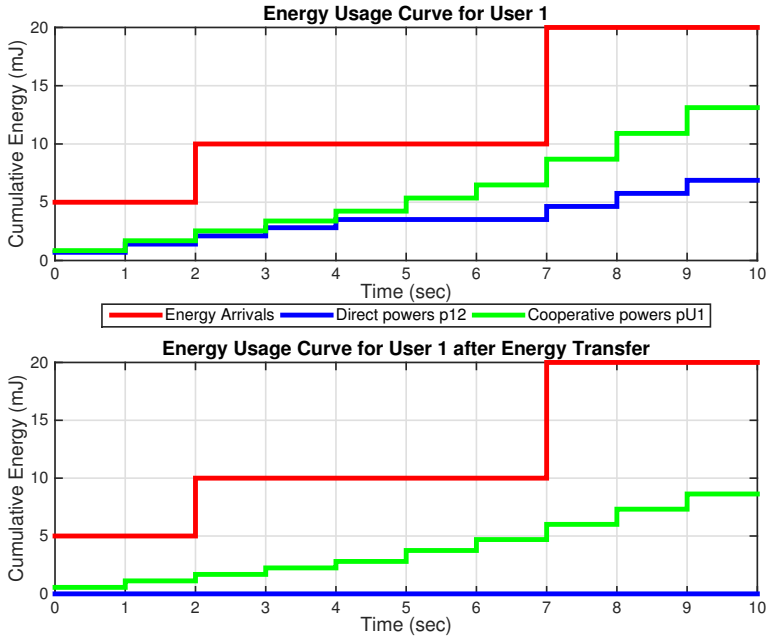

Figure 5.5: Energy usage curve for user 1 with and without energy cooperation for $\mu_1 = 0.6$ and $\mu_2 = 1$

optimal policy, in which the single user rate constraints in each time slot are tight. Then, we formulated the departure region maximization problem as a weighted sum rate maximization in terms of rates only. Next, we proposed a sequential convex approximation method and showed that it converges to the optimal solution. Finally, we solved the approximate problems with an inner outer decomposition method. Numerically, we observed that higher data rates can be sustained using the same amount of energy.

In the second part of the chapter, we considered a cooperative MAC with data and energy cooperation. We found the optimal offline transmit power and rate allocation policy that maximizes the departure region. We first showed that, the cooperative powers in each slot must be non-zero for both users. Next, we showed

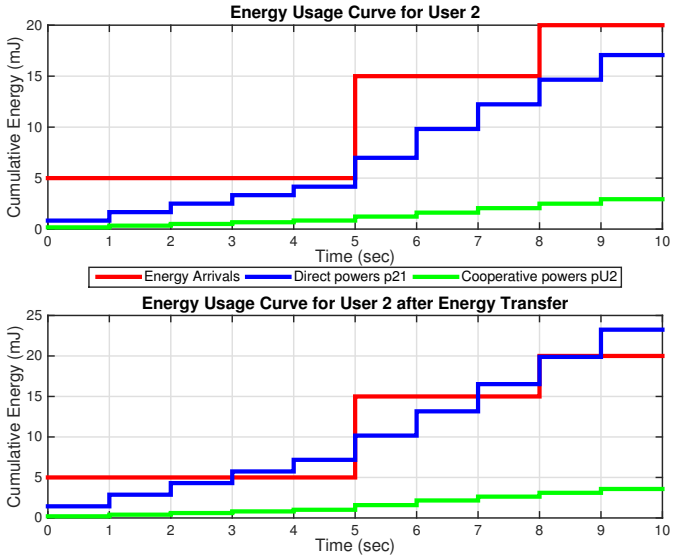

Figure 5.6: Energy usage curve for user 2 with and without energy cooperation for $\mu_1 = 0.6$ and $\mu_2 = 1$

that, data cooperation always precedes energy cooperation. In other words, excess energy must first be used to increase cooperative powers and then to assist the other user via energy cooperation. Then, we showed that if a high priority user transfers energy to a low priority user, the higher priority user must already be transmitting at a higher data rate than the other user. Finally, we showed the existence of procrastinating policies, which have the property that energy transferred in a slot must be consumed in that slot immediately.

5.7 Appendix

5.7.1 Coefficients of (5.19)

By differentiating $f(s_i/\sigma^2)$ the coefficients are,

$$A_i^n = 2^{2r_{1i}^n} + 2^{2r_{U1i}^n} + 2^{2r_{2i}^n} + 2^{2r_{U2i}^n} + 2\sqrt{(2^{2r_{U1i}^n}-1)(2^{2r_{U2i}^n}-1)} - 4 \tag{5.75}$$

$$\alpha_{1i}^n \triangleq \frac{\partial g}{\partial r_{1i}}\Big|_{r_{1i}^n} = \frac{0.5}{1+A_i^n/\sigma^2} 2^{2r_{1i}^n} \tag{5.76}$$

$$\alpha_{2i}^n \triangleq \frac{\partial g}{\partial r_{2i}}\Big|_{r_{2i}^n} = \frac{0.5}{1+A_i^n/\sigma^2} 2^{2r_{2i}^n} \tag{5.77}$$

$$\beta_{1i}^n \triangleq \frac{\partial g}{\partial r_{U1i}}\Big|_{r_{U1i}^n} = \frac{0.5}{1+A_i^n/\sigma^2} 2^{2r_{U1i}^n} \left(1 + \frac{\sqrt{2^{2r_{U2i}^n}-1}}{\sqrt{2^{2r_{U1i}^n}-1}}\right) \tag{5.78}$$

$$\beta_{2i}^n \triangleq \frac{\partial g}{\partial r_{U2i}}\Big|_{r_{U2i}^n} = \frac{0.5}{1+A_i^n/\sigma^2} 2^{2r_{U2i}^n} \left(1 + \frac{\sqrt{2^{2r_{U1i}^n}-1}}{\sqrt{2^{2r_{U2i}^n}-1}}\right) \tag{5.79}$$

$$C_i^n = \frac{1}{2}\log_2\left(1 + \frac{A_i^n}{\sigma^2}\right) \tag{5.80}$$

5.7.2 Proof of Lemma 5.2

We will prove a more general result. Assume we have two optimization problems (P1) and (P2) as given below.

$$\begin{aligned} \textbf{(P1):} \quad & \min_{\mathbf{x}} \quad f_0(\mathbf{x}) \\ & \text{s.t.} \quad f_i(\mathbf{x}) \le 0,\ i = 1, \ldots, m \\ \textbf{(P2):} \quad & \min_{\mathbf{y}} \quad f_0(h(\mathbf{y})) \\ & \text{s.t.} \quad f_i(h(\mathbf{y})) \le 0,\ i = 1, \ldots, k \end{aligned} \tag{5.81}$$

$$f_i(h(\mathbf{y})) = 0,\ i = k+1, \ldots, m \tag{5.82}$$

Here $\{f_i\}_{i=1}^m$ are convex, differentiable functions and $h(\mathbf{y})$ is a collection of one-to-one, invertible functions. (P2) is obtained from (P1) by enforcing some inequality constraints with equality and by a change of variables, $\mathbf{x} = h(\mathbf{y})$. Since (P1) is a convex optimization problem, strong duality holds [70]. We denote the primal optimal values of problems (P1) and (P2) as p_1^*, p_2^* respectively. We show the following lemma.

Lemma 5.17 *If $p_1^* = p_2^*$, then strong duality also holds for (P2).*

Proof: The dual function and the Lagrange dual problem for (P1) are,

$$g_1(\boldsymbol{\lambda}) = \min_{\mathbf{x}} \left[f_0(\mathbf{x}) + \sum_{i=1}^{m} \lambda_i f_i(\mathbf{x}) \right] \tag{5.83}$$

$$q_1^* = \max_{\boldsymbol{\lambda} \geq \mathbf{0}} g_1(\boldsymbol{\lambda}) \tag{5.84}$$

where $\boldsymbol{\lambda}$ are the Lagrange multipliers corresponding to the inequality constraints in (5.81) and q_1^* denotes the optimal dual value. Similarly for (P2),

$$g_2(\boldsymbol{\beta}, \boldsymbol{\gamma}) = \min_{\mathbf{y}} \left[f_0(h(\mathbf{y})) + \sum_{i=1}^{k} \beta_i f_i(h(\mathbf{y})) + \sum_{i=k+1}^{m} \gamma_i f_i(h(\mathbf{y})) \right] \tag{5.85}$$

$$q_2^* = \max_{\boldsymbol{\beta} \geq \mathbf{0}, \boldsymbol{\gamma}} g_2(\boldsymbol{\beta}, \boldsymbol{\gamma}) \tag{5.86}$$

where β_i and γ_i correspond to the inequality and equality constraints in (5.82), respectively. We do not have the constraints $\boldsymbol{\gamma} \geq \mathbf{0}$ since $\boldsymbol{\gamma}$ corresponds to equality

constraints. Since h is invertible, we let $\mathbf{x} = h^{-1}(\mathbf{y})$ and rewrite (5.85) as,

$$g_2(\boldsymbol{\beta}, \boldsymbol{\gamma}) = \min_{\mathbf{x}} \left[f_0(\mathbf{x}) + \sum_{i=1}^{k} \beta_i f_i(\mathbf{x}) + \sum_{i=k+1}^{m} \gamma_i f_i(\mathbf{x}) \right] \tag{5.87}$$

Now we have,

$$q_2^* \geq \max_{(\boldsymbol{\beta}, \boldsymbol{\gamma}) \geq \mathbf{0}} g_2(\boldsymbol{\beta}, \boldsymbol{\gamma}) = \max_{\boldsymbol{\lambda} \geq \mathbf{0}} g_2(\boldsymbol{\lambda}) = \max_{\boldsymbol{\lambda} \geq \mathbf{0}} g_1(\boldsymbol{\lambda}) = q_1^* \tag{5.88}$$

where the first inequality follows from the fact that $\boldsymbol{\gamma} \geq \mathbf{0}$ yields to a more restricted feasible set, the first equality is a rewriting of the problem in terms of variable $\boldsymbol{\lambda}$, the second equality follows from comparing (5.85) to (5.83). Furthermore,

$$q_2^* \geq q_1^* = p_1^* = p_2^*, \quad q_2^* \leq p_2^* \tag{5.89}$$

where $q_1^* = p_1^*$ follows from strong duality of (P1) and $p_1^* = p_2^*$ from assumption and $q_2^* \leq p_2^*$ follows from weak duality of (P2) which always holds irrespective of convexity of the problem. Then we have $q_2^* = p_2^*$ and strong duality holds. ■

The problem in (5.18) is obtained from (5.10) similar to how (P2) is obtained from (P1) without changing the primal objective value and the problem in (5.10) is a convex problem. Therefore the problem in (5.18) has strong duality.

5.7.3 Proof of Lemma 5.3

In [87] a non-convex problem is solved by a convex approximation method, in which non-convex constraints $g(\mathbf{x})$ are approximated around point $\mathbf{x}^n$ by a differentiable convex function $\bar{g}(\mathbf{x}, \mathbf{x}^n)$. Each function $\bar{g}(\mathbf{x}, \mathbf{x}^n)$ must satisfy:

- $g(\mathbf{x}) \leq \bar{g}(\mathbf{x}, \mathbf{x}^n)$ for all feasible $\mathbf{x}$,
- $g(\mathbf{x}) = g(\mathbf{x}^n, \mathbf{x}^n)$,
- $\partial g(\mathbf{x}^n)/\partial \mathbf{x}^n = \partial \bar{g}(\mathbf{x}^n, \mathbf{x}^n)/\partial \mathbf{x}^n$.

In our problem, the non-convex constraint function g is given as $r_{1i}+r_{2i}-f(s_i/\sigma^2) \leq 0$. The last two properties are satisfied when $\bar{g}$ is taken as the Taylor expansion of the function g. The function $f(s_i/\sigma^2)$ is a convex function since it is of the form $\log(\sum 2^x)$. Then, g is concave. The first property is satisfied since linear approximations are over-estimators for concave functions. By [87, Theorem 1], $\mathbf{R}^n$ converges to $\mathbf{R}^*$ where $\mathbf{R}^*$ is a Kuhn-Tucker point of the problem in (5.18). From Lemma 2, strong duality holds and therefore Kuhn-Tucker conditions are both necessary and sufficient for global optimality. Therefore $\mathbf{R}^*$ is a global optimal solution to (5.18).

5.7.4 Proof of Lemma 5.5

We discuss three cases to reach a contradiction in each case.

Case 1: Let $\exists k$ such that $p_{U1k} = 0, p_{U2k} > 0$. Then, $s_k = \sigma^2 + p_{12k} + p_{21k} + p_{U2k}$. We define a new power allocation vector as $\tilde{p}_{U2k} = p_{U2k} - \epsilon_1 - \epsilon_2, \tilde{p}_{21k} = p_{21k} + \epsilon_1, \tilde{p}_{U1k} = \alpha\epsilon_2, \tilde{p}_{12k} = p_{12k}$, for some $\epsilon_1 > 0, \epsilon_2 > 0$. Here, we have transferred ϵ_2 amount of

energy from user 2 to user 1 and consumed it in the cooperative power of user 1. Additionally, we decreased p_{U2k} by ϵ_1 and increased p_{21k} by ϵ_1. The energy causality constraints are satisfied for the new power allocation. Rate region constraints (5.39) and (5.40) become:

$$r_{1k} \leq f(1+\tilde{p}_{12k}) = f(1+p_{12k}) \tag{5.90}$$

$$r_{2k} < f(1+\tilde{p}_{21k}) = f(1+p_{21k}+\epsilon_1) \tag{5.91}$$

For constraint (5.41), we have

$$\tilde{s}_k = \sigma^2 + \tilde{p}_{12k} + \tilde{p}_{U1k} + \tilde{p}_{21k} + \tilde{p}_{U2k} + 2\sqrt{\tilde{p}_{U1k}\tilde{p}_{U2k}} \tag{5.92}$$

$$= \sigma^2 + p_{12k} + \alpha\epsilon_2 + p_{21k} + \epsilon_1 + p_{U2k} - \epsilon_1 - \epsilon_2 + 2\sqrt{\alpha\epsilon_2(p_{U2k}-\epsilon_1-\epsilon_2)} \tag{5.93}$$

$$= s_k + (\alpha-1)\epsilon_2 + 2\sqrt{\alpha\epsilon_2(p_{U2k}-\epsilon_1-\epsilon_2)} > s_k \tag{5.94}$$

where last inequality holds since $2\sqrt{\alpha\epsilon_2(p_{U2k}-\epsilon_1-\epsilon_2)} > (1-\alpha)\epsilon_2$ for small ϵ_1, ϵ_2. Therefore,

$$r_{1k} + r_{2k} < f(\tilde{s}_k/\sigma^2) \tag{5.95}$$

The constraints (5.91), (5.95) are loose and we can increase r_{2k} to get a larger optimal value which contradicts the optimality of the original profile. Therefore, case 1 cannot happen.

Case 2: Similar to case 1, we will reach a contradiction.

Case 3: Let $\exists k$ such that $p_{U1k} = 0, p_{U2k} = 0$. Then, $s_k = \sigma^2 + p_{12k} + p_{21k}$. We cannot have $r_{1k} = f(1+p_{12k}), r_{2k} = f(1+p_{21k})$ because $f(1+p_{12k})+f(1+p_{21k}) > f(s_k/\sigma^2)$ so this is not feasible. Without loss of generality, assume $r_{1k} < f(1+p_{12k})$. We define a new power allocation vector as $\tilde{p}_{12k} = p_{12k}-\epsilon_1-\epsilon_2, \tilde{p}_{U1k} = \epsilon_1, \tilde{p}_{21k} = p_{21k}, \tilde{p}_{U2k} = \alpha\epsilon_2$. Here, we have transferred ϵ_2 amount of energy from user 1 to user 2 and consumed it in the cooperative power of user 2. Additionally, we decreased p_{12k} by ϵ_1 and increased p_{U1k} by ϵ_1.

For small ϵ_1, ϵ_2 we still have $r_{1k} < f(1 + \tilde{p}_{12k})$ which implies (5.39) is satisfied. Since p_{21k} has not been changed, (5.40) is satisfied. For constraint (5.41) we have,

$$\tilde{s}_k = \sigma^2 + \tilde{p}_{12k} + \tilde{p}_{U1k} + \tilde{p}_{21k} + \tilde{p}_{U2k} + 2\sqrt{\tilde{p}_{U1k}\tilde{p}_{U2k}} \tag{5.96}$$

$$= \sigma^2 + p_{12k} - \epsilon_1 - \epsilon_2 + \epsilon_1 + \alpha\epsilon_2 + p_{21k} + 2\sqrt{\epsilon_1\alpha\epsilon_2} \tag{5.97}$$

$$= s_k + (\alpha - 1)\epsilon_2 + 2\sqrt{\epsilon_1\alpha\epsilon_2} > s_k \tag{5.98}$$

where last inequality holds for $\epsilon_1 > \epsilon_2(1-\alpha)^2/(4\alpha)$ which we enforce. Then, $r_{1k} + r_{2k} < f(\tilde{s}_k/\sigma^2)$. Now, we increase r_{1k} which is a contradiction. Therefore, case 3 cannot happen.

CHAPTER 6

Conclusion

In this dissertation, we explored the concept of energy cooperation, where energy can be transferred from one user to another through a separate wireless energy transfer unit, and investigated several multi-user scenarios that involve both energy harvesting and energy cooperation.

In Chapter 2, we investigated three channel models with energy harvesting and energy cooperation. First, we examined additive Gaussian two-hop relay channel with one-way energy transfer from the source node to the relay node where the objective is to maximize the end-to-end throughput. Next, we considered the Gaussian two-way channel with one-way energy transfer, and the two-user Gaussian multiple access channel with one-way energy transfer. For these two channel models, we determined the two-dimensional simultaneously achievable throughput regions. In particular, we developed a *two-dimensional directional water-filling algorithm* which optimally controls the energy flow in time and among users.

In Chapter 3, we considered the delay minimization problem in an energy harvesting communication network with energy cooperation. For fixed data and

energy routing topologies, we determined the optimum data rates, transmit powers and energy transfers, subject to flow and energy conservation constraints, in order to minimize the network delay. We started with a simplified problem with fixed data flows and a single energy harvest per node. For this case, with no energy cooperation, we showed that each node should allocate more power to links with more noise and/or more data flow. We then extended this setting to the case of multiple energy harvests per node over time. For this case, with no energy cooperation, we showed that, for any given node, the sum of powers on the outgoing links over time is equal to the single-link optimal power over time. Then, we considered the problem of joint flow control and energy management for the entire network. We determined the necessary conditions for joint optimality of a power control, energy transfer and routing policy.

In Chapter 4, we considered the energy harvesting diamond channel, where the source and two relays harvest energy from nature and the physical layer is modeled as a concatenation of a broadcast and a multiple access channel. We found the optimal offline transmit power and rate allocations that maximize the end-to-end throughput. For the broadcast side, we showed that there exists an optimal source power allocation which is equal to the single-user optimal power allocation for the source energy arrivals. We then showed that the fraction of the power spent on each broadcast link depends on the energy arrivals for the relays. For the multiple access side with no cooperation, with fixed source rates, we showed that the problem can be cast as a multiple access channel with both data and energy arrivals and can be formulated in terms of data transmission rates only. We used a dual decomposition

method to solve the overall problem efficiently.

In Chapter 5, we considered an energy harvesting two user cooperative Gaussian multiple access channel. We studied two scenarios within this model. In the first scenario, the data packets arrive intermittently over time. We found the optimal offline transmit power and rate allocation policy that maximize the departure region. We first showed that there exists an optimal policy, in which the single-user rate constraints in each time slot are tight, yielding a one-to-one relation between the powers and rates. Then, we formulated the departure region maximization problem as a weighted sum rate maximization in terms of rates only. Next, we proposed a sequential convex approximation method to approximate the problem at each step and showed that it converges to the optimal solution. Then, we solved the approximate problems using an inner outer decomposition method. In the second scenario, the users cooperate at the battery level (energy cooperation) by wirelessly transferring energy to each other in addition to the data cooperation. We found the jointly optimal offline transmit power and rate allocation policy together with the energy transfer policy that maximize the departure region. We provided necessary conditions for energy transfer.

Bibliography

[1] J. Lei, R. D. Yates, and L. Greenstein. A generic framework for optimizing single-hop transmission policy of replenishable sensors. *IEEE Trans. Wireless Comm.*, 8(2):547–551, February 2009.

[2] M. Gatzianas, L. Georgiadis, and L. Tassiulas. Control of wireless networks with rechargeable batteries. *IEEE Trans. Wireless Comm.*, 9(2):581–593, February 2010.

[3] V. Sharma, U. Mukherji, V. Joseph, and S. Gupta. Optimal energy management policies for energy harvesting sensor nodes. *IEEE Trans. Wireless Comm.*, 9(4):1326–1336, April 2010.

[4] J. Yang and S. Ulukus. Optimal packet scheduling in an energy harvesting communication system. *IEEE Trans. Comm.*, 60(1):220–230, January 2012.

[5] K. Tutuncuoglu and A. Yener. Optimum transmission policies for battery limited energy harvesting nodes. *IEEE Trans. Wireless Comm.*, 11(3):1180–1189, March 2012.

[6] O. Ozel, K. Tutuncuoglu, J. Yang, S. Ulukus, and A. Yener. Transmission with energy harvesting nodes in fading wireless channels: Optimal policies. *IEEE Jour. on Selected Areas in Comm.*, 29(8):1732–1743, September 2011.

[7] J. Yang, O. Ozel, and S. Ulukus. Broadcasting with an energy harvesting rechargeable transmitter. *IEEE Trans. Wireless Comm.*, 11(2):571–583, February 2012.

[8] M. A. Antepli, E. Uysal-Biyikoglu, and H. Erkal. Optimal packet scheduling on an energy harvesting broadcast link. *IEEE Jour. on Selected Areas in Comm.*, 29(8):1721–1731, September 2011.

[9] O. Ozel, J. Yang, and S. Ulukus. Optimal broadcast scheduling for an energy harvesting rechargeable transmitter with a finite capacity battery. *IEEE Trans. Wireless Comm.*, 11(6):2193–2203, June 2012.

[10] J. Yang and S. Ulukus. Optimal packet scheduling in a multiple access channel with energy harvesting transmitters. *Journal of Comm. and Netw.*, 14:140–150, April 2012.

[11] K. Tutuncuoglu and A. Yener. Sum-rate optimal power policies for energy harvesting transmitters in an interference channel. *Journal of Comm. and Netw.*, 14(2):151–161, April 2012.

[12] C. Huang, R. Zhang, and S. Cui. Throughput maximization for the Gaussian relay channel with energy harvesting constraints. *IEEE Jour. on Selected Areas in Comm.*, 31:1469–1479, August 2013.

[13] D. Gunduz and B. Devillers. Two-hop communication with energy harvesting. In *IEEE CAMSAP*, December 2011.

[14] O. Orhan and E. Erkip. Optimal transmission policies for energy harvesting two-hop networks. In *CISS*, March 2012.

[15] Y. Luo, J. Zhang, and K. B. Letaief. Optimal scheduling and power allocation for two-hop energy harvesting communication systems. *IEEE Trans. Wireless Comm.*, 12(9):4729–4741, September 2013.

[16] B. Devillers and D. Gunduz. A general framework for the optimization of energy harvesting communication systems with battery imperfections. *Journal of Comm. and Netw.*, 14(2):130–139, April 2012.

[17] K. Tutuncuoglu, A. Yener, and S. Ulukus. Optimum policies for an energy harvesting transmitter under energy storage losses. *IEEE Jour. on Selected Areas in Comm.*, 33(3):467–481, March 2015.

[18] O. Orhan, D. Gunduz, and E. Erkip. Throughput maximization for an energy harvesting communication system with processing cost. In *IEEE ITW*, September 2012.

[19] J. Xu and R. Zhang. Throughput optimal policies for energy harvesting wireless transmitters with non-ideal circuit power. *IEEE Jour. on Selected Areas in Comm.*, 32(2):322–332, February 2014.

[20] B. Gurakan, O. Ozel, J. Yang, and S. Ulukus. Energy cooperation in energy harvesting wireless communications. In *IEEE ISIT*, July 2012.

[21] B. Gurakan, O. Ozel, J. Yang, and S. Ulukus. Two-way and multiple access energy harvesting systems with energy cooperation. In *Asilomar Conference*, November 2012.

[22] B. Gurakan, O. Ozel, J. Yang, and S. Ulukus. Energy cooperation in energy harvesting two-way communications. In *IEEE ICC*, June 2013.

[23] A. Sendonaris, E. Erkip, and B. Aazhang. User cooperation diversity. Part I. System description. *IEEE Trans. Comm.*, 51(11):1927–1938, November 2003.

[24] K. Huang and V. K. N. Lau. Enabling wireless power transfer in cellular networks: Architecture, modeling and deployment. *IEEE Trans. Wireless Comm.*, 13(2):902–912, February 2014.

[25] Y. Shi, L. Xie, Y. T. Hou, and H. D. Sherali. On renewable sensor networks with wireless energy transfer. In *IEEE INFOCOM*, April 2011.

[26] R. Doost, K. R. Chowdhury, and M. Di Felice. Routing and link layer protocol design for sensor networks with wireless energy transfer. In *IEEE GLOBECOM*, December 2010.

[27] J. E. Ferguson and A. D. Redish. Wireless communication with implanted medical devices using the conductive properties of the body. *Expert Review of Medical Devices*, 8(4):427–433, July 2011.

[28] A. Yakovlev, S. Kim, and A. Poon. Implantable biomedical devices: Wireless powering and communication. *IEEE Comm. Magazine*, 50:152–159, April 2012.

[29] S. Kim, J. S. Ho, and A. Poon. Wireless power transfer to miniature implants: Transmitter optimization. *IEEE Trans. on Anten. and Prop.*, 60(10):4838–4845, October 2012.

[30] W. C. Brown. The history of power transmission by radio waves. *IEEE Trans. on Microwave Theory and Tech.*, 32(9):1230–1242, September 1984.

[31] J. O. McSpadden and J. C. Mankins. Space solar power programs and microwave wireless power transmission technology. *IEEE Microwave Magazine*, 3(4):46–57, December 2002.

[32] A. Sahai and D. Graham. Optical wireless power transmission at long wavelengths. In *Int. Conference on Space Opt. Systems and App.*, May 2011.

[33] A. Kurs, A. Karalis, R. Moffatt, J. D. Joannopoulos, P. Fisher, and M. Soljacic. Wireless power transfer via strongly coupled magnetic resonances. *Science*, 317:83–86, July 2007.

[34] A. Karalis, J. D. Joannopoulos, and M. Soljacic. Efficient wireless non-radiative mid-range energy transfer. *Annals of Physics*, 323(1):34–48, January 2008.

[35] B. Glover and H. Bhatt. *RFID Essentials*. O'Reilly Media, 2006.

[36] P. Grover and A. Sahai. Shannon meets Tesla: wireless information and power transfer. In *IEEE ISIT*, July 2010.

[37] L. Varshney. Transporting information and energy simultaneously. In *IEEE ISIT*, July 2008.

[38] R. Zhang and C. K. Ho. MIMO broadcasting for simultaneous wireless information and power transfer. *IEEE Trans. Wireless Comm.*, 12(5):1989–2001, May 2013.

[39] L. Varshney. On energy/information cross-layer architectures. In *IEEE ISIT*, July 2012.

[40] P. Popovski and O. Simeone. Two-way communication with energy exchange. In *IEEE ITW*, September 2012.

[41] A. M. Fouladgar and O. Simeone. On transfer of information and energy in multi-user systems. *IEEE Comm. Letters*, 16(11):1733–1736, November 2012.

[42] D. W. Kwan Ng, E. S. Lo, and R. Schober. Energy efficient resource allocation in multiuser ofdma systems with wireless information and power transfer. In *IEEE WCNC*, April 2013.

[43] D. Bertsekas and R. Gallager. *Data Networks*. Prentice-Hall, Inc., 1992.

[44] T. M. Cover and J. Thomas. *Elements of Information Theory*. John Wiley and Sons Inc., 2006.

[45] R. G. Gallager. A minimum delay routing algorithm using distributed computation. *IEEE Trans. Comm.*, 25(1):73–85, January 1977.

[46] D. P. Bertsekas, E. M. Gafni, and R. G. Gallager. Second derivative algorithms for minimum delay distributed routing in networks. *IEEE Trans. Comm.*, 32(8):911–919, August 1984.

[47] B. Gavish and I. Neuman. A system for routing and capacity assignment in computer communication networks. *IEEE Trans. Comm.*, 37(4):360–366, April 1989.

[48] D. Bertsekas. *Network Optimization: Continuous and Discrete Models*. Athena Scientific, 1998.

[49] H. H. Yen and FY. S. Lin. Near-optimal delay constrained routing in virtual circuit networks. In *IEEE INFOCOM*, April 2001.

[50] R. L. Cruz and A. V. Santhanam. Optimal routing, link scheduling and power control in multihop wireless networks. In *IEEE INFOCOM*, March 2003.

[51] L. Xiao, M. Johansson, and S. Boyd. Simultaneous routing and resource allocation via dual decomposition. *IEEE Trans. Comm.*, 52(7):1136–1144, July 2004.

[52] S. Cui, R. Madan, A. J. Goldsmith, and S. Lall. Cross-layer energy and delay optimization in small-scale sensor networks. *IEEE Trans. Wireless Comm.*, 6(10):3688–3699, October 2007.

[53] Y. Xi and E. M. Yeh. Node-based optimal power control, routing, and congestion control in wireless networks. *IEEE Trans. Inform. Theory*, 54(9):4081–4106, September 2008.

[54] C. K. Ho and R. Zhang. Optimal energy allocation for wireless communications with energy harvesting constraints. *IEEE Trans. Signal Proc.*, 60(9):4808–4818, September 2012.

[55] B. Gurakan, O. Ozel, J. Yang, and S. Ulukus. Energy cooperation in energy harvesting communications. *IEEE Trans. Comm.*, 61(12):4884–4898, December 2013.

[56] K. Tutuncuoglu and A. Yener. Multiple access and two-way channels with energy harvesting and bidirectional energy cooperation. In *UCSD ITA Workshop*, February 2013.

[57] K. Tutuncuoglu and A. Yener. Cooperative energy harvesting communications with relaying and energy sharing. In *IEEE ITW*, September 2013.

[58] L. Xie, Y. Shi, Y. T. Hou, W. Lou, H.D. Sherali, and S.F. Midkiff. On renewable sensor networks with wireless energy transfer: The multi-node case. In *IEEE SECON*, June 2012.

[59] X. Zhou, R. Zhang, and C. K. Ho. Wireless information and power transfer: Architecture design and rate-energy tradeoff. *IEEE Trans. Comm.*, 61(11):4754–4767, November 2013.

[60] A. M. Fouladgar and O. Simeone. Information and energy flows in graphical networks with energy transfer and reuse. *IEEE Wireless Comm. Letters*, 2(4):371–374, August 2013.

[61] B. Gurakan and S. Ulukus. Energy harvesting diamond channel with energy cooperation. In *IEEE ISIT*, June 2014.

[62] Z. Ding, C. Zhong, D. Wing Kwan Ng, M. Peng, H. Suraweera, R. Schober, and H.V. Poor. Application of smart antenna technologies in simultaneous wireless

information and power transfer. *IEEE Comm. Magazine.*, 53(4):86–93, April 2015.

[63] C. Hu, X. Zhang, S. Zhou, and Z. Niu. Utility optimal scheduling in energy cooperation networks powered by renewable energy. In *IEEE APCC*, August 2013.

[64] Y. Guo, J. Xu, L. Duan, and R. Zhang. Joint energy and spectrum cooperation for cellular communication systems. *IEEE Trans. Comm.*, 62(10):3678–3691, October 2014.

[65] J. Leithon, T. J. Lim, and S. Sun. Energy exchange among base stations in a cellular network through the smart grid. In *IEEE ICC*, June 2014.

[66] Y. K. Chia, S. Sun, and R. Zhang. Energy cooperation in cellular networks with renewable powered base stations. *IEEE Trans. Wireless Comm.*, 13(12):6996–7010, December 2014.

[67] J. Xu, L. Duan, and R. Zhang. Cost-aware green cellular networks with energy and communication cooperation. *IEEE Comm. Magazine*, 53(5):257–263, 2015.

[68] B. Schein and R. Gallager. The Gaussian parallel relay network. In *IEEE ISIT*, June 2000.

[69] V. Prelov and E. van der Meulen. Asymptotic expansion for the capacity region of the multiple-access channel with common information and almost Gaussian noise. In *IEEE ISIT*, June 1991.

[70] S. Boyd and L. Vandenberghe. *Convex Optimization*. Cambridge University Press, 2004.

[71] A. W. Marshall, I. Olkin, and B. C. Arnold. *Inequalities: Theory of Majorization and Its Applications*. Springer Science Business Media, 2011.

[72] T. S. Han. A general coding scheme for the two-way channel. *IEEE Trans. Inform. Theory*, 30(1):35–44, January 1984.

[73] D. Tse and S. Hanly. Multiaccess fading channels - Part I: Polymatroid structure, optimal resource allocation and throughput capacities. *IEEE Trans. Inform. Theory*, 44(7):2796–2815, November 1998.

[74] A. J. Goldsmith and P. P. Varaiya. Capacity of fading channels with channel side information. *IEEE Trans. on Inform. Theory*, 43(6):1986–1992, November 1997.

[75] R. M. Corless, G. H. Gonnet, D. E. G. Hare, D. J. Jeffrey, and D. E. Knuth. On the Lambert W function. *Adv. in Comp. Math.*, 5(1):329–359, December 1996.

[76] O. Orhan and E. Erkip. Throughput maximization for energy harvesting two-hop networks. In *IEEE ISIT*, July 2013.

[77] O. Orhan and E. Erkip. Energy harvesting two-hop communication networks. *IEEE Jour. on Selected Areas in Comm.*, 33(12):2658–2670, 2015.

[78] E. Uysal-Biyikoglu and A. El Gamal. On adaptive transmission for energy

efficiency in wireless data networks. *IEEE Trans. Info. Theory*, 50(12):3081–3094, December 2004.

[79] Z. Wang, V. Aggarwal, and X. Wang. Iterative dynamic water-filling for fading multiple-access channels with energy harvesting. *IEEE Jour. on Selected Areas in Comm.*, 33(3):382–395, March 2015.

[80] N. Liu and S. Ulukus. Capacity region and optimum power control strategies for fading Gaussian multiple access channels with common data. *IEEE Trans. Comm.*, 54(10):1815–1826, September 2006.

[81] O. Orhan, D. Gunduz, and E. Erkip. Source-channel coding under energy, delay and buffer constraints. *IEEE Trans. Wireless Comm.*, 14(7):3836–3849, July 2015.

[82] D. P. Bertsekas. *Nonlinear Programming*. Athena Scientific, 1995.

[83] R. Correa and C. Lemarechal. Convergence of some algorithms for convex minimization. *Mathematical Programming*, 62(1-3):261–275, February 1993.

[84] O. Ozel and S. Ulukus. Achieving AWGN capacity under stochastic energy harvesting. *IEEE Trans. Info. Theory*, 58(10):6471–6483, October 2012.

[85] N. Su, O. Kaya, S. Ulukus, and M. Koca. Cooperative multiple access under energy harvesting constraints. In *IEEE GLOBECOM*, December 2015.

[86] O. Kaya and S. Ulukus. Power control for fading cooperative multiple access channels. *IEEE Trans. Wireless. Comm.*, 6(8):2915–2923, August 2007.

[87] B. R. Marks and G. P. Wright. A general inner approximation algorithm for nonconvex mathematical programs. *Operations Research*, 26(4):681–683, August 1978.

[88] K. Tutuncuoglu and A. Yener. Energy harvesting networks with energy cooperation: Procrastinating policies. *IEEE Trans. Comm.*, 63(11):4525–4538, November 2015.